VOLUME 21 AUGUST, 1933 NUMBER 8

PROCEEDINGS
of
The Institute of Radio Engineers

Form for Change of Mailing Address or Business Title on Page X

Institute of Radio Engineers Forthcoming Meetings

NEW YORK MEETING
October 4, 1933

PITTSBURGH SECTION
September 19, 1933

SEATTLE SECTION
September 29, 1933

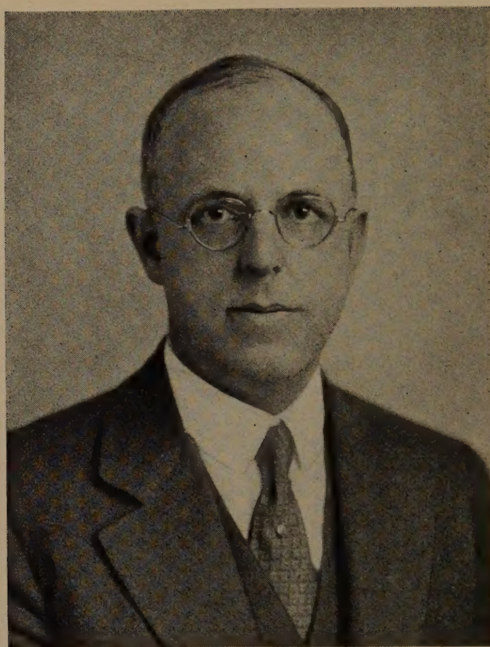

With deep regret we record the death of

Harold De Forest Arnold

who died of a heart attack on July 10.

Dr. Arnold was born in Woodstock, Connecticut on September 3, 1883. He was graduated from Wesleyan University, and in 1911 received a degree of Doctor of Philosophy from the University of Chicago. Leaving college, he entered the Research Laboratories of the Bell System, later becoming Director of Research.

His early work in the theory, design, and manufacture of vacuum tubes was of fundamental importance in the growing field of wire and wireless communication. Later, under his guidance the magnetic alloys, permalloy and perminvar, were developed.

The communications art owes a substantial debt to Dr. Arnold not only for his personal contributions but also for his leadership as the directing head of one of the world's largest research laboratories.

INSTITUTE NEWS AND RADIO NOTES

Eighth Annual Convention

The Eighth Annual Convention of the Institute was held in Chicago, Illinois, on June 26, 27, and 28.

Two-dozen papers were presented during the five technical sessions which comprised the major portion of the program. The titles and authors of these papers are listed in the June PROCEEDINGS. Some of these papers will be published in the next few issues of the PROCEEDINGS although, unfortunately, all have not been made available for publication.

Two official trips were made to the Century of Progress Expos'tion, and although substantial amounts of time were available, it was impossible to cover more than a small portion of the exhibition of interest to engineers. A large number of those in attendance stayed over for one or more additional days in order to devote the extra time to a more thorough investigation of what the Fair offered.

The Electrical and Communications Buildings which housed many exhibits of high interest were adjacent, and this assisted greatly in conserving time and effort in examining electrical developments.

Thirty-five organizations were represented by displays at the Institute's exhibition and many new pieces of equipment were introduced.

The annual banquet which was held in the Bal Tabarin of the Hotel Sherman was very well attended and devoted almost exclusively to an interesting series of entertainment acts and dancing. The short time that was devoted to serious business was occupied in the presentation of the Institute awards. The Medal of Honor was presented to Sir Ambrose Fleming for the conspicuous part he played in introducing physical and engineering principles in the radio art. This award was accepted in his behalf by British Vice Consul Henderson. The Morris Liebmann Memorial prize was awarded to Heinrich Barkhausen for his work on oscillation circuits and particularly on that type of oscillator which now bears his name. In this case, acceptance in behalf of Professor Barkhausen was by German Vice Consul Tannenberg.

The registration for the three days of the convention totaled 487 of whom 74 were ladies.

Radio Transmissions of Standard Frequencies

The Bureau of Standards transmits standard frequencies from its station WWV, Beltsville, Md., every Tuesday. The transmissions are

on 5000 kilocycles per second. The transmissions are given continuously from 12 noon to 2 P.M., and from 10:00 P.M. to midnight, Eastern Standard Time. The service may be used by transmitting stations in adjusting their transmitters to exact frequency, and by the public in calibrating frequency standards, and transmitting and receiving apparatus. The transmissions can be heard and utilized by stations equipped for continuous-wave reception through the United States, although not with certainty in some places. The accuracy of the frequency is at all times better than one cycle per second (one in five million).

From the 5000 kilocycles any frequency may be checked by the method of harmonics. Information on how to receive and utilize the signals is given in a pamphlet obtainable on request addressed to the Bureau of Standards, Washington, D. C.

The transmissions consist mainly of continuous, unkeyed carrier frequency, giving a continuous whistle in the phones when received with an oscillating receiving set. For the first five minutes the general call (CQ de WWV) and announcement of the frequency are transmitted. The frequency and the call letters of the station (WWV) are given every ten minutes thereafter.

Supplementary experimental transmissions are made at other times. Some of these are made at higher frequencies and some with modulated waves, probably modulated at 10 kilocycles. Information regarding proposed supplementary transmissions is given by radio during the regular transmissions.

The Bureau desires to receive reports on the transmissions, especially because radio transmission phenomena change with the season of the year. The data desired are approximate field intensity, fading characteristics, and the suitability of the transmissions for frequency measurements. It is suggested that in reporting on intensities, the following designations be used where field intensity measurement apparatus is not used: (1) hardly perceptible, unreadable; (2) weak, readable now and then; (3) fairly good, readable with difficulty; (4) good, readable; (5) very good, perfectly readable. A statement as to whether fading is present or not is desired, and if so, its characteristics, such as time between peaks of signal intensity. Statements as to type of receiving set and type of antenna used are also desired. The Bureau would also appreciate reports on the use of the transmissions for purposes of frequency measurement or control.

All reports and letters regarding the transmissions should be addressed to the Bureau of Standards, Washington, D. C.

Institute Meetings

Boston Section

A meeting of the Boston Section was held on May 25 at Harvard University. G. W. Kenrick, secretary, presided.

A paper by Sewell Cabot on "Resistance Tuning" was presented and included an anlytical discussion of circuits analogous to the Maxwell bridge circuit. In these circuits, the speaker stated the variations in resonant frequency are obtainable by a variation of a resistance parameter rather than a reactance parameter. Each resistance parameter includes a negative resistance component derived by the use of a dynatron characteristic.

"The Simulation of Musical Instruments by Electrical Circuits" was the subject of the second paper of the evening which was presented by E. B. Dallin. He discussed harmonic analyses of some common musical instruments, placing particular stress on the importance of musical resonant structures associated with these instruments in the emphasis of particular groups and harmonics. The paper was concluded with an experimental demonstration of the simulation of numerous musical instruments through the use of broadly tuned resonant circuits designed to produce an accentuation of harmonics similar to that obtained in the actual musical instruments being considered.

Fifty members and guests were present.

Cleveland Section

The June meeting of the Cleveland Section was held on the 2nd at the Case School of Applied Science, and was presided over by P. A. Marsal, chairman.

"The Simple Physics of Electrons" was the subject of a paper by John Victoreen of the Victoreen Instrument Company. In it, the speaker presented a general summary of known facts about electron behavior. He correlated the results of experiments in high-frequency emissions and measurements. Developments in the high-frequency field and X-ray intensity measurements were reviewed. At the close of the paper a general discussion was participated in by many of the thirty-eight members and guests in attendance. Special interest was shown in technique and quantitative measurements in the X-ray and high-frequency regions.

Detroit Section

"Some Characteristics of Five-Meter Transmission" was the subject of a paper by J. D. Kraus at the June 15 meeting of the Detroit Section which was held at the Edison Boat Club in Detroit. G. W.

Carter, chairman of the section, presided and the attendance totaled thirty-four.

In his paper, Mr. Kraus presented the history of short waves from the time of Hertz, outlining the field at the present time. He then presented detailed explanations of results of some experiments made at the University of Michigan on 5.1 meters. The purposes of these experiments were to measure field strength in absolute units, obtain a field strength survey of a specimen transmitter, determine the characteristics of the transmitting antenna used, and determine the effect of the length of the receiving antenna upon the voltage available at the receiver.

The transmitter comprised a pair of '10 tubes in a push-pull circuit feeding a full-wave antenna located on a tower of the Physics Building of the university. The antenna was arranged to permit its being swung around the tower and twisted vertically about its center. A highly sensitive superheterodyne receiver with an indicator in the second detector circuit was used for measuring field strengths. The transmitter output was about one watt.

It was then pointed out that higher field strengths were obtained when the intervening territory between the transmitter and receiver was low. The effect of hills and valleys were very prominently indicated upon the field strength maps. An antenna system giving a vertically polarized wave gave best results, and apparently regardless of how the wave leaves the antenna, it tends to become vertically polarized at a distance. Resonant receiving antenna systems gave best results, and higher voltages were obtained with long antennas working at harmonics. Phase shifting circuits located at correct points in the resonant system also proved valuable.

Philadelphia Section

The Philadelphia Section held a meeting on May 4 at the Engineers Club with H. W. Byler, chairman, presiding

A paper on "Exploring the Ionosphere" was presented by J. P. Schafer and W. M. Goodall of the Bell Telephone Laboratories. The paper covered recent experiments of the authors who showed that there are at least five layers in the upper atmosphere from which reflections of radio waves occur. The variation of ionization was indicated to be strikingly different. Considerable details of these layers and their behavior were presented. The paper was concluded with an outline of the results obtained during the solar eclipse during August, 1932.

At the close of the paper, election of officers for the following year

was held. William F. Diehl of RCA Victor was elected chairman; E. L. Forstall of the Bell Telephone Company of Pennsylvania became vice chairman; and George C. Blackwood was reëlected secretary-treasurer.

The meeting was attended by seventy-five members and guests.

San Francisco Section

A. R. Rice, chairman, presided at the June 21 meeting of the San Francisco Section held at the Bellevue Hotel, San Francisco.

L. E. Reukema, Associate Professor of Electrical Engineering at the University of California, presented a paper on "Outstanding Developments in Radio During 1932." In it, Dr. Reukema presented a very comprehensive outline of recent developments in the radio art both at home and abroad. A general discussion followed and was participated in among others by Messrs. Black, McAulay, and Whitton.

The annual election of officers was held. G. T. Royden of Mackay Radio and Telegraph Company was elected chairman; A. H. Brolly of the Television Laboratories, vice chairman; and R. C. Shermund, secretary-treasurer.

The meeting was attended by sixty-five of whom sixteen were present at the informal dinner which preceded it.

Seattle Section

A meeting of the Seattle Section was held on May 26 at the University of Washington, H. H. Bouson, chairman, presiding.

A paper was presented by W. A. Kleist of the Pacific Telephone and Telegraph Company on "Wave Filters." In it, the speaker pointed out that the proper design of filters was dependent upon the harmonic content of the signal being transmitted. He then analyzed a telegraph signal consisting of a single telegraph letter and showed it to consist of a fundamental frequency determined by the number of letters transmitted per second and all harmonics of this frequency. He then showed by a mathematical transformation that these harmonics could be divided into two groups, one being a function of the shape of the current impulse while the other contained all the intelligence carrying components. Furthermore, this second group was found to repeat itself in a series of bands, the maximum frequency component being a "dot" frequency. It was then pointed out that by use of wave filters all but one band could be removed thus permitting an increased number of telegraph channels on one line.

The paper was discussed by Messrs. Libby, Smith, Tolmie, Willson and others of the twenty-six members and guests who were present.

The June meeting of the Seattle Section was held on the 10th at the University of Washington with H. H. Bouson, chairman, presiding. Two papers were presented by graduate students of the University of Washington. The first by E. D. Scott on "A New Method of Obtaining Frequency Modulation" presented a method developed by him in connection with Professor Eastman in which an oscillator could be frequency modulated by a varying resistance through the use of a radio-frequency transmission line. He pointed out that the two principal drawbacks to the use of frequency modulation were the difficulty of producing linear modulation by means of a variable reactance and the difficulty of securing a satisfactory type of detector. He then outlined some work he has been doing which it is hoped will prove to be a solution to the second difficulty and proceeded to develop equations showing that with a line one-eighth wavelength long with a terminal resistance approximately equal to the characteristic impedance of the line, very satisfactory linear frequency modulation could be obtained. The paper was closed with a demonstration of this point by means of an experimental set-up of equipment.

The second paper presented by F. S. Allen was on "A New Type of Impedance Unit." In it, the speaker presented data taken on a quarter wavelength line to show its suitability as an impedance unit. He then demonstrated that if such lines were made of twisted pairs of conductors encased in shielding, the characteristics of the line are unchanged if the line is coiled up and inserted in a can. This gives a very compact and cheap filter unit.

The papers were discussed by Messrs. Eastman, Fisher, Levitin, Libby, Merryman, Tolmie, and Williams. Thirty-one members and guests were in attendance.

Washington Section

H. G. Dorsey, chairman, presided at the June 8 meeting of the Washington Section held at the Kennedy-Warren Apartments.

"A Solution of the Problems of Night Effect in Radio Range Beacon Systems" was the subject of a paper presented by Harry Diamond of the Radio Section of the Bureau of Standards. This paper appears in the June, 1933, issue of the Proceedings and is not abstracted here.

It was discussed by Messrs. Burgess, Robinson and others of the thirty members and guests in attendance. Fifteen were present at the informal dinner which preceded the meeting.

Proceedings of the Institute of Radio Engineers
Volume 21, Number 8 *August, 1933*

TECHNICAL PAPERS

THE APPLICATION OF GRAPHITE AS AN ANODE MATERIAL TO HIGH VACUUM TRANSMITTING TUBES*

BY

E. E. SPITZER

(Formerly, General Electric Company, Schenectady, New York; at present RCA Radiotron Company, Inc., Harrison, New Jersey)

Summary—*Graphite has been found to possess a number of advantages over materials which have heretofore been used in the construction of anodes for high vacuum transmitting tubes of the radiation-cooled type. Graphite has a higher radiation emissivity, resulting in lower glass temperatures and therefore less danger of glass electrolysis and strain cracking. Its use avoids anode warping and therefore results in tubes of much greater electrical uniformity. With proper manufacturing methods, there is no sacrifice in tube life when graphite is substituted for molybdenum.*

IT IS generally appreciated today that the communication services owe their rapid strides of the past 15 years largely to the development of high vacuum electron tubes. An entirely new tool was made available, possessing the unique property of being able to amplify faithfully electrical phenomena of the most complex character. Through this tool long-distance telephony became a reality, radiotelephony became practicable, and radio communication in general took on new life.

The action of the high vacuum tube amplifier may be briefly described as follows. The electrical impulse to be amplified is applied to the grid, and controls electrostatically the flow of electrons from an emitting cathode to the anode. The source of energy in the anode circuit is generally a high voltage direct-current supply. This energy is partly converted into an enlarged replica of the impulse applied to the grid. The efficiency of energy conversion in the anode circuit is never 100 per cent, so part of the energy is lost. This appears in the form of heating of the anode and is equal to the average energy with which the electrons bombard the anode.

Now it is readily seen that if a tube is operated under specified conditions at a given anode circuit efficiency and there are no other limiting factors, the power output is determined by the power that can be dissipated safely by the anode. In radiation-cooled tubes, which

* Decimal classification: R331. Original manuscript received by the Institute, April 14, 1933. Presented before Eighth Annual Convention, Chicago, Ill., June 26, 1933.

alone will be considered here, the anode loss is radiated largely through the glass envelope into space. Since the amount of energy that can be radiated is approximately proportional to the fourth power of the temperature, it has been found desirable to operate at anode temperatures as high as 1000 degrees centigrade in order to obtain anodes of reasonable size. Largely because of these high operating temperatures, comparatively few materials have been found suitable for anode construction. It has recently been determined that graphite is suitable and has a number of advantages over materials that have heretofore been used. Before discussing the characteristics of graphite for this purpose some of the requirements of an anode material will be considered.

1. Adsorbed Gases

The amount and kind of gases adsorbed in the anode material and the ease with which they can be desorbed are two of the most important factors in determining the suitability of the material. Gases are desorbed when materials are heated in vacuum. It is very essential that no appreciable amounts of gases be liberated by the anode during operation at the normal temperature. Liberated gases become ionized under impact by electrons and these ions partly neutralize the electron space charge which limits the flow of electron current between the cathode and anode. Increased current then flows through the tube, resulting in greater anode heating and more rapid gas liberation. This process may quickly become cumulative and lead to an arc discharge between anode and cathode. If no overload protective device is used, such a discharge generally results in an abrupt termination of the life of the tube by melting of the cathode, grid, and anode. In any case, a tube which goes out of service at short intervals is of no practical value.

The kind of gases liberated by the anode is important in the case of thoriated-tungsten cathode tubes. The electron emission of such cathodes is due to a monatomic layer of thorium adsorbed on the surface of the tungsten. Very small amounts of oxygen will oxidize the thorium layer and thereby destroy the emission of the cathode. This layer can also be destroyed by sputtering of positive ions. The lighter gases, such as hydrogen and helium, are relatively ineffective in this sputtering compared with heavier gases, such as mercury vapor.

2. Radiation Emissivity

It is desirable to have the total radiation emissivity of the anode material as high as possible because for given anode operating temperature and dissipation rating this results in an anode of minimum physical size and, therefore, also of lowest electrostatic capacitance to the other electrodes of the tube. Low interelectrode capacitances are essen-

tial if the tube is to be operated up to the highest frequencies in commercial use at the present time. In the past, high radiation emissivity has been obtained by roughening the external surface of the anode, by the addition of radiating fins and by coating the anode with carbon. The last method comes nearest the ideal of a black body.

3. Mechanical Properties

The material of the anode must have a number of mechanical properties. It must be capable of being worked into the desired shapes without undue difficulty. It must maintain these shapes at the highest temperatures necessary during the exhaust of the tube. Only a very small amount of warping can be tolerated at the normal anode temperature as warping results in a change of electrical characteristics of the tube.

4. Vapor Pressure

The vapor pressure of the anode material must be low enough to avoid noticeable deposits in the tube during exhaust. Deposits on insulators in the tube may result in excessive interelectrode leakage. Deposits on the glass envelope result in higher glass temperatures because of increased radiation absorption and may lead to strain cracks.

5. Electrical Conductivity

The electrical conductance of the anode material must be high enough so that no appreciable energy loss can be attributed to this property.

Molybdenum as Anode Material

Molybdenum, tantalum, and nickel are materials that have been used for anodes of transmitting tubes. Molybdenum is most widely used at the present time. Long manufacturing experience has shown that molybdenum anodes which have been degassed at a brightness temperature of 1400 degrees centigrade can subsequently be operated at temperatures as high as 1000 degrees centigrade without noticeable gas liberation. The recent work of Norton and Marshall[1] has shown that considerably higher temperatures are necessary to degas molybdenum completely. Fortunately, complete degassing is not necessary because, regardless of the temperature at which the degassing is carried on, the rate of gas evolution can be reduced to a negligible value by operating the anode at a sufficiently lower temperature. Furthermore, considerable gas evolution can be tolerated if the tube contains active "getter" for cleaning up the gases as fast as they are generated. In general, it may be stated that as far as adsorbed gases are concerned,

[1] F. J. Norton and A. L. Marshall, *Amer. Inst. Mining & Metallurgical Eng.*, February, (1932).

molybdenum is satisfactory as an anode material for transmitting tubes.

In regard to the second factor—radiation emissivity—molybdenum leaves considerable to be desired. Even when the surface is roughened by means of carborundum blasting, the radiation emissivity is only about half that of a black body. Thus, for the case of radiation into space, the absolute temperature of the molybdenum would have to be $\sqrt[4]{2}$ times the temperature of an equivalent black-body radiator. With the black body at 1000 degrees Kelvin the molybdenum would have to be at a temperature 190 degrees Kelvin higher.

The mechanical properties of molybdenum are not very satisfactory. It can be put through the necessary forming processes but the life of the tools and dies is comparatively short. In the case of flat anodes, warping of the molybdenum occurs due to uneven heating over the side of the anode. Special bracing is necessary to counteract this warping. Molybdenum does not soften or anneal even at much higher temperatures than are used during exhaust. This property is one of the chief reasons for the present widespread use of molybdenum for anodes.

In regard to the fourth and fifth factors, molybdenum is entirely satisfactory. Its vapor pressure is low enough so that bulb blackening can be avoided during manufacture. Its electrical conductivity is never a problem in design.

Application of Graphite

Graphite has been used for many years as an anode material in mercury pool type rectifiers. In such tubes the voltage drop is very low and consequently the anode loss is also small for a given current. Furthermore, there is no necessity for keeping interelectrode capacitances low so that it is possible to design tubes to operate at very low anode temperatures. Recently it has been found that it is possible to make successful high vacuum tubes with graphite anodes. Following the early work of H. W. Jackson of the General Electric staff, the initial application has been to the so-called "50-watt" type of tube which is designed to operate at a plate voltage of 1000 volts and a maximum anode dissipation of 100 watts. Fig. 1 shows a molybdenum and graphite anode as used in this type of tube.

Various commercial brush grades of graphite have been found applicable. In comparison with molybdenum, the amounts of gas adsorbed in typical graphite samples are quite large. Some of the best grades of artificial graphite have a gas content by volume of the order of ten times the gas content of molybdenum. By suitable treatment this gas content can be very materially reduced before the anode is built

into the tube. This makes the exhaust of the tube correspondingly easier. As in the case of molybdenum, Norton and Marshall found that complete degassing is not necessary. They found, for instance, that after a certain sample had been degassed for about one hour at 1300 degrees centigrade, no further evolution of gas could be detected when the temperature was dropped to 1000 degrees centigrade for 15 minutes. In actual manufacture it has been found that in spite of the large initial gas content of raw graphite, the exhaust of a properly pretreated graphite anode in a tube requires no more time than the exhaust of a similar molybdenum anode tube.

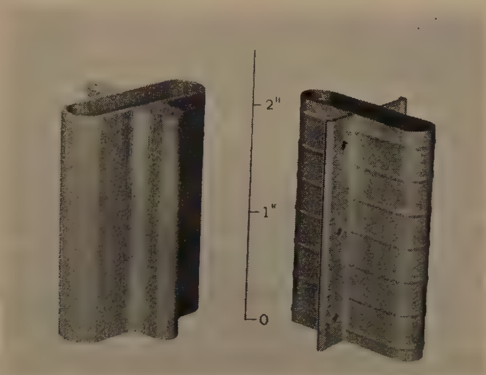

Fig. 1—New graphite and former molybdenum anode for 50-watt radio transmitting tube.

The total radiation emissivity of graphite depends on the treatment the surface has received. For rough ground surfaces, the total emissivity is probably about 90 per cent. This is a satisfactory approach to the black-body ideal. In comparison with molybdenum, graphite anodes run at a visibly lower temperature for the same power radiation. This reduction of temperature results in a decrease in the amount of heat conducted along the electrode supports to the reëntrant glass stems to which the supports are attached. For example, by introduction of the graphite anode in the "50-watt" type of tube, the temperature of the glass pinch through which the lead-in wires pass was reduced about 35 per cent at the rated anode dissipation of 100 watts. It is estimated that the glass conductivity between the lead-in wires was reduced twentyfold by this drop in temperature. It is hardly necessary to state that the danger of strain cracks and electrolysis of the pinch has been greatly reduced by this change.

One of the disadvantages of graphite as an anode material is its low tensile strength. In order to compensate for this weakness it ap-

pears desirable to make the minimum wall thickness at least one-sixteenth of an inch. There is a decided advantage in this increased wall thickness. The appearance of hot spots is a common occurrence in metal anode tubes, even when the construction is perfectly symmetrical, and is due to the fact that electrons attempt to travel from the cathode to the anode in lines normal to the anode surface. If the anode thickness is made very small so that the heat conductance in the plane of the anode surface is low, the shape of the filament can be seen outlined as a bright image on the exterior anode surface. With the anode thickness commonly used when the material is molybdenum, the center of the anode usually operates at a visibly higher temperature than the edges. This temperature difference produces warping. In the case of graphite anodes where the minimum anode thickness is one-sixteenth of an inch, the heat conductance in the plane of the anode surface is so good that hot spotting is avoided. In addition, the coefficient of expansion is so much lower for graphite that warping practically does not occur. Consequently, the electrical characteristics of graphite anode tubes are much more uniform, not only from tube to tube, but also for the same tube under various conditions of load.

The absence of hot spotting when graphite anodes are used means that the anode loss is radiated much more uniformly over the anode surface. The glass bulb also operates at a more uniform temperature. In the case of the "50-watt" type of tube, an 8 per cent reduction of bulb temperature opposite the anode was obtained when graphite was substituted for molybdenum.

Because of its softness, graphite does not present any serious difficulties in machining. Grades of graphite which have been graphitized at the highest temperatures are easiest to work but also have the least strength.

The vapor pressure of graphite is so low that bulb blackening can be avoided during exhaust. However, if the material has been graphitized at a low temperature, volatile materials other than graphite may be present and result in bulb darkening. Such grades of graphite are quite likely to be difficult to degas properly too. By choice of the proper grade of graphite these difficulties can be avoided.

The electrical conductivity of graphite is low compared with metals, but at the same time the temperature coefficient is usually negative, so that as the temperature is increased the difference becomes less. As the thickness of a graphite anode has to be about tenfold greater than the thickness of an equivalent metal anode for purely mechanical reasons, the resultant conductance is low enough to avoid appreciable loss, even at frequencies as high as 60 megacycles.

Finally a word should be said about the comparative costs of molybdenum and graphite anodes. Fundamentally, graphite is a much cheaper material than molybdenum. Whether a saving can be effected in the last analysis depends upon the construction adopted and the amount of pretreatment necessary for the graphite. It is hoped that in most cases the substitution of graphite for molybdenum will result in a somewhat lower cost.

Proceedings of the Institute of Radio Engineers
Volume 21, Number 8 *August, 1933*

VACUUM TUBE CHARACTERISTICS IN THE POSITIVE GRID REGION BY AN OSCILLOGRAPHIC METHOD*

By

H. N. Kozanowski and I. E. Mouromtseff

(Westinghouse Research Laboratories, East Pittsburgh, Pa.)

Summary—*A method of determining "complete" plate and grid characteristics of vacuum tubes in the positive grid region by means of oscillographic recording has been developed. A condenser of high capacity furnishes a single pulse of grid excitation which can be made to cover the entire region from any desired positive grid voltage to zero. Due to the rapidity of this excitation instantaneous power input to the tube of twenty to thirty times nominal rating has been recorded without danger to the tubes.*

Several typical complete charts of plate and grid characteristics obtained by this method for an experimental tube of the so-called "50-watt" type are given. The experimental procedure in obtaining these characteristics is discussed in detail. Also the circuit for obtaining oscillographically the highly important "composite diode line," with $E_p = E_g$, is described. The inadequacy of the usual logarithmic extrapolation of zero-grid characteristics into the positive grid region is discussed.

The complete plate and grid current charts, which can be obtained accurately only by an oscillographic method, are practically indispensable in precalculation of class B and class C performance. The method has been successfully used in studying the characteristics of the smallest and the largest existing tubes in this country.

In THE use of transmitting vacuum tubes the familiar curves of plate current against plate voltage for various negative grid voltages have long been an almost indispensible source of information to the radio engineer. Thus, in the case of the class A amplifier he has been able to determine easily and accurately such factors in tube operation as optimum load for a given output, grid excitation, distortion, and efficiency. Such charts have also been widely used in the study of modulator performance, a particular case of the class A amplifier, to determine the number of tubes necessary, percentage of modulation, and so forth. In fact, with the aid of these charts, all questions involving the action of a class A amplifier, where the grid does not swing to potentials positive with respect to the filament, can be solved graphically with ease and precision.

The increasing popularity of amplifiers where the grid is driven positive has brought out the desirability of having complete characteristic charts covering all regions into which the plate and the grid may swing during operation.

* Decimal classification: R131. Original manuscript received by the Institute, April 13, 1933. Presented before Eighth Annual Convention, Chicago, Ill., June 26, 1933.

In the class B audio amplifier where the problem of power output at minimum distortion is paramount, the chart allows the direct determination of distortion and the selection of operating paths along which the distortion is a minimum. For the class B amplifier at radio frequencies, and the class C amplifier, or oscillator, the complete charts would give such information as: grid excitation voltage and power for a desired output, optimum operating region, efficiency and many other important factors. Thus with the aid of complete charts, the performance of an amplifier, or self-oscillator, can be precalculated precisely, whereas, without this information, the process is rather empirical and indefinite.

For a complete solution of the operation of vacuum tubes, the values of grid current corresponding to the various plate-current—plate-voltage characteristics are also quite essential.

Possible Methods of Extension of Characteristics

There are three methods by which one might expect to arrive at information concerning the positive grid region. They are:

(a) Point-by-point static curves
(b) Logarithmic extrapolation
(c) Oscillographic recording.

Let us examine these possibilities in some detail.

(a) The *point-by-point static curves* are undoubtedly the most straightforward way of exploring the positive-grid region, as with suitable circuit arrangements, the values of the four variables, plate and grid current, and plate and grid voltage can be directly measured. In this way the region of comparatively low positive plate and grid voltages can be accurately investigated. However, the fact that the voltages must be applied for a time interval long enough to allow the reading of indicating meters furnishes a distinct limitation to carrying the observations to the most interesting region of comparatively high positive grid voltages. It is evident that in this region the dangerous heat dissipations for the plate and also for the grid are soon reached. With sustained voltages of the order in which we are interested, the tube might easily be damaged, if not destroyed, during the few seconds necessary for taking the corresponding meter readings. There is also the point that might be made concerning the effect of high plate and grid temperatures on the electron emission from the cathode and the possible distortion of the tube elements with consequent changes in normal tube characteristics. This is the reason why a point-by-point method cannot be successfully used for complete mapping of the positive-grid region.

(b.) *Logarithmic extrapolation method* is an attempt to calculate the plate currents for positive grid voltages from the zero-grid static curve by application of the basic vacuum tube equation. This plate-current plate-voltage characteristic at zero grid voltage can be determined statically in a point-by-point manner with accuracy; it gives a straight line on log-log paper which may be extended in the direction of higher plate currents. In the basic equation,

$$I_p = 1/k(E_p + \mu E_g)^\alpha,$$

α is the slope of this log-log line and $1/k$ is its intercept. It is evident that if the constants α and $1/k$ have been determined, I_p can be calculated for *any* combination of values of plate and grid voltages, assuming that μ, the amplification factor is also known. Therefore, the value of I_p can be read directly from a linear extrapolation of the original zero grid voltage curve plotted against "plate diode voltage" (or "grid diode voltage"),[1] which is given by

$$E_{pd} = E_p + \mu E_g$$

thus referring all voltages to the plate (or to the grid) as though the tube were a diode. The method is open to the following criticisms:

1. The amplification factor is not constant.
2. The slope of the log-log curve is not necessarily a constant; it varies essentially in the region of low plate currents and also as the saturation region is approached.
3. The slope is seldom equal to 1.5, the theoretical slope of the ideal tube characteristic, and varies from tube to tube, even of the same type.
4. No means exists in the equation for the separation of grid and plate current.
5. Secondary emission which may greatly affect grid and plate currents does not appear in the picture at all.

The verdict one is compelled to arrive at from the above considerations is that the method of logarithmic extrapolation can be applied safely only for regions of high plate and low grid voltages with negligible grid current, and also where the situation is not complicated by a limited thermionic emission from the cathode.

[1] When "plate-diode voltage" is considered, a three-electrode tube is treated as a diode tube having identical plate and filament structure and the original grid voltage is transferred to the plate of this diode according to the relation above. The sum of plate and transferred grid voltage is what we call, "plate-diode voltage." "Grid-diode" voltage is referred to a diode in which the original grid of the tube is considered the anode and the plate voltage is transferred to it according to the relation $E_{gd} = E_p/\mu + E_g$. This "grid-diode" voltage corresponds exactly to the German "Steuerspannung."

(c) *An oscillographic-recording method* is free from the limitations just discussed. With it the actually observed values of the four parameters are permanently recorded under conditions comparable with those which prevail during vacuum tube operation. But even such a method may involve some limitations connected with plate and grid temperatures. One must note that in such a method the power supply sources are required to deliver instantaneous currents which usually exceed the capacity of standard equipment. Therefore, a method which may be described as "*condenser-discharge oscillographic method*" has

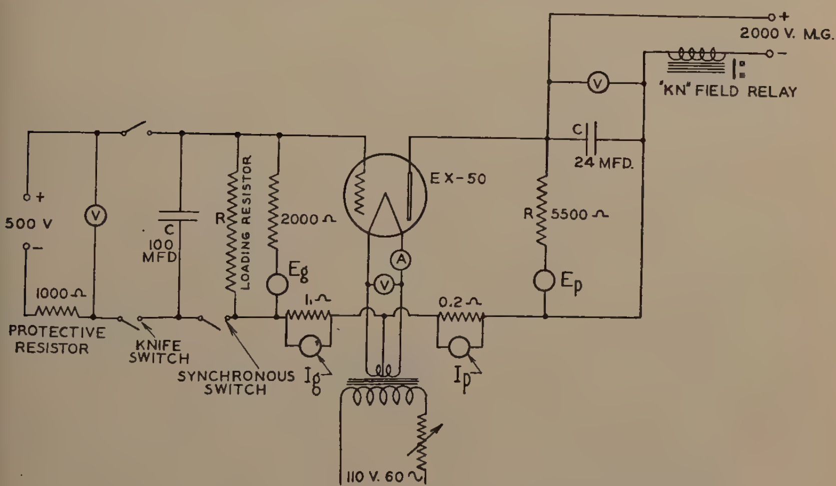

Fig. 1—Oscillograph circuit for recording triode characteristics in positive grid region.

been developed. It can be outlined as follows: A high capacity—high voltage condenser is charged to any desired potential difference and is then discharged in a comparatively short time interval to furnish excitation to the grid of the tube being studied. Normal plate voltage is supplied by the conventional direct-current generator. Four oscillograph elements suitably placed give deflections corresponding to the instantaneous values of plate current, grid current, and grid and plate voltages. The experimental arrangement is shown in the schematic diagram of Fig. 1.

Details of the Circuit and its Calibration

For this work five elements of a standard Westinghouse 9-element oscillograph were used. The grid excitation condenser, C, and the loading resistor, R, are so chosen that the discharge curve falls to zero within the length of a single exposure of the recording camera film,

with the camera drum driven at a suitable speed. A 60-cycle per second timing wave, which is also recorded on the film, aids in the checking and adjustment of the discharge time. A condenser of 100 microfarads capacity, rated at 500 volts, and a loading resistor of approximately 2500 ohms are suitable for the study of tubes rated from 50 to 500 watts. It should be pointed out that the grid is never "floating," but is always connected to the center tap of the filament transformer by the grid voltmeter element and loading resistor in parallel.

The connections of all oscillograph elements are shown in Fig. 1. All shunts and resistors are noninductive, preventing the possibility of phase-shift in recording. The grid current shunt has a resistance of one ohm and is used with a high-sensitivity oil-damped element. The plate current shunt consists of two equal 0.2-ohm sections connected to a high sensitivity element. This allows the selection of such deflections for a given plate current that accuracy is preserved even at lower plate current values. The grid and plate voltmeter elements are of standard sensitivity (of about 100 milliamperes per inch deflection).

The calibration of elements was carried out in the usual way, by applying to the individual elements a series of standard voltages and currents measured by laboratory standard meters, and measuring the deflection of the spot of light on a graduated ground-glass screen. The deflections are stable and linear over the range used in actual recording. Additional calibration checks were obtained by actually recording zero lines and constant deflections photographically.

Synchronization of Excitation and Recording

In this type of oscillogram it is necessary that the beginning of the grid excitation coincide with the beginning of the exposure. This is carried out in the standard 6- and 9-element oscillograph by the "remote control" relay which can be adjusted to close the grid excitation circuit and open the recording light shutter simultaneously. A commutating segment located on the camera drum-shaft can be so adjusted that the trip-solenoid operates the shutter and excitation circuit only when the film is in the correct position.

Procedure in Oscillographic Recording

The tube under investigation is operated at rated filament voltage. Plate power is supplied by a 5-kilowatt direct-current high voltage generator shunted by a condenser of 24 microfarads capacity. The plate voltage is adjusted to a desired value indicated by a standard voltmeter. The maximum voltage is governed by the plate temperature of the tube at zero grid voltage. The grid excitation circuit is opened and

interlocked with the shutter trip mechanism. The grid condenser is then charged through a high "protective" resistance from a generator, or vacuum tube rectifier of comparatively small capacity, to a potential of about 500 volts, and the charging switch is opened. The condenser is thus isolated and holds its charge for an appreciable time as leakage is small. The camera is operated at a predetermined speed with the safety shutter open. When the overvoltage switch of the oscillograph is closed, the light intensity increases, and at the instant the beginning of the film reaches the recording slit, the shutter is automatically opened and excitation applied. At the end of the trace the shutter is closed and the lamp circuit is opened. Once adjusted the recording and synchronizing circuit is entirely automatic.

Thus with a single exposure we have a permanent record of plate current, grid current, and plate voltage for a continuous range of grid voltages from about 400 volts positive to zero. Experiments have shown that a very complete record of the characteristics of medium power tubes such as UV-203A or UV-849 can be obtained with six exposures, using arbitrarily chosen plate voltages of 1000, 750, 625, 500, 250, and 100 volts. With the apparatus once set up and calibrated, complete characteristics of an individual tube can be recorded in 20 to 30 minutes.

Analysis of Oscillographic Records

After the records are developed, the four zero lines are extended across the entire film, consisting of three exposures, from the middle exposure, where they are photographically recorded. This is done in preference to recording zero lines for each individual exposure, because confusion due to the line width and superposition at small deflections is eliminated. A typical exposure at $E_p = 900$ volts is shown in Fig. 2.

Distances equal to a selected series of grid voltages, as given by calibration data, are measured from the grid zero or base line, E_{g0}, to the discharge curve, E_g. A template with appropriately spaced holes allows these distances to be quickly and accurately located. Lines drawn perpendicular to the zero lines and passing through the points corresponding to the selected grid voltages, intersect the plate-current, grid-current, and plate-voltage curves. The perpendicular distance of each deflection from its zero line, multiplied by its appropriate calibration factor gives the value of each variable recorded.

The grid voltages arbitrarily selected for reading the oscillograms start from zero and increase by 25-volt intervals up to positive voltages of the order of 300 to 400 volts. It can be seen from the oscillogram of Fig. 2 that the initial plate-current surge due to the closing of the ex-

citation circuit causes a highly damped transient state in the plate voltage. This does not affect the results in this region as there is no phase displacement in the recording of the elements. The voltages actually recorded during this transient state can be read from the film records and the corresponding values of currents used in compiling the data.

Initially it was found that a generator without a filter condenser gives a plate voltage which varies throughout the entire record, making the interpretation of the data tedious. By placing a condenser of 24

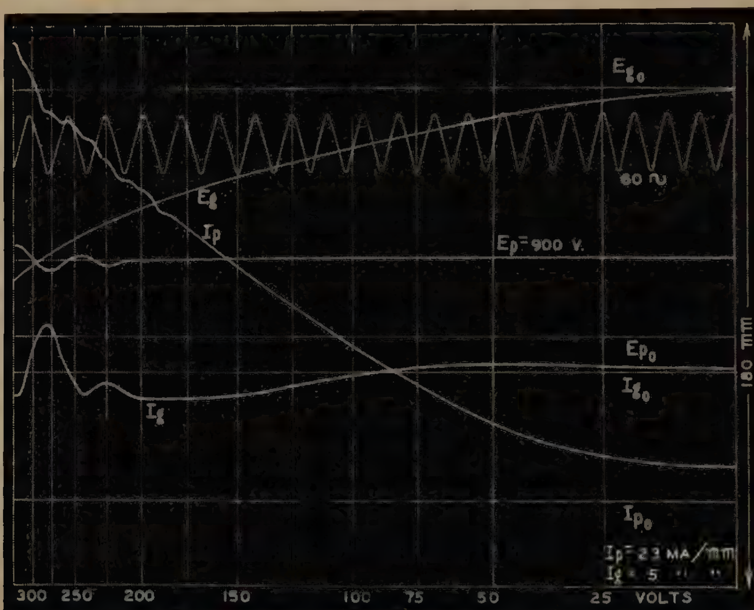

Fig. 2—Typical oscillographic record for EX-50 tube. A replica of the actual oscillogram, prepared by tracing over the original, is shown since this offers better reproduction.

microfarads capacity across the generator, and making all connecting leads short and of large cross-section, it is possible to maintain a plate voltage which is sensibly constant after the first two or three timing cycles of the exposure. Such a constant plate voltage greatly simplifies the analysis and interpretation of the record.

It will be noted that the magnitude and *direction* of the grid current can be accurately determined from the oscillograms. This recorded grid current is in reality the difference between the number of electrons arriving at the grid, and the number of secondary electrons leaving the grid at any given instant. The very interesting and important problem of the separation of incident and secondary electrons will be discussed in a later publication.

Thus, six oscillograms at appropriately chosen plate voltages make it possible to obtain complete data on the plate- and grid-current characteristics in the positive grid region. Charts prepared from these data for a special EX-50 tube of the so-called "50-watt" type resembling the UV-203A are given in the following figures. In Fig. 3 the plate current

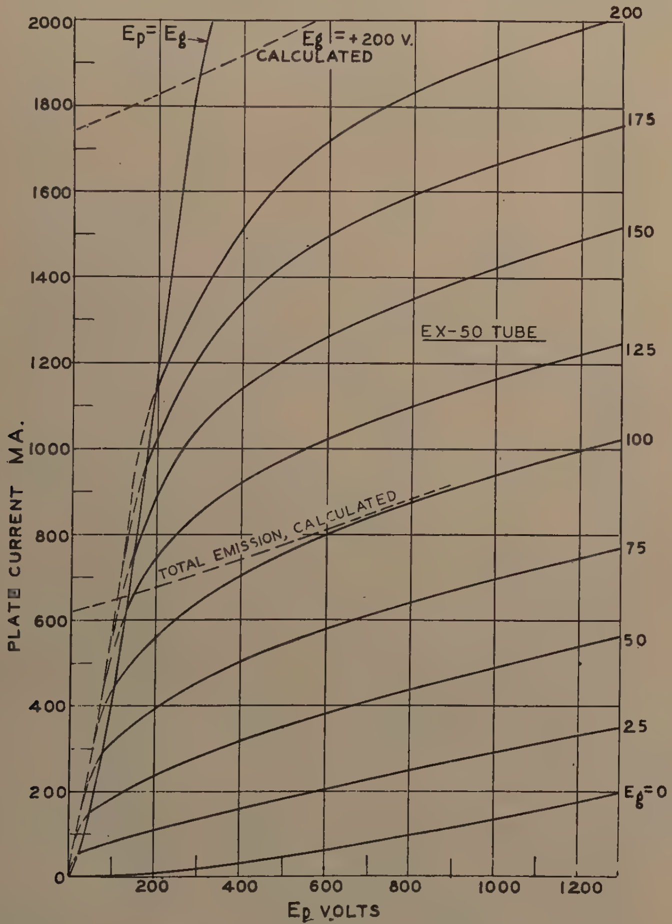

Fig. 3—Plate characteristics from oscillographic data.

is plotted as function of the plate voltage for a series of positive grid voltages. It is interesting to note that peak currents of 2 amperes at a plate voltage of 1000 volts, corresponding to instantaneous plate dissipations of 2 kilowatts, have been recorded without danger or injury to the tube, although the rated plate dissipation is only 100 watts.

In addition, the value of the plate current calculated from logarith-

mic extrapolation has been indicated in broken lines in the same chart for particular values of grid voltage of +100 and +200 volts. One must note that the discrepancy between calculated and recorded curves becomes more and more marked throughout the entire voltage range as

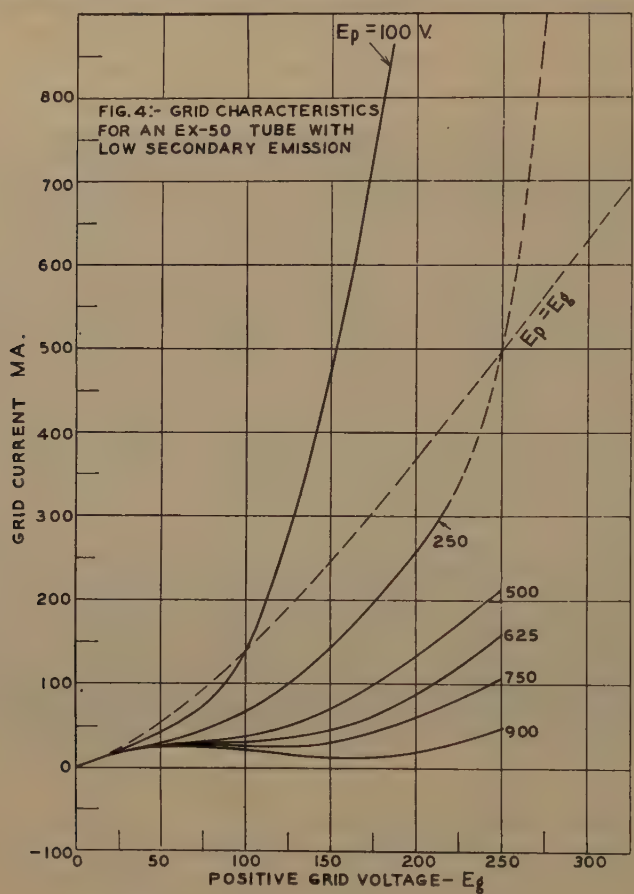

Fig. 4

the saturation region, due to a limited thermionic emission from the cathode, is approached.

The grid current curves are shown in Figs. 4 and 5 corresponding to two extremes from the standpoint of secondary emission. The presence of secondary emission is evident in both; but Fig. 4 shows grid characteristics of a tube in which measures were taken to reduce secondary emission, while in Fig. 5 it is so pronounced that in certain regions large negative grid currents are observed. The same data in more

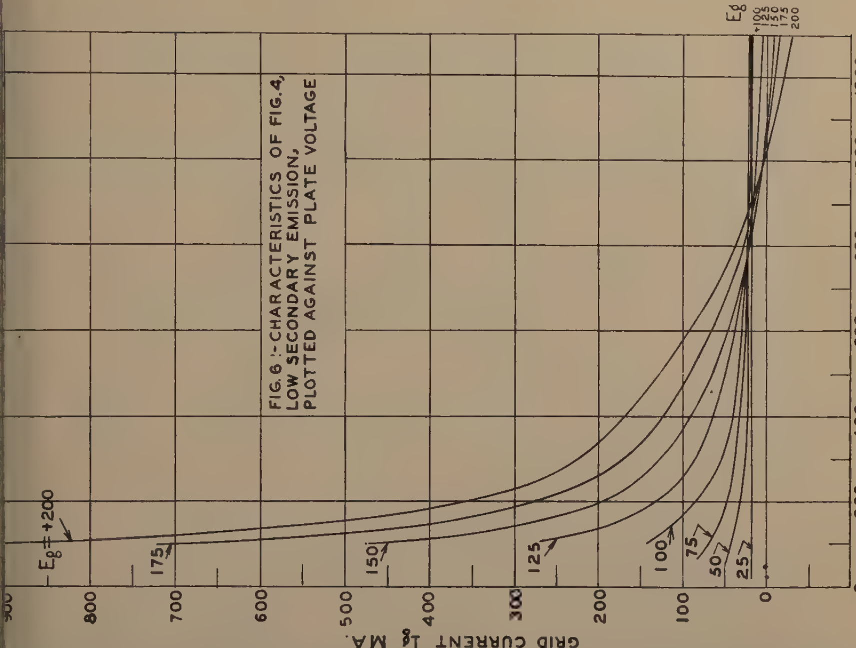
FIG. 6 :- CHARACTERISTICS OF FIG. 4, LOW SECONDARY EMISSION, PLOTTED AGAINST PLATE VOLTAGE
GRID CURRENT I_g MA.
PLATE VOLTAGE I_p
E_g = +200
E_g
175
150
125
100
75
50
25
0
200
400
600
800
1000
1200

Fig. 6

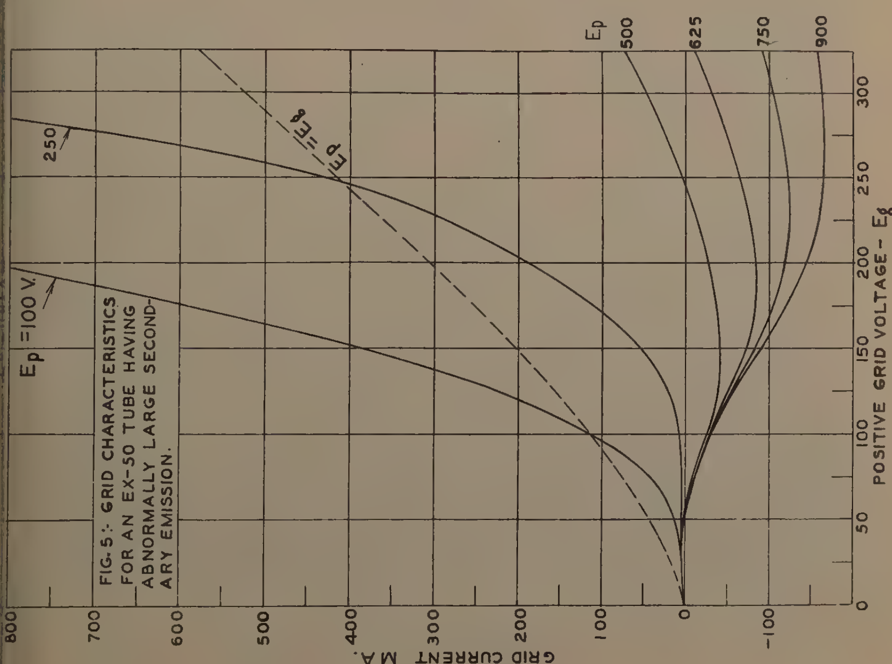
FIG. 5 :- GRID CHARACTERISTICS FOR AN EX-50 TUBE HAVING ABNORMALLY LARGE SECONDARY EMISSION.
GRID CURRENT MA.
POSITIVE GRID VOLTAGE - E_g
E_p = 100 V.
250
$E_p = E_g$
E_p
500
625
750
900
-100
0
50
100
150
200
250
300

Fig. 5

useful form for the design engineer are given in Figs. 6 and 7. Here grid current is plotted against plate voltage with the grid voltage as a parameter.

In Fig. 3 the curves of plate current have been terminated on the "composite-diode" line; that is, with $E_p = E_g$. This line can be obtained by logarithmic extrapolation of point-by-point determinations of plate

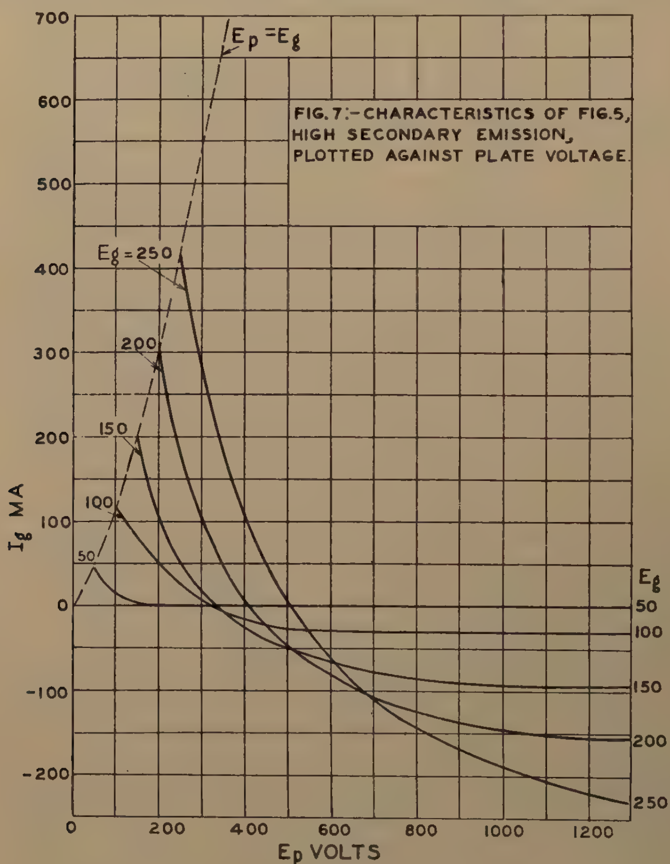

Fig. 7

current from the region of low voltages, or by oscillographic recording using the circuit shown in Fig. 8. Such an oscillographic record is represented in Fig. 9, while Fig. 10 contains the curves of plate and grid current for $E_p = E_g$ plotted from this record. This diode line is most useful in verifying the shape of the characteristics in Fig. 3 in the region of low plate voltage. To the left of the diode line in Fig. 3 the various curves of plate current (shown in dotted lines) descend steeply to

zero and practically coincide with each other and at the same time depart but little from the diode line itself. Therefore, this part of the

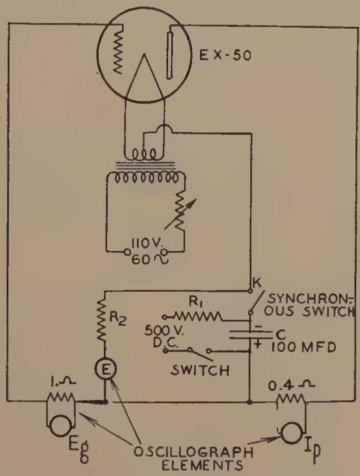

Fig. 8—Circuit for oscillographic recording of composite diode line, $E_p = E_g$.

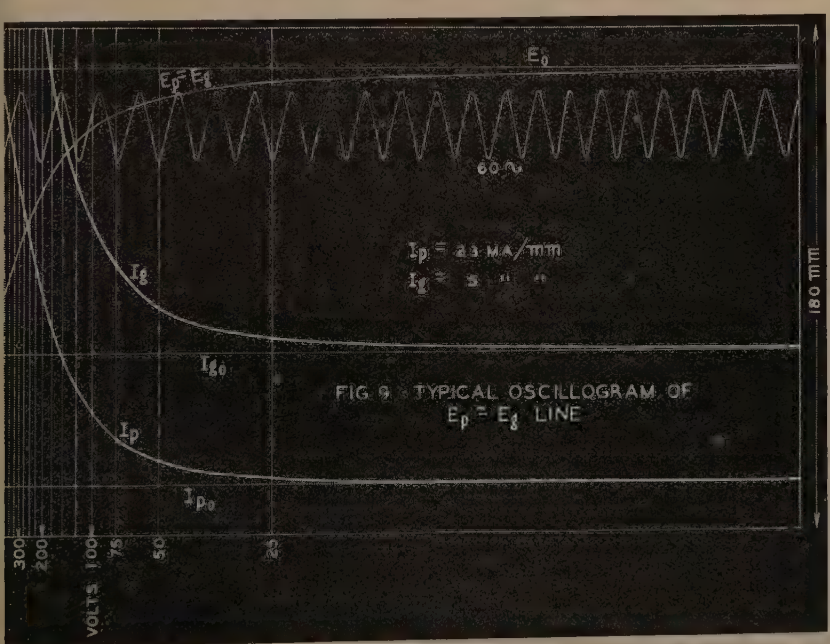

Fig. 9—A replica of the actual oscillogram, prepared by tracing over the original, is shown since this offers better reproduction.

chart is of little technical importance. In fact, it can readily be seen that there is little to be gained by allowing the grid to swing into the region to the left of this line, as such a condition increases the grid dissipation and driving power greatly without contributing appreciably to the power output of the tube.

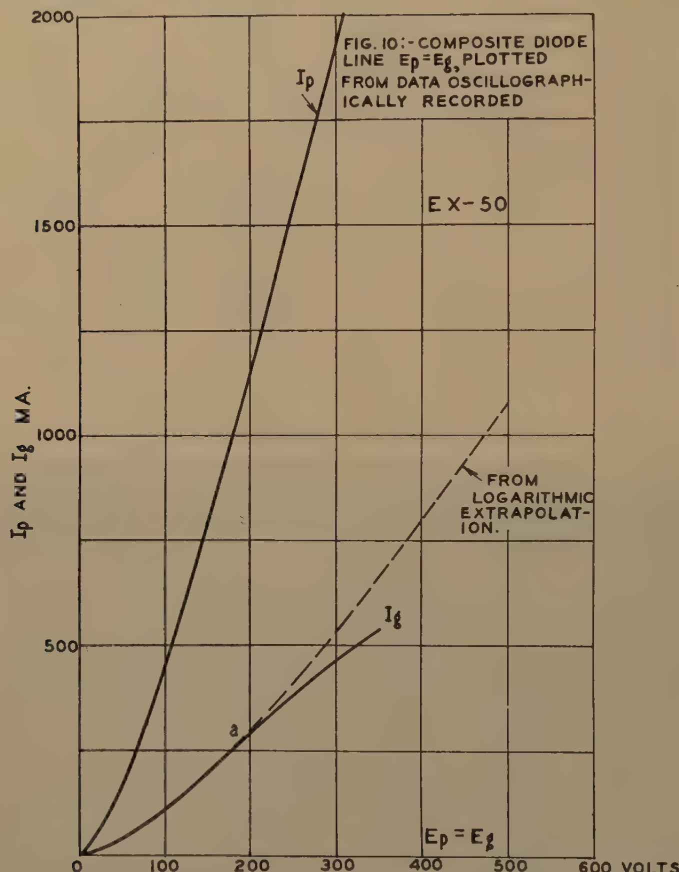

Fig. 10

The curves of Fig. 10 show that the effect of saturation with the tube investigated begins with plate current somewhat below 1.5 amperes (point *a*), although the total emission of the thoriated filament used is above 3 amperes. The influence of saturation is particularly clear from the comparison of the logarithmically extrapolated plate and grid current lines for $E_g = E_p$ and the actually recorded currents, as is shown in Fig. 11. Early saturation can also be observed on the

plate-current chart, where the upper curves have the tendency to crowd together. With some individual tubes this effect is even more pronounced.

One may note that variation in the amplification factor, μ, in the vicinity of the diode line is very pronounced, if one considers plate-current—plate-voltage characteristics of Fig. 3. There it acquires any values between the normal (about 28) and zero. But if one plots

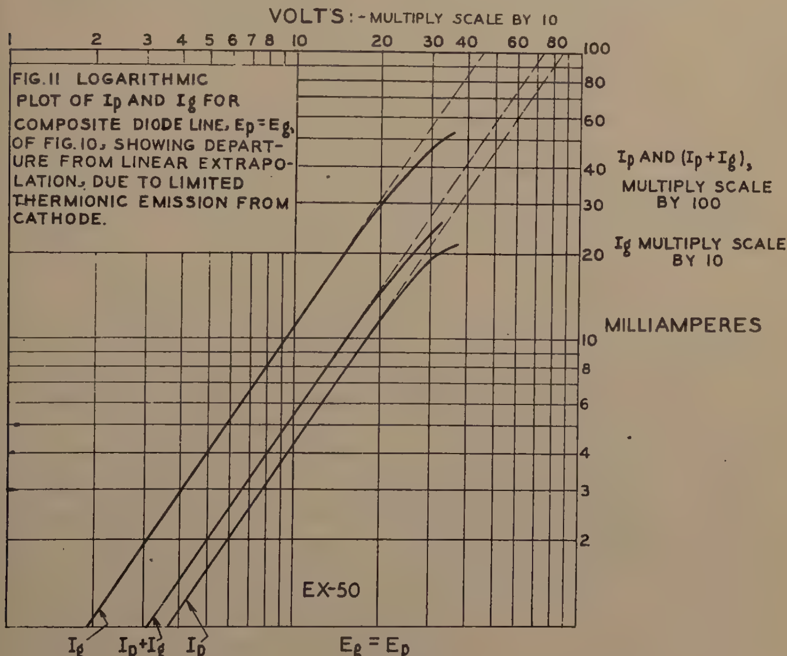

Fig. 11

(I_p+I_g) curves as function of plate voltage with E_g = constant as a parameter (Fig. 12), μ comes out more constant and does not drop to zero even at zero plate voltage. It is quite evident that μ in the basic vacuum tube equation must be considered for total space current, (I_p+I_g) rather than for plate current alone.

Conclusion

The oscillographic charts obtained by recording the actual picture of the internal relations between voltages and currents within a tube, over a wide region of feasible tube applications, are very useful for precalculation of all desired data for any preconceived operating condition taking into account all possible tube limitations. Thus, for in-

stance, the grid-current charts are indispensable in determination of driving or excitation power and, hence, for the design of preceding stage exciter tubes and circuits.

The oscillographic method is particularly well adapted for the study of the more complicated phenomena in multigrid tubes, such as the screen-grid type, in which secondary emission plays a decided role in

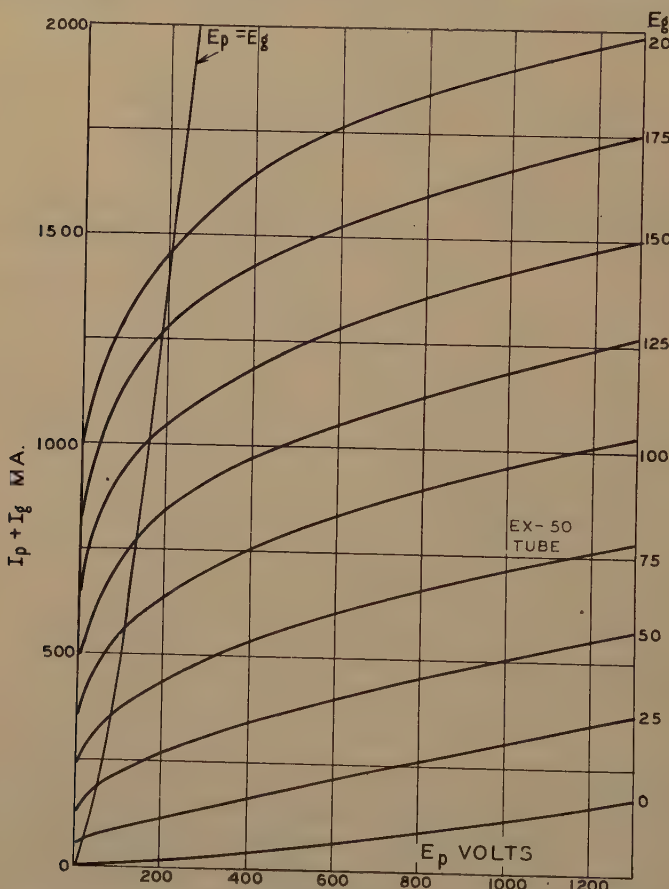

Fig. 12—Sum of I_p and I_g as functions of E_p, for E_g as parameter, showing details of characteristics to left of $E_p = E_g$ line. (Compare with Fig. 3.)

determining tube performance. A study of screen-grid transmitter tubes from this viewpoint is now being carried out.

This method is applicable, and in fact has been used, in the study of the largest as well as the smallest tubes made in this country.

Proceedings of the Institute of Radio Engineers
Volume 21, Number 8 *August, 1933*

A LIFE TEST POWER SUPPLY UTILIZING THYRATRON RECTIFIERS*

By

H. W. Lord

(Vacuum Tube Engineering Department, General Electric Company, Schenectady, New York)

Summary—*Thyratron rectifiers for supplying high voltage direct current to radio transmitting tube life test racks are superior to motor-generator sets where quietness, flexibility, low operating cost, and safe operation over long intervals of time are desirable.*

An installation for supplying typical voltages, in conjunction with usual forms of electric power supplies is described. This consists of two high power rectifiers for 425 and 1000 volts direct current plate supplies and a low power 125-volt direct current rectifier for bias voltage. A control circuit provides complete protection against faults detrimental to tube operating conditions such as low filament voltage, low bias, and resumption of power after failure, insuring a maximum of life testing hours available consistent with safe operation.

An installation, including two Thyratron rectifiers, for supplying 425 volts and 1000 volts direct current to life test racks for radio transmitting tubes is a useful auxiliary to vacuum tube manufacturers. It is often desirable to have the power supply in the same room with the test racks where the noise of a motor-generator set would be objectionable. The rectifiers provide a quiet unit, are flexible as to voltage ratings, have low operating cost and may be operated safely at long intervals without attention, permitting operation of the life test over week-ends.

Typical direct current voltage requirements for small transmitting tube life test purposes are:

	Plate Supply	*Bias Potentiometer Supply*	
(a)	1125	0	
(b)	1000	−125	
(c)	425	±125	(See Fig. 1.)
(d)	250	±125	

In the equipment to be described the available power sources are:

250v/125v d-c with grounded neutral

230v/115v a-c with grounded neutral

550v—3-phase a-c (Selsyn excitation source)

* Decimal classification: R366.2. Original manuscript received by the Institute, April 14, 1933. Presented before Eighth Annual Convention, Chicago, Ill., June 28, 1933.

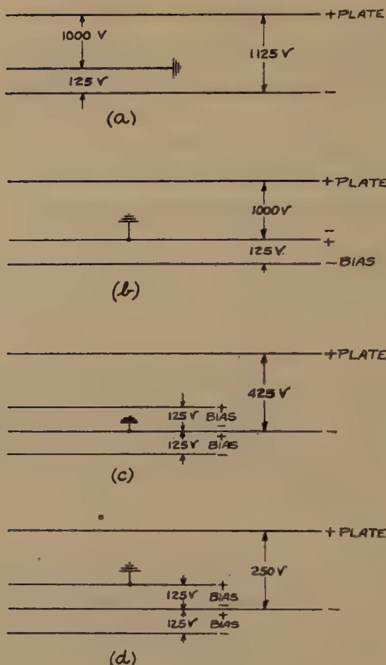
+PLATE
1000 V
1125 V
125 V
(a)
+PLATE
1000 V
125 V
−BIAS
(b)
+PLATE
425 V
125 V BIAS
125 V BIAS
(c)
+PLATE
250 V
125 V BIAS
125 V BIAS
(d)

Fig. 1

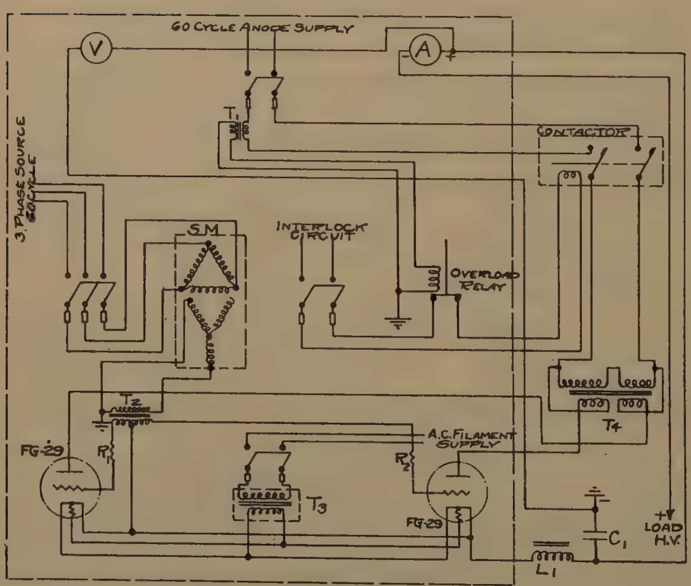
60 CYCLE ANODE SUPPLY
V
A
T1
CONTACTOR
3 PHASE SOURCE 60 CYCLE
S.M.
INTERLOCK CIRCUIT
OVERLOAD RELAY
T2
FG-29
R1
A.C. FILAMENT SUPPLY
R2
T3
T4
FG-29
C1
L1
+ LOAD H.V.

Fig. 2

The voltage requirements are met by two rectifiers, rated at 1000 volts and 425 direct-current output, with the negatives tied to the common neutral of the power sources, and a third low power rectifier rated at 125 volts direct-current output with the positive tied to the −125-volt direct-current source. Fig. 1 shows how the different required voltages are obtained.

The two high voltage rectifiers are similar in circuit and construction. The tube and control panels are identical. Fig. 2 is a schematic wiring diagram of one of these rectifiers and shows two FG-29 Thyratrons with an anode supply consisting of power transformer T_4 con-

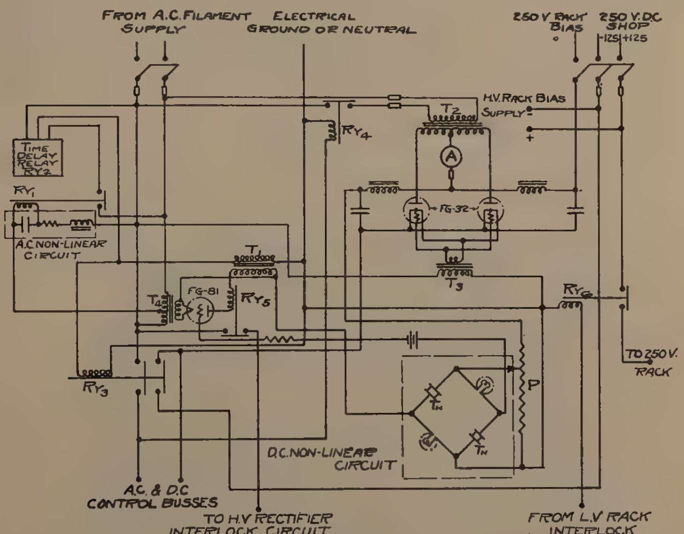

Fig. 3

nected as an autotransformer. The autotransformer connection is used in the 425-volt rectifier to reduce the kva rating of transformer T_4 and in the 1000-volt rectifier to obtain 1000 volts direct current from a standard 2300/1150- to 230/115-volt distribution transformer. This connection makes the neutral of the alternating current source the center tap of the anode supply and thus gives an inherent tie-in between the neutral of the source and the negative terminal of the rectifier. The FG-29 variable phase grid excitation for control is supplied through transformer T_2 from Selsyn *SM*, which in turn is supplied from a three-phase source of which the anode supply is a part. Current transformer T_1 in conjunction with a trip free overload relay provides overload and short-circuit protection. The interlock circuit is supplied

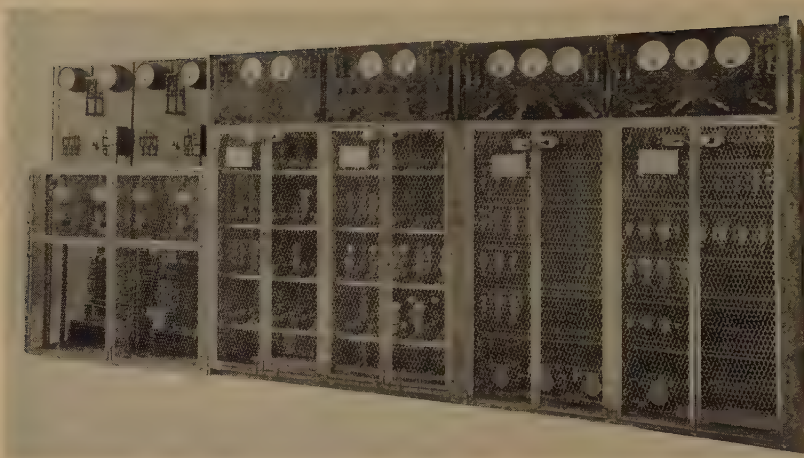

Fig. 4—Vacuum tube life test racks and thyratron rectifiers.

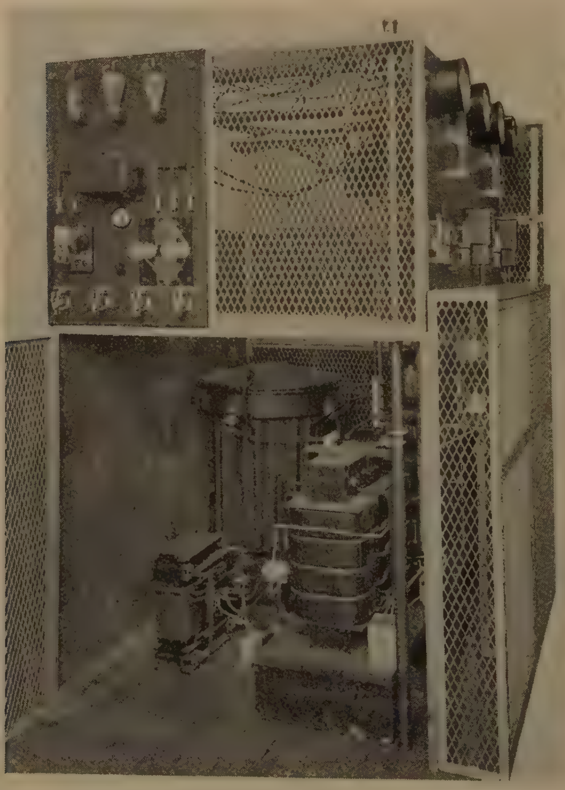

Fig. 5—Thyratron rectifiers. Side view showing bias panel.

from a main control panel through the gate interlocks on the test racks.

The bias rectifier is mounted on a panel which also functions as a main control panel. The circuit of this panel is shown in Fig. 3.The rectifier includes two FG-32 Phanotrons supplied by the anode transformer T_2 and two filter circuits, one for the output and the other for supplying the underbias protective circuit.

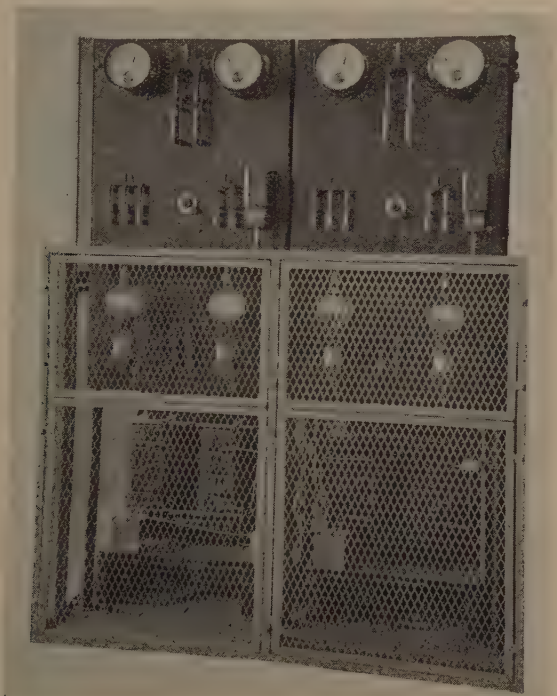

Fig. 6—Thyratron rectifiers for vacuum tube life test racks.

Only a reduction of negative bias is harmful so potentiometer P is placed across the bias rectifier and the -125 volt direct-current source in series. A part of this voltage is fed to a tungsten-thyrite bridge, the output of which controls the grid of the FG-81 Thyratron. Relay R_{y5} operates to open the interlock circuit to the high voltage rectifiers when the bias voltage drops below a predetermined value and recloses as soon as the voltage exceeds the drop-out value by a few volts.

Relay R_{y1} in conjunction with an alternating current nonlinear[1]

[1] C. G. Suits, "Non-linear circuits for relay applications," *Electrical Engineering,* vol. 50, pp. 963–965; December, (1931).

circuit provides a simple but dependable alternating current under-voltage release. This relay opening drops out the cathode protection time delay relay R_{y2} and requires the full time delay for reclosing after an undervoltage failure. The contacts of R_{y2} control excitation to the underbias protective relay and the alternating and direct current control bus contactor R_{y3}. These alternating and direct current control busses supply excitation to interlock circuits and contactors with either alternating or direct current type coils when the life test circuits required a cathode heating time before application of anode voltage.

The protective circuits are so interconnected that all cathodes are allowed a definite heating time, set by the time delay relay, after an interruption or undervoltage condition of the alternating current filament supply while loss or reduction of bias removes the plate supply to the vacuum tube racks only for the period of the fault, still permitting other life test circuits unaffected by the loss of direct current to continue operating. With such a control the operation is entirely automatic and may be safely operated without attention for long periods of time.

The accompanying photographs show the installation described above. Fig. 4 shows the rectifier and test racks, Fig. 5 the rectifiers, and Fig. 6 the control panel. This installation has been in operation for several months with a very satisfactory service record.

Proceedings of the Institute of Radio Engineers
Volume 21, Number 8 *August, 1933*

THE LIMITING POLARIZATION OF DOWNCOMING RADIO WAVES TRAVELING OBLIQUELY TO THE EARTH'S MAGNETIC FIELD*

By

W. G. Baker and A. L. Green
(Radio Research Board, Sydney, Australia)

Summary—*The paper is a theoretical discussion of the limiting polarization of downcoming electromagnetic waves propagated at oblique angles to the earth's magnetic field. The main conclusions arrived at are:*

(a). The polarization of the downcoming wave tends to a definite limit on leaving the Kennelly-Heaviside layer. The limiting polarization has been shown to be very nearly independent, for conditions that are likely to hold in practice, of the presence of large numbers of heavy negative ions in addition to the electrons, and of the occurrence of collisions between electrons and gas molecules.

(b). The shape of the ellipse of polarization is determined by the frequency of the wave relative to the critical frequency, and by the angle between the direction of propagation and the lines of force of the earth's magnetic field.

(c). The orientation of the ellipse is such that the principal axes are perpendicular to the direction of propagation, the major axis being in the plane containing the direction of the earth's magnetic field and the direction of propagation.

(d). The sense of rotation of the electric vector contained by the ellipse is left-handed when the direction of propagation of the "ordinary" downcoming ray makes an acute angle with the earth's field; the rotation is right-handed when the angle is obtuse. Either form of rotation can therefore occur even for the "ordinary" ray in either hemisphere, but, for moderate distances from the transmitter, in temperate and polar latitudes, and for waves of broadcast frequency, the polarization is left-handed in the Northern Hemisphere, and right-handed in the Southern. In the contrary case, the angle of incidence of the downcoming ray must be greater than the magnetic dip, which is usually large. The sense of rotation in the "extraordinary" ray is the reverse.

(e). By a simple transformation of the principal components of electric force, namely those along the axes of the ellipse, to components respectively in the vertical plane containing the sending and the receiving station, and parallel to the ground, it has been shown to be possible to predict the polarization of the downcoming rays (as measured at the ground), for any given distance and in any direction from the transmitter. As a practical example, maps have been drawn on which there are marked lines of equipolarization, the conditions being those for transmission from station 2BL, Sydney, New South Wales, frequency, 855 kilocycles. The contours show (1) the ratio of the abnormally to the normally polarized component of electric force, and (2) the phase difference between the components. The two maps, taken together, are sufficient to determine both the shape of the polarization ellipse, and the sense of rotation of the electric vector in the ellipse.

(f). It is pointed out that, in the Kennelly-Heaviside layer, the true direction of propagation is oblique to the wave front. Practically this suggests that a wave propa-

* Decimal classification: R113.6. Original manuscript received by the Institute, January 12, 1933.

gated obliquely to the earth's field, would be laterally deviated; the amount of deflection depends on the gradient of ionization in the layer.

(g). The relative attenuation factors of the "ordinary" and the "extraordinary" rays have been plotted for oblique propagation to the earth's field, assuming simple conditions. For angles, between the directions of propagation and of the earth's field, less than about 30 degrees, the "ordinary" downcoming ray is much the stronger. At about 60 degrees the attenuation factors are equal, and, at right angles to the field, the "extraordinary" ray suffers the less absorption.

I. Introduction

(1). Scope of the Paper

APPLETON and Ratcliffe[1] have found, experimentally, that the polarization of downcoming waves of broadcast frequency is predominantly circular, with a left-handed sense of rotation of the electric vector, when propagation is along the lines of force of the earth's magnetic field. In a recent investigation[2] by one of us, circular polarization has also been measured, but with a right-handed sense of rotation; the experimental conditions were for propagation parallel to but against the lines of force of the earth's field in the Southern Hemisphere.

No general tests of polarization have yet been made in either hemisphere for directions of propagation oblique to the earth's field, so that the object of the present paper is to predict the elliptical characteristics of downcoming radio waves as received at any given distance and in various directions from the transmitting station.

(2). Previous literature

Early work by Eccles and Larmor paved the way for the discussion of propagation in directions parallel to and perpendicular to the earth's magnetic field by Appleton, Nichols and Schelleng, Appleton and Barnett, Taylor and Hulburt, Breit and Tuve, and Pedersen.[3]

In his book, Pedersen discusses the matter in considerable detail. He assumes the electric force to be transverse to the direction of propa-

[1] E. V. Appleton and B. A. Ratcliffe, *Proc. Roy. Soc.* (London), sec. A, vol. 117, pp. 576–588; February 1, (1928).

[2] A. L. Green, to be published.

[3] W. H. Eccles, *Proc. Roy. Soc.* (London), sec. A, vol. 87, pp. 79–99; August 13, (1912). J. Larmor, *Phil. Mag.*, ser. 6, vol. 48, pp. 1025–1036; December, (1924). E. V. Appleton, *Proc. Phys. Soc.* (London), vol. 37, pp. 16D–22D; February 15, (1925). H. W. Nichols and J. C. Schelleng, *Bell Sys. Tech. Jour.*, vol. 4, pp. 215–234; April, (1925). E. V. Appleton and A. F. Barnett, *Proc. Cambridge Phil. Soc.*, vol. 22, pp. 672–675; July, (1925), *Electrician* (London), vol. 94, p. 398; April 3, (1925). A. H. Taylor and E. O. Hulburt, *Phys. Rev.*, ser. 2, vol. 27, pp. 189–215; February (1926). G. Breit and M. A. Tuve, *Phys. Rev.*, ser. 2, vol. 28, pp. 554–575; September, (1926). P. O. Pedersen, "Propagation of Radio Waves Along the Surface of the Earth and in the Atmosphere," Copenhagen, (1927).

gation. However, in the case of transmission at right angles to the earth's field (*loc. cit.* p. 107), there is an electron motion in the direction of propagation, this constituting a current; there is no displacement current to offset it. The current does not, therefore, lie in the wave front. As the current is the same at any point of the wave front, it follows that its "divergence" is not equal to zero, which it must be in order that Maxwell's equations may be satisfied. In this case it seems that Pedersen's results fail to hold.

Transmission oblique to the direction of the earth's field has been considered by Breit, Goldstein, Appleton, Hartree, and Burnett.[4]

No distinction has been made between the direction of a ray and the normal to the wave front, whereas these actually coincide only when the dielectric constant is a maximum or a minimum as regards a variation in direction. In particular, the ray and the normal to the wave front agree in the principal cases of transmission along and at right angles to the earth's field.

Goldstein derived an expression from which may be obtained the limiting polarization of the downcoming wave. He applied this to the special experimental conditions used by Appleton and Ratcliffe for the west-to-east, and the south-to-north directions of propagation in England, but did not further consider oblique transmission in general. It would appear to be difficult to modify Goldstein's analysis in order to allow for collisions and for the presence of heavy ions.

Appleton has extended his earlier work to include oblique propagation. In particular, he has used the modified formulas in an experimental investigation[5] of the maximum electronic density of ionization in the Heaviside layer.

Hartree has pointed out the importance of a term which allows for the discontinuous distribution of electronic charge in the Heaviside layer; earlier work had assumed a constant electric charge per unit volume, but the concentration of charge on discrete particles renders this assumption untenable, in the limit. However, we have been able to show that the limiting polarization of the "ordinary"[6] ray is not altered by the inclusion of the new factor.

Burnett was concerned chiefly with waves of very low frequency.

[4] G. Breit, Proc. I.R.E., vol. 15, pp. 709–723; August, (1927). S. Goldstein, *Proc. Roy. Soc.* (London), sec. A, vol. 121, pp. 260–285; November 1, (1928). E. V. Appleton, International Union of Scientific Radio Telegraphy. Papers, vol. 1, pt. 1, pp. 2–3, (1927). D. R. Hartree, *Proc. Cambridge Phil. Soc.*, vol. 25, pp. 97–120; January, (1929); vol. 27, pp. 143–162; January, (1931). D. Burnett, *Proc. Cambridge Phil. Soc.*, vol. 27, pp. 578–587; October, (1931).

[5] E. V. Appleton, *Nature*, vol. 127, p. 197; February 7, (1931).

[6] Waves longer than about 180 meters, on entering the Heaviside layer, are resolved into two components. The ray, for which the refractive index at first decreases from unity, we have called "ordinary," and the other "extraordinary."

(3). Definitions

In Fig. 1, a downcoming wave is incident at the ground at an angle i. It is assumed that the electric force in the sky wave is, in general, elliptically polarized and that the components of this rotating force are E_1, the normally polarized component which is in the vertical plane containing the sender and the receiver, and E_1', the abnormally polarized component, being at right angles to E_1 and to the direction of propagation. The angular phase difference between the components is denoted[7] by ξ.

Dissociating the downcoming wave, for the moment, from its orientation with the ground and looking at Fig. 2, it is seen that OP

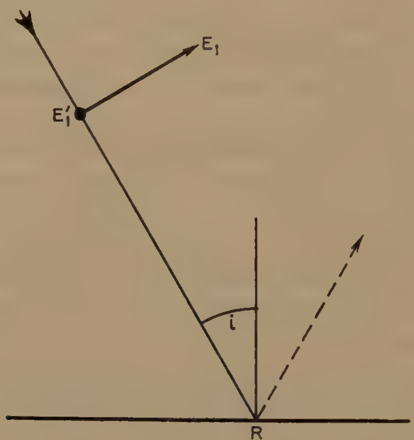

Fig. 1

and OQ are the normal and the abnormal components of value $E_1 \cdot \sin pt$ and $E_1' \cdot \sin (pt+\xi)$, respectively, where p is the angular frequency of the wave. In this figure, the direction of propagation is through the paper and away from the reader, and the sense of the system of axes is such that OQ points to the right for an observer looking from the sending to the receiving station.

Combination of the two component alternating forces then gives the rotating electric vector OE, whose instantaneous value depends on the shape of the ellipse of polarization, and on the position of the vector in the ellipse at any given moment. The definition of the sense of rotation of OE is then as follows: Looking from the sending to the receiving stations, and for increasing values of the time t, the sense of rotation is

[7] The nomenclature is mainly that of Appleton and Ratcliffe.

left-handed if ξ lies between 0 and 180 degrees, and right-handed when ξ is between 180 and 360 degrees.

For example, with the polarization circular and the sense of rotation right-handed, the component forces OP and OQ are equal but in quadrature, in time as well as in space, the normally polarized component OP leading the abnormally polarized component OQ, in time. The description of the polarization is then that the ratio of components

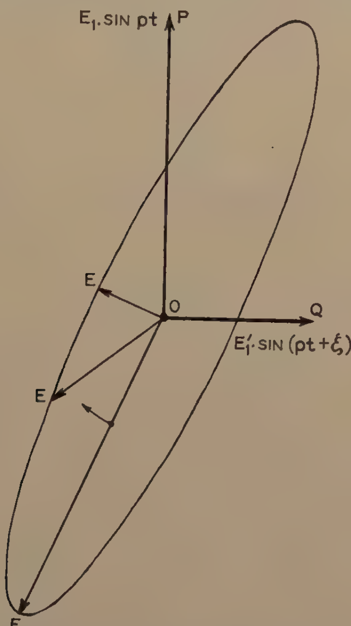

Fig. 2—The alternating electric forces OP and OQ are the components of the rotating vector OE, of periodically varying amplitude. The shape of the ellipse of polarization and the sense of rotation of OE are completely specified when the quantities E_1'/E_1 and ξ are known both in magnitude and sign.

E_1'/E_1, denoted by R_c, is unity, and that the phase difference between them, ξ, is 270 degrees.

II. Electron Motions in the Heaviside Layer

It will be necessary briefly to review the application of classical theory to the problem.

In Fig. 3, let OX, OY, and OZ denote three axes at right angles, of which OZ lies along the positive direction of the earth's magnetic field, of which the vertical component in the Southern Hemisphere is directed upwards. OX lies in the plane which contains the direction of propagation and the direction of the earth's field; let OX make an acute angle

with the former direction. The sense[8] of the axes is such that OX is to the right of OZ when looking in the direction OY.

Let E_x, E_y, and E_z denote the components of electric force, there being similar components of magnetic force H, and electric displacement D. The electric quantities are measured in electrostatic units,

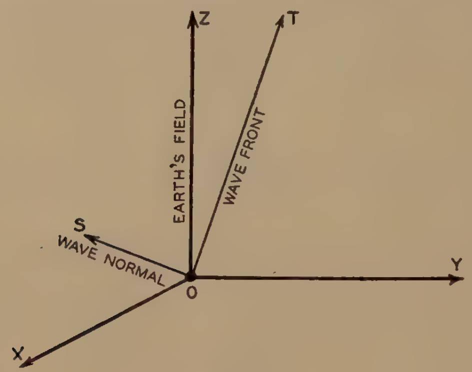

Fig. 3

and the magnetic in electromagnetic units. Then Maxwell's equations state,

$$\text{curl } H = \frac{1}{c} \cdot \frac{\partial D}{\partial t}, \text{ and curl } E = -\frac{1}{c} \cdot \frac{\partial H}{\partial t} \tag{1}$$

where c is the velocity of light in vacuo. We also have that,

$$\text{div } H = 0, \text{ and div } D = 0, \tag{2}$$

but it is not necessary that div E should be zero.

In setting down the equations of motion of the ions in the Kennelly-Heaviside layer, the effect of the electrons alone will be considered at first, the treatment of the heavier ions being given later. For the present, also, we shall neglect the effects of collisions between electrons and gas molecules; discussion of this point will be found in the sequel. A further assumption, later to be modified, is that there are equal positive and negative charges in the ionized region, per unit volume.

Let $-e$ and m be the charge and mass of an electron, u, v, and w its three velocity components at time t, and $\mathcal{H}$ the total intensity of the earth's magnetic field. The equations of motion are then,

$$m \cdot \frac{du}{dt} = -e \cdot E_x - \frac{\mathcal{H}ev}{c} \tag{3}$$

[8] The symbolism of this paper follows that of Nichols and Schelleng; they, however, used a left-handed system of axes.

$$m \cdot \frac{dv}{dt} = -e \cdot E_y + \frac{\mathcal{H} eu}{c} \tag{4}$$

$$m \cdot \frac{dw}{dt} = -e \cdot E_z. \tag{5}$$

Since the velocity and field components all involve an exponential factor whose index is jpt, their time derivatives are obtained by multiplying by jp, where j has its usual operational significance; we can also put,

$$p_0 = \frac{\mathcal{H} e}{mc} \tag{6}$$

p_0 being the electronic critical angular frequency. We then have for the velocity components,

$$u = \frac{-e}{m} \cdot \frac{(jp \cdot E_x - p_0 \cdot E_y)}{(p_0^2 - p^2)}$$

$$v = \frac{-e}{m} \cdot \frac{(jp \cdot E_y + p_0 \cdot E_x)}{(p_0^2 - p^2)}$$

$$w = \frac{-e}{m} \cdot \frac{E_z}{jp} \cdot$$

The constants of integration are the initial velocities, distributed at random, and hence equal to zero on the average.

If there are N electrons per unit volume, the current per unit area will be $-Ne$ times the velocity. This is the current carried by the electrons, to which must be added the Maxwellian displacement current, equal to $1/4\pi \cdot dE/dt$.

To shorten the expressions, let us put

$$\epsilon_1 = 1 + \frac{4\pi \cdot Ne^2}{m(p_0^2 - p^2)} \tag{7}$$

$$\epsilon_2 = 1 - \frac{4\pi \cdot Ne^2}{mp^2} \tag{8}$$

$$\alpha = \frac{p_0}{p} \cdot \frac{4\pi \cdot Ne^2}{m(p_0^2 - p^2)} \tag{9}$$

and the current components are given by,

$$4\pi \cdot C_x = \epsilon_1 \cdot \frac{dE_x}{dt} + j\alpha \cdot \frac{dE_y}{dt}$$

$$4\pi \cdot C_y = \epsilon_1 \cdot \frac{dE_y}{dt} - j\alpha \cdot \frac{dE_x}{dt}$$

$$4\pi \cdot C_z = \epsilon_2 \cdot \frac{dE_z}{dt}$$

so that the components of electric displacement are,

$$D_x = \epsilon_1 \cdot E_x + j\alpha \cdot E_y \tag{10}$$

$$D_y = \epsilon_1 \cdot E_y - j\alpha \cdot E_x \tag{11}$$

$$D_z = \epsilon_2 \cdot E_z. \tag{12}$$

From the last three equations, it is apparent that the displacement does not agree with the electric force in direction, except in certain special cases. Hence, there will be an effective dielectric constant for each direction[9] of propagation of the wave.

Let us now choose OX in the plane containing the directions of propagation, and of the earth's field; then the normal to the wave front makes angles with the axes whose cosines are respectively l, zero, and n. Let cV be the phase velocity, and cU its component normal to the wave front; then the phase of the wave at the point (x, y, z) at time t, is

$$\phi = \phi_0 + p\left\{t - \frac{(lx + nz)}{cU}\right\}$$

so that differentiation of a vector with respect to t, x, y, or z is the same as multiplication by a constant quantity times unity, $-l/cU$, zero, or $-n/cU$, respectively.[10]

[9] It is interesting to notice, qualitatively, two aspects of the phenomenon of there being a difference between the directions of phase propagation and of the normal to the wave front. In the first place, it appears that a ray incident vertically at the Kennely-Heaviside layer would keep its wave front horizontal, but would be bent over and come down again vertically at a different place, which, for the ordinary ray, would be at a point closer to the magnetic pole. Second, for propagation not in the magnetic meridian, there will be a deflection of the ray in the plane containing the earth's field and the direction of ray propagation. For example, for east-to-west transmission in the Southern Hemisphere, the ordinary downcoming ray will appear to come from a direction somewhat north of the true bearing of the transmitter. The amount of lateral deviation depends on the gradient of ionization in the layer, being zero for the case of sharp reflection.

Dr. D. F. Martyn has concluded from observations of natural fading in Victoria that there is present a considerable degree of lateral deviation of downcoming waves, and he has suggested that this deviation may be produced, in part, by the influence of the earth's magnetic field.

[10] We are indebted to M. René Mesny for helpful criticism as to the method of performing this differentiation, and consequently as to the form of equations (13) to (19).

On expanding Maxwell's equations (1), we have

$$nH_y/U = \epsilon_1 \cdot E_x + j\alpha \cdot E_y \tag{13}$$

$$(lH_z - nH_x)/U = \epsilon_1 \cdot E_y - j\alpha \cdot E_x \tag{14}$$

$$lH_y/U = -\epsilon_2 \cdot E_z \tag{15}$$

$$nE_y/U = -H_x \tag{16}$$

$$(lE_z - nE_x)/U = -H_y \tag{17}$$

$$lE_y/U = H_z. \tag{18}$$

On the elimination of E_x, E_y, E_z, H_x, H_y, and H_z from these six equations, an expression for U is left, namely

$$U^4\{\epsilon_2(\epsilon_1^2 - \alpha^2)\} - U^2\{l^2(\epsilon_1^2 - \alpha^2) + (1 + n^2)\epsilon_1\epsilon_2\} + \{n^2\epsilon_2 + l^2\epsilon_1\} = 0, \tag{19}$$

the solution of which is,

$$1 - \frac{1}{U^2} = \frac{(1 - \epsilon_1)\{p^2\epsilon_2 - \frac{1}{2}l^2p_0^2 \pm \sqrt{\frac{1}{4}l^4p_0^4 + n^2\epsilon_2^2p_0^2p^2}\}}{\{\epsilon_1p^2 + n^2p_0^2(1 - \epsilon_1)\}}, \tag{20}$$

agreeing with Goldstein and Hartree.

Having chosen the value of U, the ratios of the electric and magnetic components may be obtained by the elimination of five of them from any five of the above equations. On putting, $A = U\epsilon_1$, $B = U\epsilon_2$, and $C = U\alpha$, we have

$$KE_x = -nB(AU - 1) \tag{21}$$

$$KE_y = -jnBCU \tag{22}$$

$$KE_z = lU(A^2 - C^2) - lA \tag{23}$$

$$KH_x = jn^2 \cdot BC \tag{24}$$

$$KH_y = -BU(A^2 - C^2) + BA \tag{25}$$

$$KH_z = -jlnBC \tag{26}$$

in which K is the same for all the components, but otherwise arbitrary. The components of electric displacement and magnetic force normal to the wave front are now zero, as required by (2).

In order to describe the polarization more simply, we may take the components of displacement and magnetic force in and perpendicular to the plane containing the earth's field and the normal to the wave front. We shall call the components in the above plane D_t and H_t, and their values may be obtained from (21) to (26). It should be noted that D_y, D_t, H_y, and H_t all lie in the wave front. It follows that,

$$\frac{D_y}{D_t} = -\frac{H_t}{H_y} = \frac{-j\alpha \cdot n}{\{(\epsilon_1^2 - \alpha^2) \cdot U^2 - \epsilon_1\}}. \tag{27}$$

III. Polarization of the Downcoming Rays

As the wave comes down through regions of decreasing ionization, the direction of propagation comes into coincidence with the normal to the wave front, in the limit when the ionization density tends to zero. The limiting polarization may therefore be found by fixing the direction of the wave normal, and taking the limit of the polarization as the ionization density tends to zero. In this case all the expressions (21) to (26) for the field components vanish, so that it is necessary to find their ratios.

It is convenient, at this stage, to change the directions of the axes of Fig. 3. Choose OS, OT, and OY, such that OY is unchanged, and OS and OT lie in the plane ZOX. Then OS is along the wave normal, OT is at right angles to OS and makes an acute angle with OZ, the direction of the earth's field. We then have,

$$E_s = lE_x + nE_z, \text{ and } E_t = lE_z - nE_x,$$

with similar expressions for the magnetic components. The values of the latter in (16) to (18) may be substituted in (13) to (15), giving

$$n^2E_x - lnE_z = U^2\cdot(\epsilon_1 E_x + j\alpha\cdot E_y) \tag{28}$$

$$E_y = U^2\cdot(\epsilon_1 E_y - j\alpha\cdot E_x) \tag{29}$$

$$l^2E_z - lnE_x = U^2\epsilon_2 E_z. \tag{30}$$

Any two of these three equations are sufficient; they are compatible for the correct value of U. From (29) and (30), we have

$$\frac{E_y}{E_t} = -\frac{j\alpha}{n\epsilon_2}\cdot\frac{(l^2 - U^2\epsilon_2)}{(1 - U^2\epsilon_1)} \tag{31}$$

and, for the component along the wave normal,

$$\frac{E_s}{E_t} = \frac{l(1 - U^2\epsilon_2)}{nU\epsilon_2}. \tag{32}$$

As the ionization tends to zero, both U and ϵ_2 tend to unity, so that the ratio in (32) tends to zero. The wave thus has its electric force transverse, as it ought to have, since the component along the wave normal vanishes. From (31) it is seen that E_y and E_t are in quadrature, so that it follows from (31) and (32) together, that the major and minor axes of the ellipse of polarization are along the directions OT and OY.

The final states of polarization of the rays are then determined completely by the limit of (31) as N tends to zero, if such a limit exists. Let us put

$$-E_y/j\cdot E_t = R_a, \tag{33}$$

where R_a may be known as the ratio of axes of the ellipse of polarization in the downcoming ray. We then may obtain the value of U^2 from (31) and put it into (19). This eliminates U, and gives the relation between R_a, the direction cosines l and n, and the principal dielectric constants ϵ_1, ϵ_2, and α.

From (7), (8), and (9), using the abbreviations

$$g = 4\pi \cdot Ne^2/m \cdot (p_0^2 - p^2) \tag{34}$$

$$q = p_0/p \tag{35}$$

it follows that,

$$\epsilon_1 = 1 + g \tag{36}$$

$$\epsilon_2 = 1 + g(1 - q^2) \tag{37}$$

$$\alpha = gq. \tag{38}$$

Let us take the limit of the polarization as g tends to zero. The terms of the first degree yield nothing, but the terms containing g^2 give,

$$R_a^2 + \frac{l^2}{n} \cdot q \cdot R_a - 1 = 0 \tag{39}$$

which, therefore, shows first that the limiting polarizations[11] of the downcoming rays are determined by the angle between the direction of propagation and that of the earth's field, and second by the frequency of the wave relative to the critical frequency. From this equation we may calculate the ratio of axes of the ellipses of polarization for both the ordinary and the extraordinary rays. The ray with U greater than unity may be termed the ordinary ray and that with U less than unity the extraordinary ray.

Solutions of (39), for directions of propagation oblique to the earth's field are readily had with the help of a table of $\sin\theta \cdot \tan\theta$, since this is

[11] An alternative method of obtaining the limiting polarization is to deal directly with the electric displacement. From (27) we have

$$R_D = -D_y/j \cdot D_t = \alpha \cdot n/\{(\epsilon_1^2 - \alpha^2)U^2 - \epsilon_1\}.$$

After eliminating U^2 with the help of (19), we have

$$R_D^2 + \frac{l^2}{n} \cdot \frac{(\epsilon_1^2 - \alpha^2 - \epsilon_1\epsilon_2)}{\alpha \cdot \epsilon_2} \cdot R_D - 1 = 0,$$

which, in the absence of heavy ions in the layer, reduces to

$$R_D^2 + \frac{l^2}{n} \cdot \frac{q \cdot R_D}{\epsilon_2} - 1 = 0.$$

Now, as the density of ionization tends to zero, ϵ_2 tends to unity, and further

$$jR_D = \frac{(j\alpha \cdot E_x + \epsilon_1 E_y)}{\{n(\epsilon_1 E_x - j\alpha \cdot E_y) - l\epsilon_2 E_z\}} \rightarrow \frac{E_y}{nE_x - lE_z} = jR_a,$$

since α tends to zero, and ϵ_1 to unity. Hence the limiting polarization is again given by (39) above.

the same as l^2/n, if θ is the angle between the direction of propagation and the earth's field, and is also equal to $(\sec\theta - \cos\theta)$. Having selected θ to correspond to the direction of transmission required, the value of $\sin\theta \cdot \tan\theta$ obtained from the table is multiplied by q. Thus the sum of the roots of (39) is known. The table is then read inversely for the angle ψ corresponding to $\sin\psi \cdot \tan\psi = q \cdot \sin\theta \cdot \tan\theta$. The two possible roots of (39) are then given by the cosine and the negative secant of the new angle ψ, since we have that the product of the roots is -1.

These two roots are for the ordinary and the extraordinary rays, and it is necessary to distinguish between them, this being done in the following way: The values of U^2 may be found in terms of q, g, l, and n, from (31). As the density of ionization tends to zero, we have

$$\underset{g\to 0}{Lt}\ \frac{1 - U^2}{g} = 1 - \frac{qn}{R_a}\cdot \tag{40}$$

For the value of R_a numerically less than unity, R_a and n are of the same sign. In the case when p is less than p_0, then n is greater than R_a, so that the right-hand side of (40) is negative, and therefore U^2 tends to unity from above. The value of R_a numerically less than unity therefore corresponds to the ordinary downcoming ray. For the other value of R_a, n, and R_a are of opposite sign, so that the right-hand side of (40) is positive, and U^2 tends to unity from below, thus corresponding to the extraordinary ray. Hence, in distinguishing between the two possible roots of (39), the cosine root is applicable to the ordinary ray.

It is now possible to specify more definitely the orientation of the ellipse of polarization. For the ordinary downcoming ray, the axes of the ellipse are perpendicular to the direction of propagation, and the major axis is in the plane containing the earth's field and the direction of propagation; the minor axis is perpendicular to that plane.

The values obtained for R_a show that the resultant force in the downcoming ray is, in general, elliptically polarized. When R_a is positive, the rotation is like a left-handed screw when looking along the ray path from the transmitter to the receiver; with R_a negative, the sense of rotation is right-handed.

The ordinary downcoming ray will have a left-handed sense of rotation of the resultant electric force when the direction of propagation makes an acute angle with the lines of force of the earth's magnetic field; the rotation will be right-handed when the angle is obtuse. Either form of rotation can occur, even for the ordinary ray, in either hemisphere, but for moderate distances from the transmitter, in temperate and polar latitudes, and for waves of broadcast frequency, the

polarization will be left-handed in the Northern Hemisphere, and right-handed in the Southern. In the contrary case, the angle of incidence of the downcoming ray must be greater than the magnetic dip, which is usually large.

IV. Polarization of the Downcoming Rays as Measured at the Ground

In the previous section, the orientation of the ellipse of polarization was specified with respect to the plane containing the directions of propagation and of the earth's field. However, the experimental methods of measuring ellipticity in downcoming waves make use of receiving

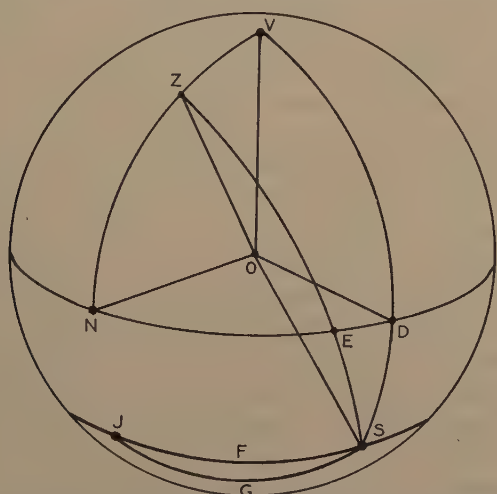

Fig. 4—Spherical triangles used in the transfer of the principal components of electric force, namely those along the major and minor axes of the ellipse of polarization, to components of electric force respectively in the vertical plane containing the sending and the receiving stations, and parallel to the ground.

aerials placed in planes either parallel or perpendicular to the earth's surface. It will therefore be necessary to transform the principal components of electric force, which were along the axes of the ellipse, to components respectively in and perpendicular to the plane containing the direction of propagation and the normal to the earth's surface, for which we will need to consider the spherical triangles of Fig. 4. It will be remembered that the principal components were in quadrature, in time as well as in space; the new components will not necessarily be quadrate in time.

O is the center of the sphere, OV the vertical line, OZ the earth's field, OS the direction of propagation, NED the horizontal plane

through O, JFS a horizontal small circle through S, and JGS the great circle through S perpendicular to the great circle ZES. The great circle distances through VZ and VS, respectively, cut the plane NED in N and D. Then ON is magnetic north, the angle ZON is the magnetic dip, the angle NOD measured clockwise around the circle DEN is the magnetic bearing of the receiver from the transmitter, and VOS is the supplement of the angle of incidence of the wave. ZOS is the angle between the direction of the earth's field and the direction of propagation.

The principal components of electric force in the sky wave are tangents at the point S, one to the arc SZ and the other to the arc SGJ. The component forces as measured at the ground are tangents at the point S to the arcs SDV and SFJ. These latter are known as the normally and the abnormally polarized components of electric force in the downcoming wave, and are denoted by E_1 and E_1' respectively. The angular phase difference between them is ξ, and the ratio of components, E_1'/E_1, is denoted by R_c.

For a given point of reception, we know VZ, VS, and the angle ZVS, so that the triangle ZVS can be solved. The side SZ determines R_a, and the angle ZSV is that through which the tilted axes have to be turned into the new directions.

In order to make the procedure clearer, the detailed calculations are given for a point 110 kilometers west, magnetic, of station 2BL, Sydney, New South Wales. The height of the Kennelly-Heaviside layer is assumed to be 110 kilometers, this being a figure known to be close to the average height as measured by one of us during a period of about six months in 1930, using 2BL as the source of the frequency-change transmissions. The frequency of 2BL is 855 kilocycles, so that p is equal to 5.35 megaradians per second. The horizontal and vertical components of the earth's magnetic field are approximately 0.268 and 0.515 for Sydney. The dip is 62.5 degrees south, and the total value of the field is 0.581. The value of e/m being taken as 1.77×10^7 e.m.u./gm., p_0 is 1.026×10^7, corresponding to a critical wavelength of about 183 meters for Sydney conditions. Now p_0 is very nearly double p, so that, since the magnetic field is liable to small variations with time and with the position of the receiving station, it will be sufficient to assume $p_0 = 2p = 10^7$, and consequently $q = 2$.

In the triangle VZS, we have that $z = 153°26'$, $s = 27°20'$, and $V = 90°$, so that $v = 142°30'$ and $S = 49°20'$. From the table of $\sin\theta \cdot \tan\theta$, we have that $\sin v \cdot \tan v = -0.4672$, and the angle ψ which corresponds to q times this value is $129°36'$. Now $\cos\psi$ is -0.6365, and this is R_a.

In the transfer to the directions OV, OD, and their common per-

pendicular ON, certain auxiliary formulas are useful. A quantity ρ is required, defined by the relation

$$(1 + \rho) \cdot R_c^2 = (1 - \rho).$$

The values of ρ and ξ, are then determined from the relations,

$$\cot \xi = \sin v \cdot \tan v \cdot \sin 2S$$

where $\sin \xi$ has the sign of R_a, and

$$\rho = \frac{(1 - \cos 2\psi)}{(3 + \cos 2\psi)} \cdot \cos 2S$$

these two expressions being easily established.

In the numerical case under discussion, ξ works out to be 294°48′, and R_c to 1.061. Thus, for transmission from east to west, the polarization is elliptical and, for the distance quoted, the ratio of component electric forces at the ground is nearly unity: the normally polarized component leads the abnormally polarized by an angular phase difference of 65°12′, indicating right-handed rotation of the resultant electric vector.

Since it happens that the abnormally polarized component is always associated with $\cos i$ in measurements of the polarization at the ground, it is better to express the results in terms of $(E_1' \cdot \cos i)/E_1$ rather than in terms of E_1'/E_1, so that, in preparing values of the ratio of components at the ground, we have calculated $R_c \cdot \cos i$ instead of R_c; here, i is the angle of incidence of the downcoming wave at the ground.

The polarization of signals from the broadcast station 2BL has been calculated by the methods outlined above. Two maps are reproduced in Figs. 5 and 6, these showing in the form of contours, the phase difference ξ, and second, the quantity $R_c \cdot \cos i$.

In reading Fig. 5, it should be remembered that values of the phase difference ranging from 180 to 360 degrees indicate a right-handed sense of rotation. No values less than 210 degrees occur on the map, so that, in the region covered, there is no instance of left-handed polarization. It will also be noticed that the phase difference alters very slowly from 270 degrees for receivers placed to the south of the transmitter. For the same area, see Fig. 6, the ratio of components is never far from unity, so that the polarization would be circular and right-handed for a large number of locations of the receiver approximately south of the transmitting station.

North of the transmitter, the phase difference varies rapidly for receiving stations a little way off the magnetic meridian. Going in a

northerly direction, the ratio of components decreases markedly, so that the polarization of downcoming waves as received in an area north of the transmitter would be elliptical. An interesting point, which might have a practical application, is that the intensity of the abnormally polarized component is very small at distances of about 300 kilometers from the transmitter in a northerly direction; this follows from the low

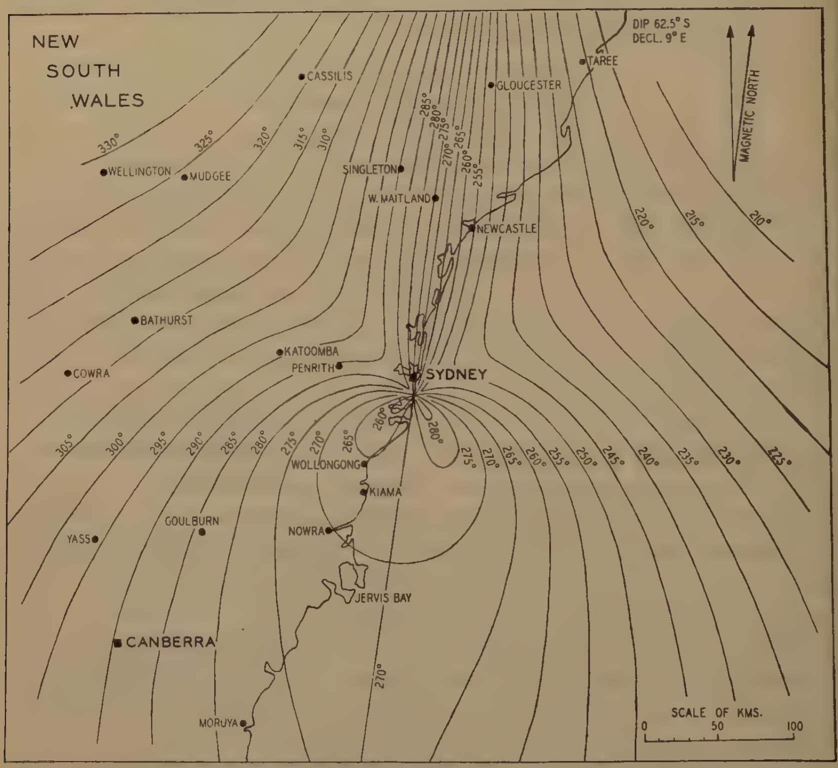

Fig. 5—Map showing the variation of the angular phase difference ξ, between the normally and the abnormally polarized components of electric force in the ordinary downcoming ray, as measured at the ground. Angles between 180 and 360 degrees indicate a right-handed sense of rotation of the equivalent electric vector in the ray. The phase difference for the extraordinary ray differs from that for the ordinary ray by 180 degrees.

values of the ratio of components found north of the transmitter, of the order 1/10 for the distance just quoted.

The meaning of this is that one would expect errors in radio direction finding to be small at night for this particular orientation of sender and receiver. There is, however, the possibility of the presence of the extraordinary ray, especially at this distance and in this direction, and,

in that case the resultant polarization should occasionally still be plane, but it would be capable of assuming almost any state of ellipticity as the two downcoming rays moved in and out of phase.

A number of assumptions have been made in constructing the maps of Figs. 5 and 6. In the first place they are for the ordinary downcoming ray alone. Second, they are drawn for conditions in the Southern Hem-

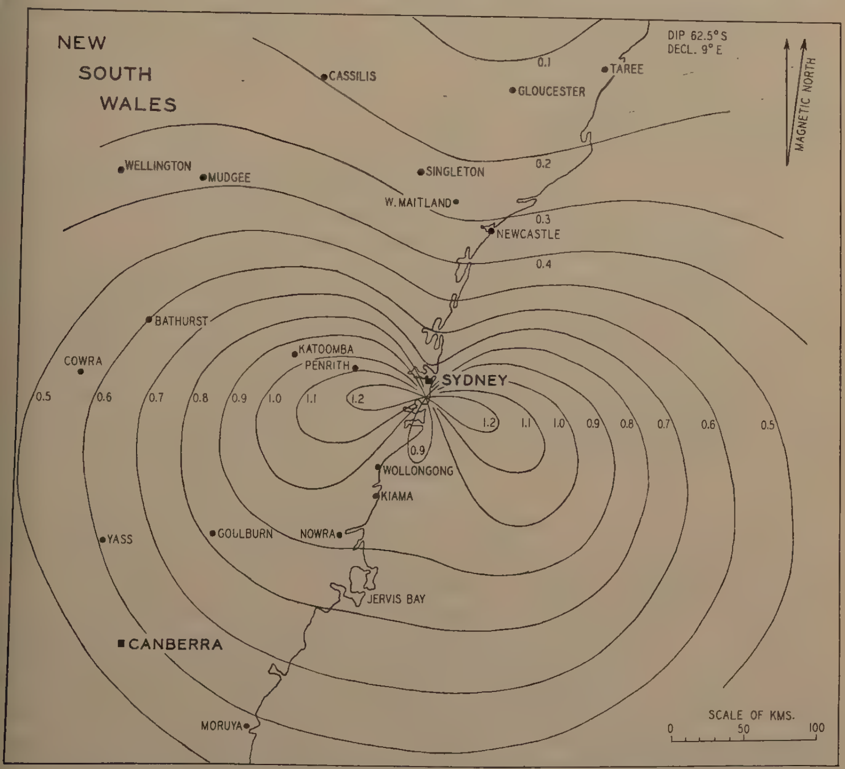

Fig. 6—Map showing the variation of the ratio of the abnormally to the normally polarized component of electric force in the ordinary downcoming ray, as measured at the ground. For practical convenience, this ratio has been multiplied by cos i, where i is the angle of incidence of the downcoming wave at the ground. The ratio of components for the extraordinary ray is the reciprocal of that for the ordinary ray.

isphere where the value of the critical wavelength is about 180 meters instead of the 214 meters correct for England, where the total intensity of the earth's magnetic field is less. Again, the frequency of transmission is 855 kilocycles, and the lines of equipolarization would be differently placed for other frequencies; other maps can, however, be drawn after reading the appropriate conditions into the mathematical analysis detailed above.

The other assumptions are:

(1). The height of the Kennelly-Heaviside layer has been taken to be 110 kilometers.

(2). The value of the critical angular frequency p_0 has been assumed to be exactly twice p.

(3). No account has been taken of the earth's curvature, and in particular, no allowance has been made for the difference in magnetic bearing of a line at its two ends.

(4). No account has been taken of variation in magnetic intensity or dip at different points of the map.

(5). The lower boundary of the ionized layer has been assumed to be horizontal, and the height of the layer, that reached by a wave traveling along an ideal triangular path such as would correspond with the angle of incidence at the ground.

(6). No correction has been made for imperfect reflection at the ground. Such errors as will be made here are likely to be small, and will principally affect the phase difference between the components.

(7). No allowance has yet been made for the effects of collisions between electrons and gas molecules.

(8). No allowance has yet been made for the presence of massive ions in the ionized region, in addition to the electrons.

Most of the errors due to inaccuracies in these assumptions are likely to be small, so that the maps should represent the distribution of polarization of the ordinary downcoming ray fairly closely.

The polarization of the extraordinary ray, if it should happen to come down in appreciable intensity, is easily determined from that of the ordinary ray. The phase difference is changed by 180 degrees, which reverses the sense of rotation. The ratio of components is the reciprocal of that for the ordinary ray, so that, in preparing a map for the extraordinary ray, one would have that $R_c' \cdot \cos i = (\cos^2 i)/R_c \cdot \cos i$, where R_c' is for the extraordinary ray.

If both ordinary and extraordinary rays are returned to the earth with comparable intensity, the effect would be that the resultant phase difference would be variable, except in the principal case of quadrature, and there would be a fluctuation in the measured ratio of components as the two waves moved in and out of phase due to changes in the lengths of their paths.

In the next section, the effects of collisions between electrons and gas molecules are considered. In that part of it dealing with the relative absorptions of the ordinary and extraordinary rays, it will be found that theoretical evidence is against the return to the earth of

the extraordinary ray when the direction of propagation makes an angle with the earth's field less than about 30 degrees; for very oblique transmission, however, the extraordinary ray may even be the stronger of the two downcoming rays.

V. Electronic Collisions

In the preceding pages it has been assumed that the electrons are free to move in accordance with the applied electromagnetic field. However, each electron will make a large number of collisions with other particles in the layer, and, according to Pedersen[3] the estimated number of collisions per second is 10^5 at a height of 100 kilometers above the earth's surface, changing tenfold for a change in height of 20 kilometers, and decreasing on ascending.

On the average, there will be very little relation[12] between the velocity of an electron before and after a collision. As far as the wave is concerned, a collision destroys the motion built up, and collisions occurring at a certain average rate mean a corrseponding rate of decrease of current.

Using the same notation as before, the equations of motion of the electrons are still those given by (3), (4), and (5). If there are N electrons per cubic centimeter, the current per square centimeter will be increasing at a rate given by

$$\frac{dC_x'}{dt} = \frac{Ne^2}{m} \cdot \left\{ E_x + \frac{v\mathcal{H}}{c} \right\}$$

$$\frac{dC_y'}{dt} = \frac{Ne^2}{m} \cdot \left\{ E_y - \frac{u\mathcal{H}}{c} \right\}$$

$$\frac{dC_z'}{dt} = \frac{Ne^2}{m} \cdot E_z,$$

in the absence of collisions.

If there are ν collisions per electron per second, each of these electrons carrying a current $-eu$, $-ev$, and $-ew$, then this current is annulled at the rate of $N\nu$ times per second. The rate of decrease of current due to collisions alone is then given by

$$\frac{dC_x''}{dt} = - N\nu \cdot eu = - \nu \cdot C_x''$$

with similar expressions for the other components.

[3] *Loc. cit.*, p. 43.

[12] This assumption has been made by W. G. Baker and C. W. Rice, *Trans. A.I.E.E.*, vol. 45, pp. 302–332; February, (1926).

The net rate of increase of current will be obtained by subtracting the decrease due to collisions, and we then have

$$(jp + \nu)\cdot C_x + p_0\cdot C_y = \frac{Ne^2}{m}\cdot E_x$$

$$(jp + \nu)\cdot C_y - p_0\cdot C_x = \frac{Ne^2}{m}\cdot E_y$$

$$(jp + \nu)\cdot C_z = \frac{Ne^2}{m}\cdot E_z$$

from which the current components are easily obtained. To these must be added the Maxwellian displacement currents, and we then have for the components of displacement,

$$D_x = \epsilon_1\cdot E_x + j\alpha\cdot E_y$$

$$D_y = \epsilon_1\cdot E_y - j\alpha\cdot E_x$$

$$D_z = \epsilon_2\cdot E_z$$

which are of exactly the same form as (10), (11), and (12), except that ϵ_1, ϵ_2, and α now have different values, given by

$$\epsilon_1 = 1 + 4\pi\cdot\frac{Ne^2}{m}\cdot\frac{(jp + \nu)}{jp\{p_0^2 + (\nu + jp)^2\}} \tag{41}$$

$$\epsilon_2 = 1 + 4\pi\cdot\frac{Ne^2}{m}\cdot\frac{1}{jp(jp + \nu)} \tag{42}$$

$$\alpha = \frac{p_0}{p}\cdot 4\pi\cdot\frac{Ne^2}{m}\cdot\frac{1}{\{p_0^2 + (\nu + jp)^2\}}\cdot \tag{43}$$

These new values of ϵ_1, ϵ_2, and α are now available for the analysis following (10): they should be compared with (7), (8), and (9).

If now, corresponding with (34) and (35), we use

$$g' = 4\pi\cdot\frac{Ne^2}{m}\cdot\frac{(jp + \nu)}{jp\{p_0^2 + (\nu + jp)^2\}} \tag{44}$$

$$q' = p_0/(p - j\nu) \tag{45}$$

we have, similarly to (36), (37), and (38)

$$\epsilon_1 = 1 + g' \tag{46}$$

$$\epsilon_2 = 1 + g'(1 - q'^2) \tag{47}$$

$$\alpha = q'g' \tag{48}$$

where the new expressions may be referred to as the "collision" values of ϵ_1, ϵ_2, and α.

With these modifications, it will be unnecessary to repeat any more of the previous work; it will be sufficient to note a few results.

(1). Limiting Shape of the Polarization Ellipse

As the density of ionization tends to zero, g' vanishes, and, by analogy with (39), it must follow that the limiting polarization, when allowing for collisions, is

$$R_a{}^2 + \frac{l^2}{n} \cdot q' \cdot R_a - 1 = 0. \tag{49}$$

Because of the substitution of q' for q, the value of R_a is now complex, so that the axes of the ellipse must be rotated a little. Let us find the probable maximum shift of the axes, for which it will be permissible to assume the practical conditions, $p_0 = 2p = 20\nu$. Then the collision frequency is about 5.10^5, which should hold at a height of about 90 kilometers above the earth's surface. For these conditions

$$q' = 2/(1 - j/10).$$

To find the amount of change in R_a, due to the effects of collisions, we have from (49)

$$\frac{\Delta R_a}{\Delta q'} = - \frac{R_a \cdot l^2/n}{2R_a + q' \cdot l^2/n}$$

and it will be necessary to find for which direction of propagation the effect is greatest. Again from (49), we have

$$\frac{l^2}{n} = \frac{(1 - R_a{}^2)}{q' \cdot R_a}$$

so that,

$$\frac{\Delta R_a}{\Delta q'} = \frac{R_a(R_a{}^2 - 1)}{q' \cdot (R_a{}^2 + 1)}.$$

Differentiating logarithmically with respect to R_a, we find for the maximum value of $\Delta R_a/\Delta q'$,

$$\frac{1 - 4R_a{}^2 + R_a{}^4}{R_a(1 + R_a{}^2)} = 0.$$

The value of R_a less than unity which satisfies this equation is, for the ordinary ray,

$$R_a = 2 - \sqrt{3} = 0.268$$

for which value of R_a it follows that $l^2/n=\sqrt{3}$, and the direction of transmission for which the shift of the axes is greatest, makes an angle of about 63 degrees with the direction of the earth's magnetic field.

We can now use in (49), this value of l^2/n and that already assigned to q', and hence determine the new value of R_a: it is

$$R_a = 0.263 + 0.157j$$

showing that the ellipse of polarization no longer has its principal axes in the same direction as when collisions were assumed to be negligible. Let us rotate the axes through an angle ϕ, and find the components a and b, along the new directions; they are

$$a = \cos\phi - 0.263j\cdot\sin\phi + 0.157\sin\phi$$

$$b = \sin\phi + 0.263j\cdot\cos\phi - 0.157\cos\phi.$$

For these to be the new principal axes, the ratio of a to b must be purely imaginary, which occurs when

$$\tan^2\phi + 5.77\tan\phi - 1 = 0$$

from which ϕ is approximately 10 degrees.

It is then easy to show that the ratio of the new axes is 0.256, whereas when neglecting collisions it was 0.268, while the ellipse has been rotated nearly through 10 degrees. These are likely to be maximum errors, since the collision frequency has been assumed to have a value slightly greater than that which we expect to hold in practice.

It follows that the limiting shape and orientation of the polarization ellipse are given with sufficient accuracy by the analysis which neglects collisions.

(2). Attenuation Factors of the Ordinary and Extraordinary Rays

Equation (19) is of the same form as before, except that U is now complex; suppose its value is the reciprocal of $(\mu-j\zeta)$, then μ will be the refractive index, and ζ the logarithmic attenuation factor of the wave traveling a distance equal to c/p.

The solution of (19) is still that given in (20), except that there must be substituted the collision values of ϵ_1, ϵ_2, and α; also q must be replaced by q'. We then have that

$$\frac{1}{U^2} = (\mu - j\zeta)^2 = 1 + \frac{(1-\epsilon_1)\left\{\epsilon_2 - \frac{1}{2}l^2q'^2 \pm \sqrt{\frac{1}{4}l^4q'^4 + n^2\epsilon_2{}^2q'^2}\right\}}{\left\{\epsilon_1 + n^2q'^2(1-\epsilon_1)\right\}}.$$

A simple solution of this general case may be had for the condition $p_0=2p$, when both the ionization density and the frequency of col-

lision are low. The result is,

$$(\mu - j\zeta)^2 = 1 + \frac{k}{9p^2}\cdot\left[3p\left\{1 - 2l^2 \pm 2\sqrt{l^4 + n^4}\right\}\right.$$

$$\left. - j\nu\cdot\left\{(5 + 2l^2) \pm \frac{2(l^4 - 2n^2)}{\sqrt{l^4 + n^2}}\right\}\right]$$

$$= R + jI, \text{ say, where } k = 4\pi\cdot Ne^2/mp.$$

Then,

$$\mu - j\zeta = \sqrt{R} + \frac{jI}{2\sqrt{R}}$$

and hence,

$$\zeta = -I/2\mu$$

whence,

$$\zeta = \frac{2\pi\cdot Ne^2\nu}{9\mu\cdot mp^3}\cdot\left\{(5 + 2l^2) \pm \frac{2(l^4 - 2n^2)}{\sqrt{l^4 + n^2}}\right\}$$

and the logarithmic attenuation factor per unit distance is $\zeta . p/c$.

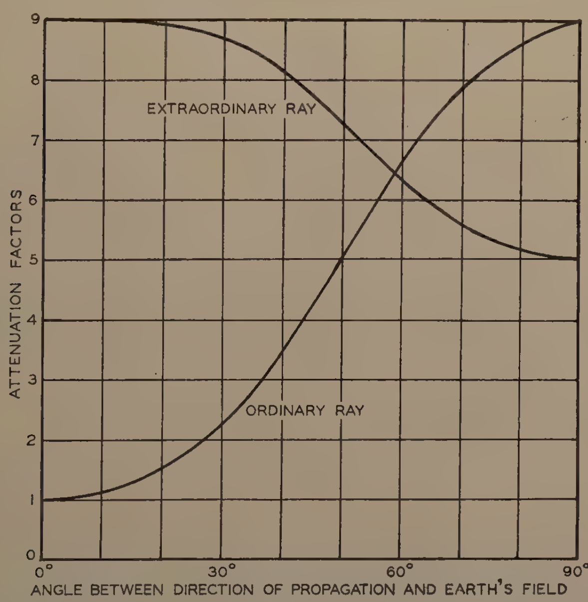

Fig. 7—Relative logarithmic attenuation factors per unit distance, of the ordinary and extraordinary rays. The transmission frequency is one half of the electronic critical frequency, and both the collision frequency and the density of ionization have been assumed small. The abscissas are the angles between the directions of the earth's field and of propagation, and the ordinates can be converted into absolute units on multiplying by the factor

$$2\pi\cdot Ne^2\nu/9\mu\cdot mc\cdot p^2.$$

We have drawn, in Fig. 7, curves showing the relative attenuations of the two rays, ordinary and extraordinary. The abscissas are for the angle θ between the direction of propagation and the earth's field; $\sin\ \theta=1$, and $\cos\ \theta=n$. The ordinates should be multiplied by $2\pi\cdot Ne^2\nu\cdot/9\mu\cdot mcp^2$ to obtain the logarithmic attenuation factors per unit distance, it being understood that both the density of ionization and the frequency of collision have been assumed to be low. The frequency of the wave is one half of the critical frequency.

For propagation at small angles to the earth's field, the ordinary ray is favored; for example, at 30 degrees the ratio of attenuation factors is about 4/1. Approximately for an angle of 60 degrees, the two rays are equally attenuated, and, for transmission perpendicular to the field, the attenuation factor for the extraordinary ray is less than that for the ordinary, in the ratio 5/9. Hence for propagation at very oblique angles to the earth's magnetic field, one would expect the extraordinary and the ordinary rays to be returned to the earth in comparable intensity.

VI. Heavy Ions

Chapman[13] has pointed out that, chiefly owing to the known electron affinity of oxygen atoms, there must be a large excess of negative ions over electrons in the Kennelly-Heaviside layer. Lunar daily magnetic variations, if caused by the tidal circulation of Foucault currents, require an ion density of the order 10^8 per cubic centimeter. On the other hand, Appleton's measurements[14] of maximum electronic density are of the order 3.10^4, for the greater part of a midwinter night.

Since the large numbers of negative oxygen atoms, and molecules, may cause an appreciable reduction in the dielectric constant it will be important to know whether the limiting polarization of the downcoming wave is affected.

Let there be N' heavy negative ions each of mass M. Then the ionic critical angular frequency is, by analogy with (10),

$$P_0 = \frac{\mathcal{H}\cdot e}{Mc} \tag{50}$$

which has a value of approximately 300 for the same conditions that make p_0, the electronic critical angular frequency, about 10^7.

Modifications to the equations of motion, (3), (4), and (5) need not be given; it will be sufficient to quote the new expressions for ϵ_1, ϵ_2, and α, as a comparison with (7), (8), and (9); they are

[13] S. Chapman, *Proc. Roy. Soc.* (London), sec. A, vol. 132, pp. 353–374; August 1, (1931).

[14] E. V. Appleton, *Nature*, vol. 127, p. 197; February 7, (1931).

$$\epsilon_1 = 1 + \frac{4\pi \cdot Ne^2}{m(p_0^2 - p^2)} + \frac{4\pi \cdot N'e^2}{M(P_0^2 - p^2)} \tag{51}$$

$$\epsilon_2 = 1 - \frac{4\pi \cdot Ne^2}{mp^2} - \frac{4\pi \cdot N'e^2}{Mp^2} \tag{52}$$

$$\alpha = \frac{p_0}{p} \cdot \frac{4\pi \cdot Ne^2}{m(p_0^2 - p^2)} + \frac{P_0}{p} \cdot \frac{4\pi \cdot N'e^2}{M(P_0^2 - p^2)}. \tag{53}$$

Now, P_0 is very small compared with p, so that it will be valid to assume that the ionic contributions to ϵ_1 and ϵ_2 are the same. Further, on using the abbreviations

$$Q = P_0/p \tag{54}$$

$$G = 4\pi \cdot N'e^2/M(P_0^2 - p^2) \tag{55}$$

which should be compared with (34) and (35), we have, corresponding to (36), (37), and (38)

$$\epsilon_1 = 1 + g + G \tag{56}$$

$$\epsilon_2 = 1 + g(1 - q^2) + G \tag{57}$$

$$\alpha = qg + QG. \tag{58}$$

Now, with regard to α, the ratio of the ionic to the electronic contributions is given by

$$\frac{QG}{qg} = \frac{N' \cdot m^2 \cdot (p_0^2 - p^2)}{N \cdot M^2 \cdot (P_0^2 - p^2)}.$$

If M is for negative oxygen atoms, m^2/M^2 is about 10^{-9}; also, for the practical case of $p_0 = 2p$, we have approximately

$$\frac{QG}{qg} = -\frac{N'}{N} \cdot 3 \cdot 10^{-9}.$$

We may therefore consider two cases, (a) when QG is negligible compared with qg, that is to say when there is at least one electron to each million of ions, and (b) when QG cannot be neglected.

As the downcoming wave descends through regions of decreasing electronic density, even assuming that the ionic density remains sensibly constant, there will be a height at which the number of electrons is so small that double refraction has ceased to operate. It is important to notice that, since the ionic critical frequency is of the order of 50 cycles, a wave, such as we are considering, behaves in a purely ionic medium as if its wavelength were very short; the two values of

the refractive index, for any direction of propagation, are equal, to a high degree of precision. Hence, it is only by the agency of electrons that a wave can be resolved into two components.

The limiting polarization of the ordinary ray may then be considered when the number of electrons is very small, and yet a large enough fraction of the ionic density to make qg greatly preponderate over QG. At a lower height, where there are ions but no electrons, there is no longer any mechanism capable of altering the polarization, except the effect of a rotation of the ellipse of polarization by simple ionic refraction.

Our two conditions are therefore, (a) $\alpha = qg$, and (b) $\alpha = QG$. The limiting shape of the polarization ellipse is had from the first, when g becomes small, and, the final orientation of the axes of the ellipse can be found from the second, by calculating the total change in the direction of propagation as the downcoming wave passes through the ionic region.

(1). The Limiting Shape of the Ellipse of Polarization

The conditions are,

$$\alpha = qg$$

$$\epsilon_1 = 1 + g + G$$

$$\epsilon_2 = 1 + g(1 - q^2) + G.$$

With these modifications, equation (27) still holds, so that

$$R_D = -\frac{D_y}{j \cdot D_t} = \frac{\alpha n}{\left\{(\epsilon_1^2 - \alpha^2)U^2 - \epsilon_1\right\}}.$$

Eliminating U through (19), we have

$$R_D^2 + \frac{l^2}{n} \cdot \frac{(\epsilon_1^2 - \alpha^2 - \epsilon_1\epsilon_2)}{\epsilon_2 \cdot \alpha} \cdot R_D - 1 = 0$$

which is the same as,

$$R_D^2 + \frac{l^2}{n} \cdot \frac{q(1 + G)}{\left\{1 + g(1 - q^2) + G\right\}} \cdot R_D - 1 = 0. \tag{59}$$

As the electronic density becomes small, so does g, and (59) becomes

$$R_D^2 + \frac{l^2}{n} \cdot q \cdot R_D - 1 = 0$$

and holds independently of the value assigned to N', the number of heavy ions. On exactly similar lines it may be shown that, as the electronic density becomes small,

$$R_D = -D_x/j\cdot D_t \rightarrow -E_y/j\cdot E_t = R_a,$$

so that, even when heavy ions are present, the limiting polarization is given by

$$R_a^2 + \frac{l^2}{n}\cdot q\cdot R_a - 1 = 0,$$

which is (39). Hence, the limiting polarization of the downcoming wave is that which holds for the lowest height at which free electrons exist, even if there is, at this height, a large concentration of heavy ions. There remains to be considered a possible twist of the polarization ellipse as the wave descends through the ionic region.

(2). Ionic Refraction of the Downcoming Wave

The conditions are, $p_0 = 2p = 10^7$, and

$$\alpha = QG$$
$$\epsilon_1 = \epsilon_2 = 1 + G.$$

Assuming that there are as many as 10^8 ions per cubic centimeter at the height at which the electron density of ionization becomes small, the refractive index, as calculated from ϵ_1 or ϵ_2, is 0.77.

Let us consider the special case of a ray traveling along the direction of the lines of force of the earth's field, the dip angle being 62.5 degrees. Then it is easy to show that the change in direction of the ray path is only 9 degrees, this being the difference between the direction of propagation at the height at which the limiting shape of the polarization ellipse was found, and the final direction after passing through the region of purely ionic ionization.

Hence, the point on the earth's surface at which the downcoming wave is actually received, is not very different from that for which the polarization, as shown in Figs. 5 and 6, is circular.

VII. The Hartree Modification

Hartree[4] has suggested the value of 1/3 for a term β which allows for the discontinuous distribution of electric charge on discrete particles in the Heaviside layer. Other workers have either assigned a zero value, or alternatively left β unspecified. In this paper, which is particularly concerned only with the *limiting* polarization of the downcoming wave, β has been disregarded. It will be necessary, therefore, to justify the omission.

Since it will be shown that the limiting polarization is not affected by the inclusion of β, we do not propose to do more than quote the new

values which must be assigned to ϵ_1, ϵ_2, α, and q, in order to allow for Hartree's term. They will be

$$\epsilon_1'' = \frac{4 + 7\epsilon_2 - 2\epsilon_2^2 - 9q^2}{\{(4 - \epsilon_2)^2 - 9q^2\}}$$

$$\epsilon_2'' = \frac{1 + 2\epsilon_2}{4 - \epsilon_2}$$

$$\alpha''^2 = (\epsilon_1'' - 1)(\epsilon_1'' - \epsilon_2'')$$

$$q'' = 3q/(4 - \epsilon_2).$$

With these interpretations, the polarization expression (27) still holds, and we have, after the elimination of U through (19),

$$R_D^2 + \frac{l^2}{n} \cdot \frac{q''}{\epsilon_2''} \cdot R_D - 1 = 0 \tag{60}$$

in which we are interested in the factor

$$\frac{q''}{\epsilon_2''} = \frac{3q}{1 + 2\epsilon_2}.$$

As the ionization density tends to zero, ϵ_2 tends to unity, so that the expression for q''/ϵ_2'' becomes q. For the same condition, ϵ_1'' tends to unity, and α'' to zero, so that

$$R_D = -D_y/j \cdot D_t \rightarrow -E_y/j \cdot E_t = R_a,$$

and (60) becomes,

$$R_a^2 + \frac{l^2}{n} \cdot q \cdot R_a - 1 = 0,$$

which is the limiting polarization expression as given in (39).

VIII. Conclusion

In the preceding pages we have been able to show, by comparatively simple modifications of the fundamental expressions for ϵ_1, ϵ_2, and α, how to allow for the effects of collisions between electrons and gas molecules, and for the presence of large numbers of heavy negative ions in the Kennelly-Heaviside layer. The limiting polarization of the downcoming wave is apparently not much affected by the modifications, and is given, with an accuracy sufficient for comparison with experimental values which may later become available, by the simple theory which neglects the refinements just quoted.

Without wishing to labor the versatility of ϵ_1, ϵ_2, and α, we would point out that it is a simple matter to allow for the effects of collisions between the heavy negative ions and other particles in the Heaviside layer. The modifications would be on very similar lines to those for electronic collisions, but, for broadcast frequencies of transmission, there seems to be no necessity to consider the point.

IX. Acknowledgments

The paper describes a theoretical investigation undertaken during the course of experiments forming a part of the program of the Radio Research Board of the Australian Commonwealth Council for Scientific and Industrial Research, to whom the authors are indebted for permission to publish their results.

The authors wish to express their indebtedness to Dr. L. G. H. Huxley, to Dr. D. F. Martyn, and to M. René Mesny, for a number of suggestions as to the presentation of the paper, and they take pleasure in acknowledging to Professor J. P. V Madsen, of the P. N. Russel School of Electrical Engineering of the University of Sydney, their appreciation of his interest in the progress of the investigation.

Proceedings of the Institute of Radio Engineers
Volume 21, Number 8 *August, 1933*

A NOTE ON THE THEORY OF THE MAGNETRON OSCILLATOR*

By

J. Barton Hoag

(Ryerson Physical Laboratory, University of Chicago, Chicago, Ill.)

It has been shown by K. Okabe[1] that the half period of the electromagnetic wave generated by a magnetron oscillator corresponds to the time for an electron to travel from the filament to its tangential position along the inner wall of the anode. When the accelerating voltage V and the field strength H (gauss) have been adjusted so that the anode current starts to decrease rapidly, high-frequency oscillations are observed whose wavelength is λ centimeters. Then, according to Okabe's theory,

$$\lambda H = 10{,}650.$$

His experimental value of 13,000 for this constant, and as well, the value of D. S. Mohler of 13,230, taken as the average of twelve readings on four different tubes, is obviously much higher. It is here proposed to derive the above equation in a more elementary fashion and to indicate a simple correction which gives a constant in much better agreement with experiment.

First, we shall assume that the electrons which leave the filament are given their full acceleration within a negligible distance from the filament and then travel with a uniform velocity v. Under these conditions, they will be deflected by the magnetic field in perfect circles, touching the anode tangentially and returning to the filament when the accelerating voltage and magnetic field are properly adjusted. This serves as a simple oscillator, producing a radiation whose wavelength is, from Okabe's theory

$$\lambda = cT,$$

where c is the velocity of light and T is the period of the radiation as well as the time of transit of the electron in its orbit. If r is the radius of the anode, this time of transit is obviously

$$T = \frac{\pi r}{v}\cdot$$

* Decimal classification: R133×R355.9. Original manuscript received by the Institute, September 2, 1932.

[1] K. Okabe, Proc. I.R.E., vol. 17, p. 652, (1929).

Further, we may equate the magnetic deflecting force and the centrifugal force in the usual manner, so that

$$Hev = \frac{mv^2}{r/2}$$

where e is the charge, m is the mass and v is the velocity of an electron. Solving for v and substituting in the two preceding equations gives

$$\lambda H = \frac{2\pi mc}{e} = 10{,}650.$$

However, Langmuir[2] has shown that, due to the space charge in the neighborhood of the filament, the actual path of the electron is a cardiod whose length is 1.23 times that of the circle. Since the velocity is practically the same in both cases, the time of oscillation is 1.23 times as great and the last equation becomes

$$\lambda H = \frac{2\pi mc}{e} 1.23 = 13{,}100$$

which is in much better agreement with experimental values. Corrections for the initial velocities of emission and for the finite size of the filament are omitted, but this equation is sufficiently accurate for practical purposes.

[2] Hull. *Phys. Rev.*, vol. 18, p. 31, (1921).

Proceedings of the Institute of Radio Engineers
Volume 21, Number 8 *August, 1933*

DETERMINATION OF GRID DRIVING POWER IN RADIO-FREQUENCY POWER AMPLIFIERS*

By

H. P. Thomas

(Radio Engineering Department, General Electric Company, Schenectady, N. Y.)

Summary—*An approximate method of determining the power required to drive the grid circuit of a vacuum tube power amplifier of the class C type when operating at radio frequencies is developed, and a comparison given between the results obtained by this method, and more exact measurements made at sixty cycles. The only quantities which need to be known for the method described are the grid excitation voltage and the direct grid current, the driving power being given by the formula* $W_d = \sqrt{2}E_g I_c$.

General

MOST present-day radio transmitters employ a number of stages of radio-frequency amplification, as the oscillator is usually of the piezo-electric type or a lightly loaded master oscillator, from which the available power is in the order of a few watts, and this must be amplified to the output power level, which may be many kilowatts. The number of stages required in the amplifier chain, and the size tubes needed in each stage are determined by the power necessary to excite the successive grid circuits. Very little information on the magnitude of the grid driving power which must be supplied is available to the designer, with the result that he must do considerable experimental work, or else run the risk either of having too little exciting power to obtain the required output, or of having too many stages or larger tubes than are required.

In an article by E. E. Spitzer,[1] it was shown, from measurements made at sixty cycles using a wattmeter to measure the input power, that the driving power could be divided into two parts, first that lost in the bias device, and second the actual input to the grid. The loss in the bias device is simply E_cI_c, and the input to the grid of the tube itself was found to be expressible by the formula $W_g = AI_c^{1.34}$, where I_c is the direct grid current, E_c the bias voltage, and A is a constant. However, A is a function of the tube and also of the plate circuit load, so its value must be determined experimentally for various values of plate load impedance for each tube in order to have complete data available. Since the use of sixty-cycle frequency makes the tank circuits

*Decimal classification: R355.7. Original manuscript received by the Institute, February 9, 1933.

[1] Proc. I.R.E., vol. 17, pp. 985–1005; June, (1929).

large and clumsy, and the wattmeters needed to measure the grid power are apt to be of sizes not commonly available, this method of measurement is not convenient. The method described below was evolved in order to make it possible to make measurements at radio frequencies with the usual types of radio-frequency and direct-current instruments with at least a fair degree of accuracy.

Derivation

The power lost in the grid circuit of a power amplifier tube is given by the expression

$$W_d = 1/T \int_0^T e_g i_g dt \tag{1}$$

where,

e_g = instantaneous value of the input voltage.
i_g = instantaneous value of the grid current.
T = period.

If e_g is assumed to be sinusoidal, as is usually the case, since ordinarily a tank circuit with sufficient kilovolt-amperes is used to prevent serious distortion of the wave shape, this expression may be changed to

$$W_d = E_g\omega/\sqrt{2}\pi \int_0^{2\pi/\omega} i_g \sin \omega t dt \tag{2}$$

E_g = root-mean-square value of the grid circuit input voltage.

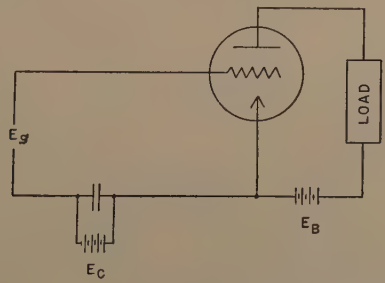

Fig. 1

Now i_g may be expressed as a series

$$\begin{aligned} i_g = {} & a_0 + a_1 \sin \omega t + a_2 \sin 2\omega t + \cdots \\ & + b_1 \cos \omega t + b_2 \cos 2\omega t + \cdots . \end{aligned} \tag{3}$$

If (3) is substituted for i_g in (2) it is seen that the driving power becomes

$$W_d = E_g a_1/\sqrt{2}. \tag{4}$$

The grid current is some function of ωt, say $f(\omega t)$ from which the value of the constant a_1 can be determined, if the function is known.

$$a_1 = \omega/\pi \int_0^{2\pi/\omega} f(\omega t) \sin \omega t dt. \tag{5}$$

Now if we determine the value of a_0 of (3), which is the direct grid current,

$$a_0 = \omega/2\pi \int_0^{2\pi/\omega} f(\omega t) dt \tag{6}$$

we see that a_1 would be equal to $2a_0$ except that the expression for a_1 has a factor $\sin \omega t$ under the integral sign. This means that the ordinates of a curve of $f(\omega t)$ vs. ωt are multiplied by $\sin \omega t$, and then the area under the curve found. An examination of the normal grid current

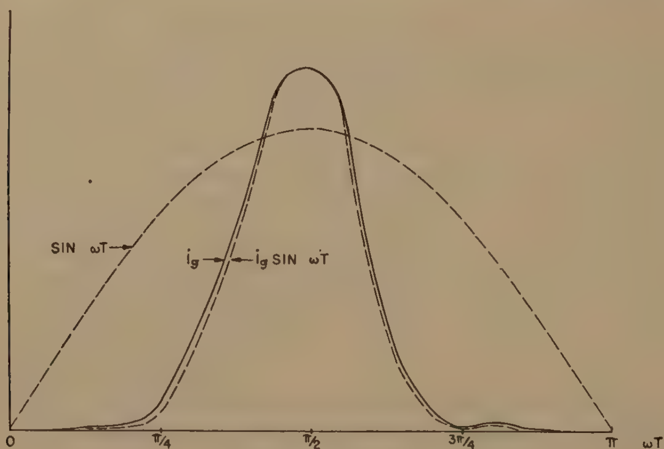

Fig. 2

wave shape shows that the greater part of the current flows when $\sin \omega t$ is nearly unity, and at points where $\sin \omega t$ is considerably less than unity the magnitude of the grid current is small. Fig. 2 shows an oscillogram of grid current for a UV-851 under class C operation (solid line), and $i_g \sin \omega t$ (dotted line). By inspection of these two curves it can be seen that the difference in area is small. This suggests that as an approximation we may set $\sin \omega t$ equal to unity in (5). Then $a_1 = 2a_0$, and (4) becomes

$$W_d = \sqrt{2} E_g a_0 = \sqrt{2} E_g I_c, \tag{7}$$

where E_g is the root-mean-square value of the radio-frequency voltage applied to the grid circuit, and I_c is the direct grid current. W_d is the total power lost in the grid circuit, comprising both the loss in the grid of the tube and that in the bias device.

Results

The validity of the assumption made in arriving at (7) can be determined most easily by comparing values of driving power calculated

TABLE I

Tube type	E_b v	I_b a	E_c v	I_c ma	E_g v	L/RC ohms	Output watts	W_d meas.	W_d calc.	Per cent error
UV-211	1000	0.175	100	19	160	3100	122	3.9	4.3	10
UV-203-A	1000	0.175	75	35	145	3100	123	6.7	7.18	7.2
UV-204-A	2000	0.275	175	131	328	4030	405	56	60.8	8.4
UV-849	2000	0.350	200	57	240	2860	562	18	19.35	7.5
UV-851	2000	0.900	200	300	274	979	1420	111	116.3	5.0
UV-861*	3000	0.350	200	40	455	4300	665	22.5	25.7	14.8

* $E_d = 500$ volts.

by this formula with actual measured values. For this purpose the experimental results obtained by E. E. Spitzer were used for comparison purposes, the calculation of driving power by (7) being made from the

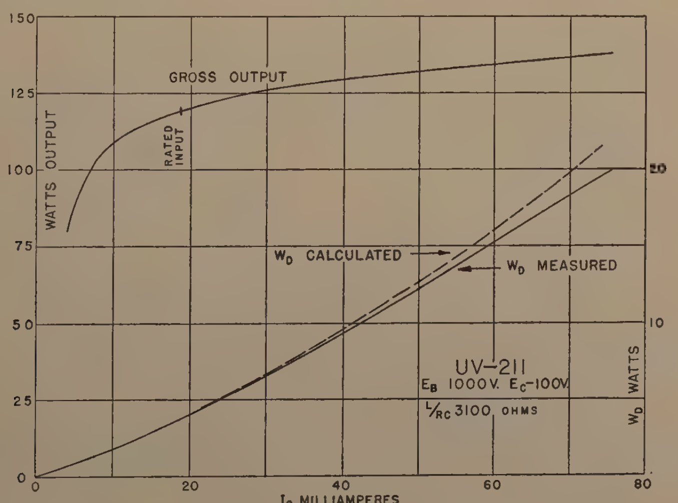

Fig. 3

values of grid voltage and grid current shown in the curves of his article. That the approximate formula gives results very close to the correct value can be seen by an examination of the curves shown in Figs. 3 to 8 for six different types of tubes. Table I gives a comparison

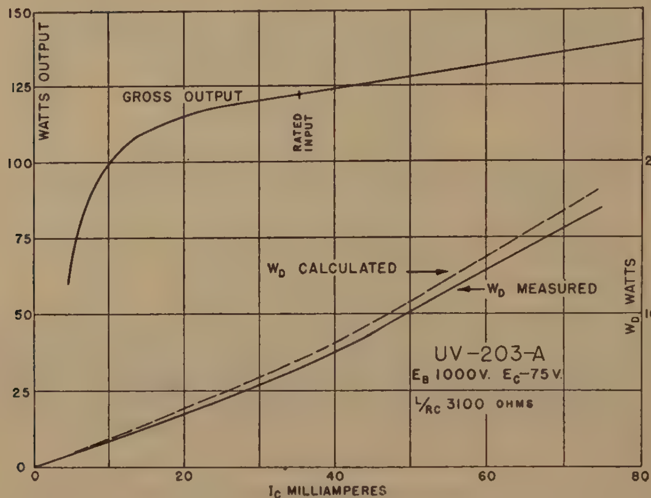
WATTS OUTPUT
GROSS OUTPUT
RATED INPUT
W_D CALCULATED
W_D MEASURED
W_D WATTS
UV-203-A
E_B 1000V. E_C-75V.
L/RC 3100 OHMS
I_C MILLIAMPERES

Fig. 4

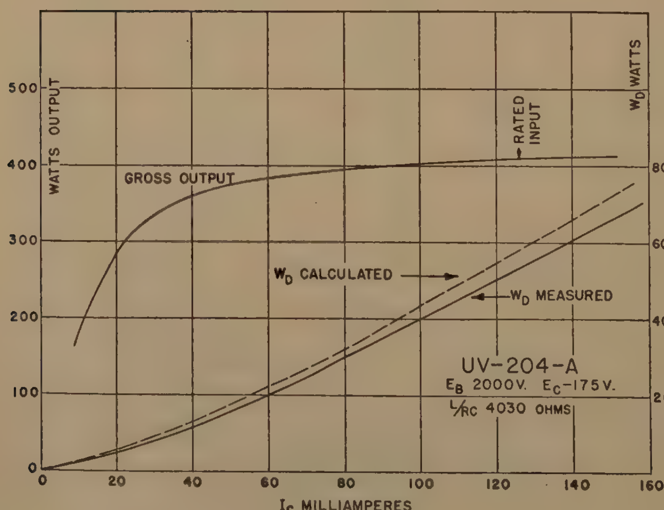
WATTS OUTPUT
W_D WATTS
RATED INPUT
GROSS OUTPUT
W_D CALCULATED
W_D MEASURED
UV-204-A
E_B 2000V. E_C-175V.
L/RC 4030 OHMS
I_C MILLIAMPERES

Fig. 5

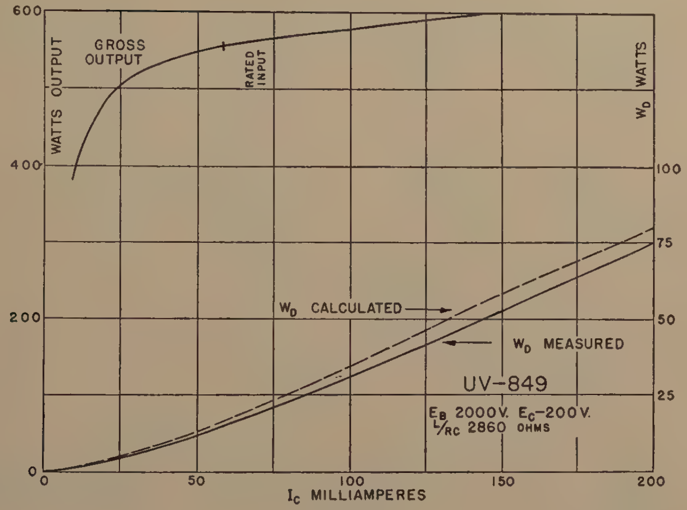
600
400
200
0
WATTS OUTPUT
GROSS OUTPUT
RATED INPUT
W_D WATTS
100
75
50
25
W_D CALCULATED
W_D MEASURED
UV-849
E_B 2000V. E_C-200V.
L/RC 2860 OHMS
0
50
100
150
200
I_C MILLIAMPERES

Fig. 6

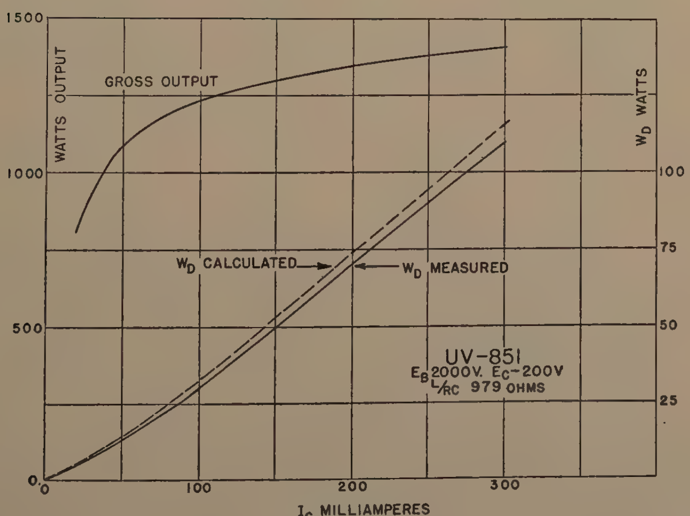
1500
1000
500
0
WATTS OUTPUT
GROSS OUTPUT
W_D WATTS
100
75
50
25
W_D CALCULATED
W_D MEASURED
UV-851
E_B 2000V. E_C-200V
L/RC 979 OHMS
0
100
200
300
I_C MILLIAMPERES

Fig. 7

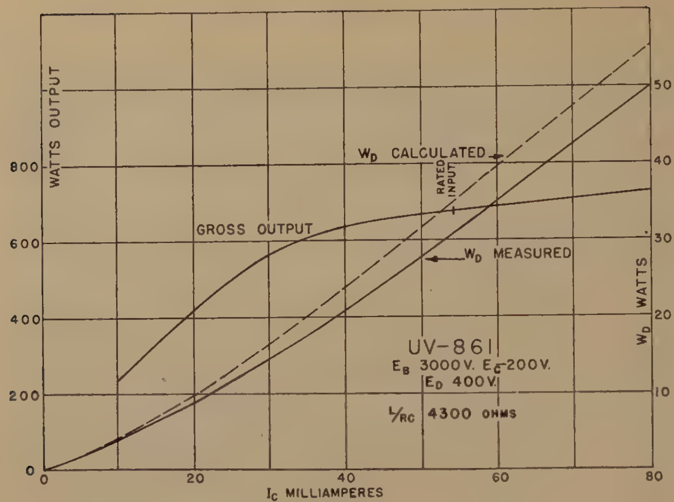

Fig. 8

of the calculated and measured values when the tubes are operated with rated input.

Discussion

To utilize the approximate formula it is necessary to know the direct grid current and the radio-frequency excitation voltage. Most radio transmitters have grid current meters, or one can easily be inserted, but there is usually no provision made for measuring the ex-

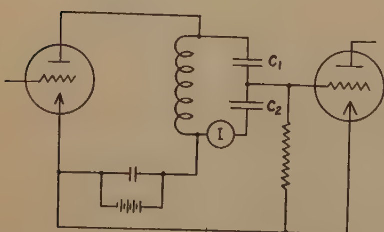

Fig. 9

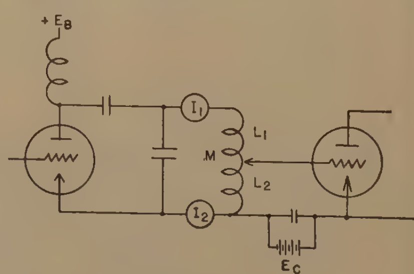

Fig. 10

citation voltage. However, it is a fairly simple matter to measure this quantity. A vacuum tube voltmeter may be used, but probably a simpler method in most cases is to insert a radio-frequency ammeter in the grid tank circuit, and calculate the voltage from the current and the reactance of that portion of the circuit across which the excitation voltage is obtained. For instance, if the grid of the power amplifier is excited by connecting it across a section of the tank condenser of the

previous stage as shown in Fig. 9, the voltage will be $I/C_2\omega$. Similarly, for the circuit shown in Fig. 10, $E_g = I_2 L_2\omega + I_1 M\omega$, or if the kilovolt-amperes in the tank circuit is sufficiently large so that $I_1 = I_2$ approximately, $E_g = I(L_2 + M)\omega$. Another method which may be convenient

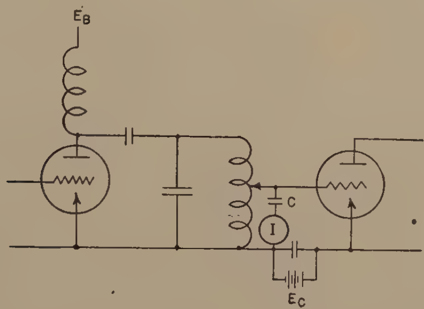

Fig. 11

in some cases is to connect a small capacity in series with a low range ammeter from grid to filament of the power amplifier, the capacity acting as a voltmeter multiplier (Fig. 11). This makes it unnecessary to use two ammeters as in Fig. 10 although the additional capacity may change the circuit conditions slightly.

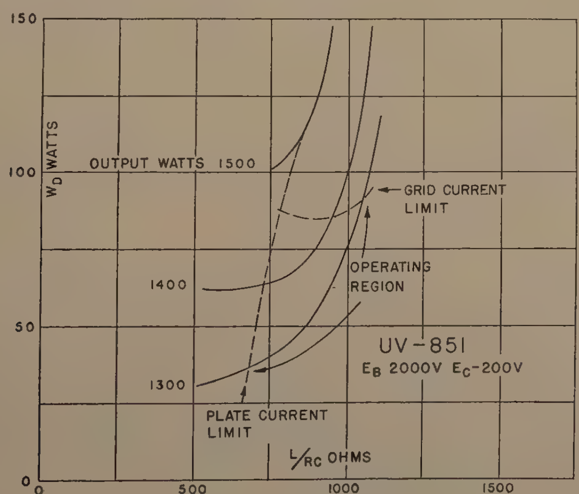

Fig. 12

Fig. 12 is given as an example of the data which can be obtained fairly quickly and easily by this method of calculation, showing data obtained on a UV-851, of grid driving power required for various plate circuit load impedances to obtain a given amount of output power.

Proceedings of the Institute of Radio Engineers
Volume 21, Number 8 *August, 1933*

AMPLITUDE CHARACTERISTICS OF COUPLED CIRCUITS HAVING DISTRIBUTED CONSTANTS*

By
Ronold King
(Electrical Engineering Department, University of Wisconsin, Madison, Wisconsin)

Summary—*A general solution for the amplitude characteristics (resonance curves) for bridge-coupled circuits having distributed line constants is obtained and applied to typical circuit arrangements including those encountered in wavelength measurement using parallel wires. The physical conditions under which the theory may be applied are analyzed; theoretical curves are computed for a typical selection of constants, and are shown to be in excellent agreement with corresponding experimental ones. A new precision method for measuring ultra-short waves is described; the maximum deflection and the minimum deflection methods are shown to be exact. A method is devised for experimentally determining the characteristics of short-wave detectors, and for measuring their input impedance at ultra-high frequencies. The screen-grid resonance indicator is shown to have a linear resonance current-deflection characteristic, and its input impedance is measured at 434 centimeters wavelength.*

IN A recent paper[1] the wavelength characteristics of coupled circuits having distributed constants were theoretically derived and compared with experimental results. It is the purpose of this paper to obtain a general expression for the amplitude characteristics of the same type of circuit, and to compute from it resonance curves for a number of typical and important circuit arrangements. Among these

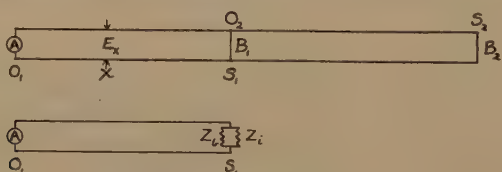

Fig. 1—Circuit diagrams.

are circuits which were experimentally studied and qualitatively discussed in an earlier paper;[2] they also include as a special case the arrangement examined by Takagishi.[3] Definite conclusions will then be drawn regarding the accuracy of several methods of wavelength standardization using parallel wires.

The circuit to be analyzed is shown in Fig. 1. It consists of a primary pair of parallel conductors 0_1s_1 with their ends at $x_1 = 0_1$ bridged by a

* Decimal classification: R140. Original manuscript received by the Institute, March 10, 1933
[1] R. King, Proc. I.R.E., vol. 20, p. 1368, (1932).
[2] R. King, *Ann. der Phys.*, Band 5, Folge 7, p. 805, (1930).
[3] Takagishi, Proc. I.R.E., vol. 18, p. 513, (1930).

perfect conductor, and their ends at $x_1=s_1$ shunted by a terminal impedance Z_r. This impedance consists of a bridge B_1 (with impedance Z_b) in parallel with the input impedance Z_i of a secondary pair of parallel conductors extending from $x_2=0_2=s_1$ to $x_2=s_2$, where they are in turn connected by a second bridge B_2. A potential difference E_x of sinusoidal form is maintained between the parallel conductors at a point x along the primary. It is desired to derive an expression for the current amplitude I_0 through an impedanceless current indicator (corresponding to the perfect conductor mentioned above) connecting the ends of the primary at $x_1=0_1$ in terms of the length s_1 of the primary, the length s_2 of the secondary, and the point of application x of the induced electromotive force E_x.

I. The General Solution

The current I_x flowing at any point x in a pair of parallel conductors of length s_1, which are bridged at the end $x=s_1$ by a terminal impedance Z_r, and to which a sinusoidal electromotive force E_0 is applied at the end $x=0$, is given by Cohen[4] to be:

$$I_x = \frac{E_0 K}{lp+r}\left\{\frac{\cosh K(s_1-x) + \dfrac{Z_r K}{lp+r}\sinh K(s_1-x)}{\sinh Ks_1 + \dfrac{Z_r K}{lp+r}\cosh Ks_1}\right\}. \tag{1}$$

Here, $K=\sqrt{(lp+r)(cp+g)}$ and l, r, c, and g are, respectively, inductance, resistance, capacitance, and leakance per loop unit length of the parallel conductors. The differential operator p becomes $j\omega$ using the notation $E_0=\overline{E}_0 e^{j\omega t}$.

By setting $y=(s_1-x)$, and defining the surge impedance N as follows,

$$N = K/(cp+g) = \sqrt{\frac{lp+r}{cp+g}}$$

equation (1) is more compactly written in the form:

$$I_x = \frac{E_0}{N}\left\{\frac{Y_r N\cosh Ky+\sinh Ky}{Y_r N\sinh Ks_1+\cosh Ks_1}\right\}. \tag{2}$$

By a general reciprocity theorem[5] "a sinusoidal impressed electromotive force applied at any point of the system and an impedanceless

[4] Cohen, "Heaviside's Electrical Circuit Theory," p. 119, equation (99).
[5] Pierce, "Electric Oscillations and Electric Waves," p. 204.

ammeter at any other point of the system are interchangeable without changing the amplitude or phase of the steady-state current through the ammeter." Hence, if an electromotive force E_x be applied to the wires at a point x, and the wires are bridged by an impedanceless ammeter at $x=0$, the current through this ammeter is at once given by (1) after interchanging the subscripts. It is,

$$I_0 = \frac{E_x}{N}\left\{\frac{Y_r N \cosh Ky + \sinh Ky}{Y_r N \sinh Ks_1 + \cosh Ks_1}\right\}. \tag{3}$$

The terminal impedance Z_r consists of the impedance Z_b of the bridge B_1 in parallel with the input impedance Z_i of the secondary pair of conductors. In terms of admittances the following relation is true:

$$Y_r = Y_b + Y_i. \tag{4}$$

The input admittance Y_i of the secondary is given by

$$Y_i = (I/E)_{x_2=0}. \tag{5}$$

Here, E and I have the values given by Cohen.[4] The complete expression is as follows:

$$Y_i = \frac{1}{N}\left\{\frac{Y_b N \cosh Ks_2 + \sinh Ks_2}{Y_b N \sinh Ks_2 + \cosh Ks_2}\right\}. \tag{6}$$

The terminal admittance of the secondary is, of course, simply the admittance Y_b of the second bridge B_2. The two bridges are assumed to be identical. The complete terminal admittance Y_r of the primary is, then,

$$Y_r = Y_b + \frac{1}{N}\left\{\frac{Y_b N \cosh Ks_2 + \sinh Ks_2}{Y_b N \sinh Ks_2 + \cosh Ks_2}\right\}. \tag{7}$$

With the value of Y_r obtained from (7) substituted in (3), the complete general solution for the current I_0 through the impedanceless ammeter at $x=0$ is obtained. The solution is expressed in terms of the three variables, namely, the length s_1 of the primary, the length s_2 of the secondary, and the position x (or y) of the applied electromotive force. The constants which appear in the equation are the distributed line constants of the parallel conductors, the impedances of the bridges, the frequency, and the amplitude of the induced electromotive force.

II. The Solution for First-Order Damping

The general solution for the current I_0 in the ammeter at $x=0$ given by (3) and (7) is complicated and not well suited to a study of special circuit arrangements. It is, in fact, much more general than re-

quired for an entirely adequate treatment of the circuits usually encountered in wavelength measurement, and which are the real object of study in this paper. Accordingly, the problem will be specialized by imposing restrictions upon the circuit constants. The prime purpose of this mode of attack is to simplify the mathematics, but without thereby seriously limiting the accuracy of the solution as applied to the actual circuits under consideration. In the following analytical development restrictions will be imposed and approximations will be made as required to achieve a reasonably simple result. When this has been obtained and applied to several special cases, the imposed conditions will be reviewed and their significance exposed in a general way.

A first restriction will now be imposed on the line constants of the parallel wire system. Let it be assumed that the distributed resistance and leakance of the conductors are both small compared with their inductive reactance and capacitive susceptance per loop unit length. Symbolically, $r \ll pl$; $g \ll pc$. Taking advantage of this condition, and introducing the familiar notation $v = 1/\sqrt{lc}$, the following relations are true:

$$N = \sqrt{\frac{lp + r}{cp + g}} = \sqrt{\frac{l}{c}}\sqrt{\frac{1 + r/lp}{1 + g/cp}} \doteq vl\left[1 + \frac{1}{2p}\left(\frac{r}{l} - \frac{g}{c}\right)\right] \quad (8)$$

$$\begin{aligned} K &= \sqrt{(lp + r)(cp + g)} = p/v\sqrt{(1 + r/lp)(1 + g/cp)} \\ &\doteq p/v + \frac{1}{2v}\left(\frac{r}{l} + \frac{g}{c}\right). \end{aligned} \quad (9)$$

Upon now setting $p = j\omega$ and defining the propagation constant β and the damping constant α as follows, the quantities N and K are conveniently expressed by (8a) and (9a).

$$\beta = \frac{\omega}{v} = \frac{2\pi}{\Lambda}; \quad \alpha = \frac{1}{2v}\left(\frac{r}{l} + \frac{g}{c}\right); \quad \epsilon = \frac{1}{2\omega}\left(\frac{r}{l} - \frac{g}{c}\right) \quad (10)$$

$$N = vl(1 - j\epsilon) \doteq vl \quad (8a)$$

$$K = \alpha + j\beta. \quad (9a)$$

It is well to note that both α and β are dimensionally reciprocal lengths. In terms of the constants α and β the restriction already imposed upon the line constants and an additional condition limiting the range of the impressed wavelength are expressed as follows:

Restriction a.

The line constants of the parallel wire system and the wavelength of the impressed electromotive force satisfy the inequalities:

$$\alpha <<< 1; \ \alpha \ll \beta; \ \epsilon \ll 1. \tag{a}$$

Here, α, ϵ, and β are defined by (10).

It is to be noted that condition (a) allows α to be neglected as compared with β only when the factor K (as given by (9a)) appears in an amplitude factor. Whenever K occurs in the argument of a hyperbolic function, the periodicity of the imaginary part involving β makes the real part, of which α is a factor, significant. Since the factor N defined by (8) and (8a) appears only as an amplitude factor, the small quantity ϵ was neglected in (8a).

As a second restriction a condition will now be imposed upon the constants of the identical bridges B_1 and B_2. Let it be assumed that the resistance of each bridge is negligibly small compared with its inductive reactance. In other words:

Restriction b.

The constants of the bridges B_1 and B_2 are such that the following relation is approximately true:

$$Z_b \doteq j\omega M. \tag{b}$$

Here M is the total inductance of each bridge.

With this condition and (9) the quantity Y_bN occurring in (7) becomes

$$Y_bN = N/j\omega M = vl/j\omega M = 1/j\beta k. \tag{11}$$

The quantity k here introduced is defined by the equation,

$$k = M/l. \tag{11a}$$

It is the ratio of the total inductance M of a bridge to the inductance per loop unit length of the parallel conductors. It is a kind of coupling coefficient having, however, the dimension of a length. It will be referred to as the equivalent length of the bridge B. This name will be found of descriptive significance later in the analysis. The three quantities, k, α, and β are the fundamental constants of the circuit taken as a whole.

Upon substituting (9a) and (11) in (7), the quantity Y_rN appearing in (3) becomes

$$Y_rN = 1/j\beta k + \left\{\frac{\cosh(\alpha + j\beta)s_2 + j\beta k \sinh(\alpha + j\beta)s_2}{\sinh(\alpha + j\beta)s_2 + j\beta k \cosh(\alpha + j\beta)s_2}\right\}. \tag{12}$$

A restriction will now be made upon the lengths s_1 and s_2 of the primary and secondary (and consequently also upon y).

Restriction c.

Let the lengths s_1, s_2, and y, denoted in the following by S, be not so great that the inequality

$$\alpha^2 S^2 \ll 1 \tag{c}$$

is not true. This implies that,

$$\sinh \alpha S \doteq \tanh \alpha S \doteq \alpha S; \quad \cosh \alpha S \doteq 1. \tag{c$'$}$$

As an immediate consequence of restriction (c') the next written relations are true:

$$\left.\begin{aligned} \sinh(\alpha + j\beta)S &\doteq \alpha S \cos\beta S + j\sin\beta S \\ \cosh(\alpha + j\beta)S &\doteq \cos\beta S + j\alpha S \sin\beta S. \end{aligned}\right\} \tag{13}$$

With these values inserted in (12), and upon collecting terms, the following equation is obtained:

$$Y_r N = \frac{1}{j\beta k} + \left\{ \frac{[\cos\beta s_2 - \beta k \sin\beta s_2] + j\alpha s_2[\sin\beta s_2 + \beta k \cos\beta s_2]}{\alpha s_2[\cos\beta s_2 - \beta k \sin\beta s_2] + j[\sin\beta s_2 + \beta k \cos\beta s_2]} \right\} \tag{14}$$

It will be convenient to obtain (14) in the form,

$$Y_r N = \alpha s_2 \Delta - j\theta. \tag{15}$$

Here the newly introduced quantities Δ and θ are functions only of s_2 and the three fundamental constants k, α, and β. They are completely discussed in the Appendix and their principal values are summarized in Table I.

With the value of $Y_r N$ obtained from (15) and Table I, (3) becomes

$$I_0 = \frac{E_x}{lv}\left\{ \frac{(\alpha s_2 \Delta - j\theta)\cosh(\alpha + j\beta)y + \sinh(\alpha + j\beta)y}{(\alpha s_2 \Delta - j\theta)\sinh(\alpha + j\beta)s_1 + \cosh(\alpha + j\beta)s_1} \right\}. \tag{16}$$

By now applying (13) written for s_1 and y according to restriction (c), (16) expands into the following:

$$I_0 = \frac{E_x}{lv}$$

$$\left\{ \frac{[\alpha(s_2\Delta + y)\cos\beta y + \alpha y\theta \sin\beta y] + j[(\alpha^2 y s_2 \Delta + 1)\sin\beta y - \theta\cos\beta y]}{[(\alpha^2 s_1 s_2 \Delta + 1)\cos\beta s_1 + \theta\sin\beta s_1] + j[\alpha(s_2\Delta + s_1)\sin\beta s_1 - \alpha s_1 \theta \cos\beta s_1]} \right\}. \tag{17}$$

After transforming trigonometrically and taking the absolute value, the current amplitude is found to be

TABLE I
Formulas for θ and Δ

$\varphi =$	any value	not near $n\pi$	$\varphi_n' = n\pi$	$\varphi_n'' = n\pi \pm \beta nqk/2$	$\varphi_n''' = n\pi - \frac{\beta k}{2}(1 \mp \sqrt{1-n^2q^2})$
$S_2 =$	any value	not near $\frac{\Delta}{2}$	$S_{2,n}' = \frac{n\Delta}{2} - k$	$S_{2,n}'' = \frac{n\Delta}{2} - k\left(1 \mp \frac{nq}{2}\right)$	$S_{2,n}''' = \frac{n\Delta}{2} - \frac{k}{2}(3 \mp \sqrt{1-n^2q^2})$
$\theta =$	$\frac{1}{\beta k} + \frac{1}{\alpha^2 S_2^2 \cot\varphi + \tan\varphi}$	$\frac{1}{\beta k} + \cot\varphi$	$\theta_n' = \frac{1}{\beta k}$	$\theta_n'' = \frac{1}{\beta k}\left(1 \pm \frac{1}{nq}\right) = \begin{cases}\theta_{\max}\\ \theta_{\min}\end{cases}$	$\theta_n''' = 0$
$\Delta =$	$\frac{1}{\alpha^2 S_2^2 \cos^2\varphi + \sin^2\varphi}$	$\csc^2\varphi$	$\Delta_n' = \frac{4}{(nq\beta k)^2} = \Delta_{\max}$	$\Delta_n'' = \frac{2}{(nq\beta k)^2}$	$\Delta_n''' = \frac{2}{\beta^2 k^2}\left(\frac{1}{1 \pm \sqrt{1-n^2q^2}}\right)$

$$q = \frac{\alpha\Lambda}{\beta k}; \quad \varphi = \beta(s_2 + k); \quad \beta\Lambda = 2\pi; \quad n = 1, 2, 3, \cdots$$

$$|I_0| = \frac{E_x}{lv}\left\{\frac{G_y^2 \cos^2(\beta y + \delta_y) + \alpha^2 F_y^2 \cos^2(\beta y - \gamma_y)}{G_s^2 \sin^2(\beta s_1 + \delta_s) + \alpha^2 F_s^2 \sin^2(\beta s_1 - \gamma_s)}\right\}^{1/2}. \tag{18}$$

Here the amplitude and phase factors are defined as follows:

$$\begin{aligned}
G_y^2 &= (\alpha^2 y s_2 \Delta + 1)^2 + \theta^2 & \delta_y &= \cos^{-1}\frac{\theta}{G_y} = \sin^{-1}\frac{(\alpha^2 s_2 y \Delta + 1)}{G_y}\\
G_s^2 &= (\alpha^2 s_1 s_2 \Delta + 1)^2 + \theta^2 & \delta_s &= \cos^{-1}\frac{\theta}{G_s} = \sin^{-1}\frac{(\alpha^2 s_2 s_1 \Delta + 1)}{G_s}\\
F_y^2 &= (s_2\Delta + y)^2 + y^2\theta^2 & \gamma_y &= \cos^{-1}\frac{(s_2\Delta + y)}{F_y} = \sin^{-1}\frac{\theta y}{F_y}\\
F_s^2 &= (s_2\Delta + s_1)^2 + s_1^2\theta^2 & \gamma_s &= \cos^{-1}\frac{(s_2\Delta + s_1)}{F_s} = \sin^{-1}\frac{\theta s_1}{F_s}.
\end{aligned} \tag{19}$$

The α^2 terms are not neglected in the above formulas since they are multiplied by the quantity Δ which may assume very large values. θ and Δ for the above relations are given in Table I.

Equation (18) is the complete general solution for the amplitude of the current I_0 through the impedanceless ammeter at $x=0$ for a circuit to which the restrictions imposed apply.

Before proceeding to derive simplified forms from (18) for the special cases which are to be considered, it is interesting and experimentally significant (as will become evident at a later point) to note that the amplitude I_0 given by (18) is essentially the same for certain lengths of the secondary as it is for the secondary completely absent.

The expressions for the factors given in (19) for the case of no secondary at all, but with the primary terminated by the bridge B_1 are obtained as follows. Clearly with $Y_i=0$ equations (4), (11), and (15) reduce, respectively, to the ones written below:

$$Y_r = Y_b \tag{4'}$$

$$Y_r N = Y_b N = 1/j\beta k \tag{11'}$$

$$Y_r N = \alpha s_2 \Delta - j\theta = 1/j\beta k. \tag{14'}$$

From the last equation, it is evident that

$$\Delta = 0;\ \theta = 1/\beta k. \tag{20'}$$

With these values, the array (19) simplifies to the following:

$$\begin{aligned}
G_y^2 &= G_s^2 = (1 + \theta^2)\\
F_y^2 &= y^2(1 + \theta^2);\ F_s^2 = s_1^2(1 + \theta^2)\\
\delta_y &= \delta_s = \cot^{-1}\theta\\
\delta_y &= \gamma_s = \tan^{-1}\theta.
\end{aligned} \tag{19'}$$

On the other hand for $\varphi=\beta(s_2+k)$ near $n\pi/2$, Table I shows that θ_n and Δ_n have the following values:

$$\Delta \doteq 1; \quad \theta \doteq 1/\beta k. \tag{20''}$$

With this value of Δ the quantity $\alpha^2S^2\Delta \ll 1$ according to restriction (c), so that (19) gives:

$$\left.\begin{aligned} G_y^2 &= G_s^2 = (1+\theta^2) \\ F_y^2 &= y^2[(1+s_2/y)^2+\theta^2]; \quad F_s^2 = s_1^2[(1+s_2/s_1)^2+\theta^2] \\ \delta_y &= \delta_s = \cot^{-1}\theta \\ \gamma_y &= \tan^{-1}\theta/(1+s_2/y); \quad \gamma_s = \tan^{-1}\theta/(1+s_2/s_1). \end{aligned}\right\} \tag{19''}$$

A comparison of (19′) and (19″) discloses that the major factors G^2 and δ are identical in the two cases. The minor factors, (i.e., those involving the very small quantity α^2), differ by having a term $(1+s_2/y)$ or $(1+s_2/s_1)$ appearing instead of unity. However, so long as s_2 is no greater than y or s_1, these terms are small compared with θ, so that F^2 and γ are also nearly the same in the two cases. Any difference between them is, moreover, a second order one in view of the multiplying factor α^2. In other words, so long as s_2 is not too long, and is of such a length that the relations (20″) are true, which is the case over a considerable range near $\varphi=\beta(s_2+k)-n\pi/2$, the current amplitude $|I_0|$ is the same, to a very close degree of approximation, as for no secondary present at all. This statement is the theoretical verification of the same conclusion obtained experimentally in reference 2 and invoked in reference 1.

III. Application of the Theory to Special Cases

The general equation (18) for first order damping may be applied to a large variety of possible circuit adjustments. There are, essentially, the three variables already referred to, namely, the position (x) along the primary of the source of induced electromotive force, the length (s_1) of the primary, and the length (s_2) of the secondary. Simultaneous variation of these three, or of any one with the others fixed in any desired way, leads to amplitude characteristics of many types and shapes. In the present discussion only a few of the more important special circuit arrangements will be analyzed by means of (18). Among these will be included especially the resonance curves of three useful methods of wavelength standardization and the "double hump phenomenon." A new precision method for the measurement of ultra-short waves will be outlined and compared with a similar one suggested by Hoag.[6]

[6] Hoag, Proc. I.R.E., vol. 21, p. 29; January, (1933).

Special Case 1: Variation of the position x of the induced electromotive force with the secondary detuned and the primary adjusted to give a maximum or any sufficiently large amplitude.

The requirement that the secondary be detuned prescribes that s_2 be fixed at a length such that φ is near $n\pi/2$. The array (19″) is then true for (18). Referring to this equation it is clear that the amplitude $|I_0|$ will become large only when the denominator of the quantity in brackets becomes sufficiently small. This will be the case when the following relation is true or nearly true:

$$(\beta s_1 + \delta) \doteq (\beta s_1 + \cot^{-1}\theta) = m\pi \quad (m = 1, 2, \cdots). \qquad (21)$$

Let it be supposed, then, that s_1 and s_2 are so adjusted that (20) is satisfied. Equation (18) reduces, in consequence, to the following simple form:

$$\begin{aligned} |I_0| &= \left| \frac{E_x}{lv} \left\{ \frac{1+\theta^2}{\alpha^2 F_s^2 \sin^2(\cot^{-1}\theta + \gamma_s)} \right\}^{1/2} \cos\beta x \right| . \\ &= \left| \bar{I}_0 \cos\beta x \right| . \end{aligned} \qquad (22)$$

With φ near $n\pi/2$, array (19″) applies and (19′) approximately. Using (19′) equation (22) reduces to the simple expression

$$|I_0| = \frac{E_x}{lv}\left| \frac{1}{\alpha s_1} \cos\beta x \right| . \qquad (22a)$$

Equation (22) is true for all values of x except at or near those leading to a vanishing numerator. At points where the numerator becomes vanishingly small, (i.e. whenever βx is at or near $(2n+1)\pi/2$), equation (18) gives the following expression for $|I_0|$:

$$|I_0| = \frac{E_x}{lv} \left\{ \frac{F_y^2 \sin^2(\gamma_y + \cot^{-1}\theta)}{F_s^2 \sin^2(\gamma_s + \cot^{-1}\theta)} \right\}^{1/2} \doteq \left| \frac{E_x}{lv} \quad \frac{F_y}{F_s} \right| . \qquad (22b)$$

With the same approximations as those which apply to (22a), equation (22b) becomes:

$$|I_0| \doteq \left| \frac{E_x}{lv} \right| . \qquad (22c)$$

This value is obviously small compared with the amplitude in (22a) in which there is a factor α in the denominator.

Conclusion.

If the secondary is detuned and the primary is fixed at a length which will give a large amplitude,[7] the magnitude of the current, $|I_0|$,

[7] It is to be noted that any adjustment whatsoever of s_1 and s_2 is satisfactory so long as the amplitude is sufficiently large. The form of (22) is not affected by the adjustment of s_1 and s_2.

through the ammeter varies as the absolute value of the cosine of the argument βx, where x is the position of the induced electromotive force relative to the parallel conductors of the primary. This is true except over small ranges where the cosine, instead of vanishing, reaches a minimum value. These minimum points occur at $x = n\pi/\beta = n\Lambda/2$. Here Λ is the wavelength of the source of electromotive force.

Equation (22) may also be written in the form:

$$x = \frac{1}{\beta}\cos^{-1}\left(\frac{I_0}{\bar{I}_0}\right) = \frac{\Lambda}{2\pi}\cos^{-1}\left(\frac{I_0}{\bar{I}_0}\right)$$

or,

$$\Lambda = \frac{2\pi x}{\cos^{-1}(I_0/\bar{I}_0)}\,. \tag{23}$$

From this relation it is clear that by plotting x against the arc-cosine of the ratio $(I_0/\bar{I}_0)$ a straight line is obtained. The wavelength of the generated electromotive force is proportional to the slope of this line.

Special Case 2: Variation of the secondary length s_2 with the position x of the induced electromotive force and the primary length s_1 both chosen to give a maximum or near-maximum amplitude.

From Special Case 1 it follows that the amplitude will be a maximum, in so far as the position of the induced electromotive force is concerned, when $\beta x = n\pi$. Since θ, a function alone of s_2, is now the variable, the value of s_1 determined by $\beta s_1 = m\pi$ will give a maximum or near maximum $|I_0|$ in so far as the adjustment of the primary length is effective. With values of s_1 and x so chosen, (18) becomes

$$|I_0| = \frac{E_x}{lv}\left\{\frac{G_y^2\cos^2\delta_y + \alpha^2 F_y^2\cos^2\gamma_y}{G_s^2\sin^2\delta_s + \alpha^2 F_s^2\sin^2\gamma_s}\right\}^{1/2}. \tag{24}$$

By now substituting from the array (19) the values of the several factors, this formula reduces to the simpler form given below:

$$|I_0| = \frac{E_x}{lv}\left\{\frac{\theta^2 + \alpha^2(s_2\Delta + y)^2}{(\alpha^2 s_1 s_2\,\Delta + 1)^2 + \alpha^2\theta^2 s_1^2}\right\}^{1/2}. \tag{25}$$

In the range of φ not near $n\pi$, Δ is small so that the inequality $\alpha^2 s_s^2\Delta \ll 1$ is true according to restriction (c). For this range, then,

$$|I_0| = \frac{E_x}{lv}\left\{\frac{\theta^2}{1 + \alpha^2 s_1^2\theta^2}\right\}^{1/2}. \tag{25a}$$

In the range of φ near $n\pi$, Δ is large so that $\Delta \gg y/s_2$ and equation (25) becomes

$$|I_0| = \frac{E_x}{lv}\left\{\frac{\theta^2 + \alpha^2 s_2{}^2\Delta^2}{(\alpha^2 s_2 s_1\Delta + 1)^2 + \alpha^2 s_1{}^2\theta^2}\right\}^{1/2}. \tag{25b}$$

Conclusion.

With s_1 and x chosen to give a maximum amplitude, the current I_0 through the ammeter varies with s_2 according to (25) and Table I. Equation (25a) indicates that the general shape of the characteristic resembles that of $|\theta|$.

Special Case 3: Moving the bridge B_1, corresponding to a simultaneous variation in the length of both primary and secondary, with the total length $s = s_1 + s_2$ fixed and the position x of the induced electromotive force chosen to give a near-maximum amplitude.

In proceeding from the general equation (18) it is mathematically very convenient in this case to assume the induced electromotive force concentrated at a point sufficiently near the indicator at $x = 0$ to permit the approximation $y = s_1 - x \doteq s_1$. It will be shown below that this does not seriously restrict the generality of the solution. With this condition (18) becomes

$$|I_0| = \frac{E_x}{lv}\left\{\frac{G^2 + \alpha^2 F^2}{G^2 \sin^2(\beta s_1 + \delta) + \alpha^2 F^2 \sin^2(\beta s_1 - \delta)} - 1\right\}^{1/2}. \tag{26}$$

The phase and amplitude factors are

$$\begin{aligned} G^2 &= (\alpha^2 s_1 s_2 \Delta + 1)^2 + \theta^2; \quad F^2 = s_1{}^2\left[\left(\Delta\frac{s_2}{s_1} + 1\right)^2 + \theta^2\right] \\ \delta &= \sin^{-1}\left(\frac{\alpha^2 s_2 s_1 \Delta + 1}{G}\right); \quad \gamma = \sin^{-1}\left(\frac{\theta s_1}{G}\right). \end{aligned} \tag{27}$$

After inserting the values of the coefficients given in (27) in (26) and neglecting terms in $\alpha^2 s_1{}^2$ in comparison with unity, this becomes

$$|I_0| = \frac{E_x}{lv}\left\{\frac{\theta^2 + \Delta^2\alpha^2 s_2{}^2 + 1 + 4\Delta\alpha^2 s_1 s_2}{\begin{array}{l}(\theta^2 + \alpha^2 s_2{}^2\Delta^2)(\sin^2\beta s_1 + \alpha^2 s_1{}^2\cos^2\beta s_1) \\ +(\alpha^2 s_1{}^2\sin^2\beta s_1 + \cos^2\beta s_1) + 2\alpha^2 s_1 s_2\Delta + \theta\sin 2\beta s_1\end{array}} - 1\right\}^{1/2}. \tag{28}$$

Two subcases are now of interest: (a) the total length $s = s_1 + s_2$ is near $m'\Lambda/2$, $(m' = 2, 3, \cdots)$ Or, what is the same thing, βs is near $m'\pi$; (b) the total length s is near $(2m'+1)\Lambda/4$, or βs is near $(2m'+1)\pi/2$.

Special Case 3a: The total length s is near $m'\Lambda/2$.

With $s = s_1 + s_2$ near $m'\Lambda/2$ it is clear that as s_1 approaches $m\Lambda/2$, $(m = 1, 2, \cdots)$, s_2 must approach $n\Lambda/2$, $(n = 1, 2, \cdots)$ with $m' = m$

$+n$. The range βs_2 (or φ) near $n\pi$ corresponds to the range βs_1 near $m\pi$. If a small quantity $\bar{s}_1$ is defined as the change in s_1 measured in either direction from $s_1 = m\Lambda/2$, then $s_1 = m\Lambda/2 + \bar{s}_1$, (or $\beta s_1 = m\pi + \beta\bar{s}_1$). Since $\beta\bar{s}_1$ is by definition small in the range to be considered, it is permissible to set $\sin\beta s_1 = \sin\beta\bar{s}_1 \doteq \beta\bar{s}_1$, and $\cos\beta s_1 = \cos\beta\bar{s}_1 \doteq 1$. Remembering restrictions (a) and (c), (28) becomes

$$|I_0| = \frac{E_x}{lv}\left\{\frac{\theta^2+\alpha^2 s_2^2\Delta^2+1+4\Delta\alpha^2 s_1 s_2}{(\alpha^2 s_1^2+\beta^2\bar{s}_1^2)(\theta^2+\alpha^2 s_2^2\Delta^2)+1+2\alpha^2 s_1 s_2\Delta+2\theta\beta\bar{s}_1} - 1\right\}^{1/2} \tag{29}$$

or, after neglecting the small quantities $(\beta\bar{s}_1)^2$ and $(\alpha s_1)^2$ compared with unity,

$$|I_0| = \frac{E_x}{lv}\left\{\frac{\theta^2+\alpha^2 s_2^2\Delta^2+2\alpha^2 s_1 s_2\Delta-2\theta\beta\bar{s}_1}{(\alpha^2 s_1^2+\beta^2\bar{s}_1^2)(\theta^2+\alpha^2 s_2^2\Delta^2)+2\alpha^2 s_1 s_2\Delta+2\theta\beta\bar{s}_1+1}\right\}^{1/2}. \tag{29a}$$

This equation is a good approximation so long as $\bar{s}_1$ is sufficiently small to justify the relation $\sin 2\beta\bar{s}_1 \doteq 2\beta\bar{s}_1$. If this condition is satisfied, $\bar{s}_2$ is automatically limited in the same way so that the values of θ and Δ for the range of φ near $n\pi$ apply.

Outside the range of φ near $n\pi$ or βs_1 near $m\pi$, Δ is sufficiently small so that $\Delta^2 s_2^2\alpha^2 \ll \theta^2$; also $\sin\beta s_1$ does not become vanishingly small. Hence (28) becomes

$$|I_0| = \frac{E_x}{lv}\left\{\frac{1+\theta^2}{(\theta\sin\beta s_1+\cos\beta s_1)^2+\alpha^2 s_1^2(\theta^2\cos^2\beta s_1+\sin^2\beta s_1)} - 1\right\}^{1/2}. \tag{30}$$

After rearranging terms this expression may be written in the form

$$|I_0| = \frac{E_x}{lv}\left\{\frac{1}{\sin^2(\beta s_1+\cot^{-1}\theta)+\dfrac{\alpha^2 s_1^2}{\theta^2+1}(\theta^2\cos^2\beta s_1+\sin^2\beta s_1)} - 1\right\}^{1/2} \tag{30a}$$

or,

$$|I_0| = \frac{E_x}{lv}\left\{\frac{\cos^2(\beta s_1+\cot^{-1}\theta)-\dfrac{\alpha^2 s_1^2}{\theta^2+1}(\theta^2\cos^2\beta s_1+\sin^2\beta s_1)}{\sin^2(\beta s_1+\cot^{-1}\theta)+\dfrac{\alpha^2 s_1^2}{\theta^2+1}(\theta^2\cos^2\beta s_1+\sin^2\beta s_1)}\right\}^{1/2}. \tag{30b}$$

From this last expression the general nature of the current amplitude for φ not near $n\pi$ is seen to be:

$$|I_0| \doteq \frac{E_x}{lv}\left|\cot(\beta s_1+\cot^{-1}\theta)\right|. \tag{30c}$$

This simple equation is identical with the one obtained directly from the general form (18) by neglecting all terms involving the damping factor α. In general it is only roughly correct and (30b) must be used.

Equation (30b) or (30c) shows that the current amplitude will not be large over the range φ not near $n\pi$ (or βs_1 not near $m\pi$). Equation (29a) shows, on the other hand, that large values of $|I_0|$ are to be expected in the range φ near $n\pi$ (or βs_1 near $m\pi$).

Special Case 3b: The total length s is near $(2m'+1)\Lambda/4$.

With the total length s near $(2m'+1)\Lambda/4$, it is clear that when s_1 is near $m\Lambda/2$, s_2 must be near $(2n+1)\Lambda/4$. Hence the range βs_2 near $n\pi$ implies that βs_1 is near $(2m+1)\pi/2$. The inverse is similarly true.

With βs_1 near $m\pi$, φ is near $(2n+1)\pi/2$, so that Δ is small and the following inequalities may be used: $\Delta^2\alpha^2 s_2^2 \ll \theta^2$; $\alpha^2\Delta s_2 s_1 \ll 1$. Upon now setting $\beta s_1 = \beta\bar{s}_1 + m\pi$, the restriction that βs_1 is near $m\pi$ implies that $\beta\bar{s}_1$ is sufficiently small to allow the approximation, $\sin\beta s_1 = \sin\beta\bar{s}_1 \doteq \beta\bar{s}_1$. With these conditions equation (28) reduces to the following:

$$|I_0| = \frac{E_x}{lv}\left\{\frac{\theta^2+1}{\theta^2(\beta^2\bar{s}_1^2+\alpha^2 s_1^2)+1+2\theta\beta\bar{s}_1} - 1\right\}^{1/2}. \qquad (31)$$

Upon neglecting the small quantity $\alpha^2 s_1^2$ in comparison with unity, this expression becomes

$$|I_0| = \frac{E_x}{lv}\left\{\frac{\theta^2+1+(\theta\beta\bar{s}_1+1)^2}{\theta^2\alpha^2 s_1^2+(\theta\beta\bar{s}_1+1)^2}\right\}^{1/2}. \qquad (32)$$

Upon differentiating (32) with respect to $\bar{s}_2$, noting that $\bar{s}_2 = -\bar{s}_1$, and equating the derivative to zero, $|I_0|$ is found to have a maximum at $\theta\beta\bar{s}_1 - 1 = 0$. Since φ is near $(2n+1)\pi/2$, $\theta \doteq 1/\beta k$ from Table I. Hence,

$$\bar{s}_{1,m} = -k, \text{ or } s_{1,m} = m\Lambda/2 - k \qquad (32a)$$

are the positions of the maxima.

At these points, since $\theta^2 \gg 1$,

$$|I_0| = \left|\frac{E_x}{\alpha lv}\cdot\frac{1}{s_1}\right|. \qquad (32b)$$

Since k is small compared with $m\Lambda/2$ for the larger values of m, the following expression is true:

$$|I_0| \doteq \left|\frac{2E_x}{\alpha lv\Lambda}\right|\cdot\frac{1}{m} \quad (m = 4, 5, 6, \cdots). \qquad (32c)$$

Turning now to the second possibility, viz., the adjustment with βs_1 near $(2m+1)\pi/2$, and consequently with φ near $n\pi$, it is clear that

in this case Δ is large, cos βs_1 is small, and sinβs_1 is near the value 1. Under these conditions (28) becomes:

$$|I_0| = \frac{E_x}{lv}\left\{\frac{(\theta^2 + \alpha^2 s_2{}^2\Delta^2 + 1) + 1 + 4\Delta\alpha^2 s_1 s_2}{(\theta^2 + \alpha^2 s_2{}^2\Delta^2)\sin^2\beta s_1 + 2\alpha^2 s_1 s_2\Delta + \theta\sin 2\beta s_1} - 1\right\}^{1/2} \tag{33}$$

or,

$$|I_0| = \frac{E_x}{lv}\left\{\frac{(\theta^2 + \alpha^2 s_2{}^2\Delta^2)\cos^2\beta s_1 + 2\alpha^2\Delta s_1 s_2 - \theta\sin 2\beta s_1}{(\theta^2 + \alpha^2 s_2{}^2\Delta^2)\sin^2\beta s_1 + 2\alpha^2\Delta s_1 s_2 + \theta\sin 2\beta s_1}\right\}^{1/2}. \tag{33a}$$

Since the cosine is small and the sine large over the range to which this equation applies, the numerator will always be smaller than the denominator. Consequently the current amplitude $|I_0|$ will be small over this entire range, i.e., over the range βs_1 not near $m\pi$. On the other hand in the range βs_1 near $m\pi$, to which (32) applies, large amplitudes are to be expected because of the α^2 term in the denominator.

Conclusion.

By moving the bridge B_1 with the total length s fixed, large current amplitudes should be obtained whenever s_1 is of such a length that βs_1 is near $m\pi$, i.e. whenever s_1 is near $m\Lambda/2$. The nature of the resonance curves at these points differs with the total length s. When s is near $m'\Lambda/2$ the complicated equation (30b) applies; outside this range the relatively simply equation (32) must be used. The current amplitude remains small for positions of the bridge B_1 at which s_1 is not near $m\Lambda/2$ regardless of the total length s of the parallel wires.

Returning now to consider the approximation that $y \doteq s_1$, the following is significant. From the conclusions just drawn it is clear that large current amplitudes are obtained only when βs_1 is near $m\pi$. Since the conditions of the special case require in any case that $\beta x = m''\pi$ ($m'' = 1, 2, \cdots$), the writing of s_1 for y is immaterial in the arguments of the trigonometric functions. Hence, for βs_1 near $m\pi$ the major term in the numerator of (18) will be $G_y{}^2\cos^2(\beta s_1 + \delta_y)$, while the important term in the denominator will be $\alpha^2 F_s{}^2\sin^2(\beta s_1 - \gamma_s)$. The substitution of s_1 for y is, therefore, only important in the factors $G_y{}^2$ and δ_y. Referring to (19), it is evident that even these factors will be seriously affected only near the vanishing points of θ. At these points, however, even a large difference in s_1 and y could at most affect the amplitude, hence hardly at all the general shape of the resonance curves. The conclusion therefore is that to set y equal to s_1 has no significant effect on the general nature of the amplitude characteristic even when s_1 and y are not at all the same.

The final equations for the current amplitude as derived for the three special cases just considered do not, on the whole, lend themselves to a general qualitative interpretation. It would be possible to determine the position of maxima or minima over the several ranges considered, and in this way attempt to visualize the nature of the resonance curves in each case. But expressions so obtained are, for the most part, complicated and little information is gained. It is, therefore, a much more satisfactory procedure to select definite circuit constants with the aid of which the curves or families of curves corresponding to the three special cases may be computed. However, before passing from the general treatment to a particular circuit, it is essential that the conditions imposed in the course of the analysis on the constants and on the range of the variables be reviewed and interpreted. The following section will be devoted to a study of the actual type of circuit to which the analysis applies, and to the selection of suitable circuit constants to be used in the subsequent evaluation of the resonance curves of a particular circuit.

IV. Analytical Restrictions and the Application of the Theory to Experiment

In deriving (18) from the general solution (3), the following restrictions were imposed upon the circuit constants, the impressed frequency, and the range of the three variables.

(a) $$r \ll \omega l; \; g \ll \omega c$$

$$\alpha <<< 1; \; \alpha \ll \beta; \; \epsilon \ll 1.$$

Here,

$$\beta = \omega/v; \; \alpha = \frac{1}{2v}\left(\frac{r}{l} + \frac{g}{c}\right); \; \epsilon = \frac{1}{2\omega}\left(\frac{r}{l} - \frac{g}{c}\right)$$

(b) $$Z_b \doteq j\omega M$$

(c) $\alpha^2 S^2 \ll 1$; here, S may be s_1, s_2, or y

(d) $\beta^2 k^2 \ll 1$; $k = M/l$.

The significance of each of these restrictions will now be discussed in order.

(a) Using formulas given by Hund,[8] the line constants r, l, and c of a pair of parallel No. 12 wires 10 centimeters apart are found to have the following approximate values at a frequency of $\omega = 4 \times 10^8$.

[8] A. Hund, Bureau of Standards Scientific Paper, No. 491, p. 497.

$$r \doteq 8.6 \times 10^{-3}\Omega \text{ per loop cm}$$
$$l \doteq 1.8 \times 10^{-8}\, h \text{ per loop cm}$$
$$c \doteq 6 \times 10^{-14}\, f \text{ per loop cm}$$
$$g \doteq 10^{-16}\Omega^{-1} \text{ per loop cm.}^{9}$$

With these line constants, which at least represent the order of magnitude, the circuit constants α, β, and ϵ assume the following values:

$$\alpha = \frac{8.6 \times 10^{-3}}{6 \times 10^{10} \times 1.8 \times 10^{-2}} = 0.8 \times 10^{-5}\text{ cm}^{-1}$$

$$\beta = \frac{4 \times 10^{8}}{3 \times 10^{10}} = 1.33 \times 10^{-2}\text{ cm}^{-1}$$

$$\epsilon = \alpha/\beta = 0.6 \times 10^{-3}.$$

For a maximum value of α ten times that computed above, i.e., $\alpha = 8 \times 10^{-5}$, an error of not over 5 per cent in neglecting α in comparison with β, or ϵ in comparison with unity, requires that $\beta \geqq 1.6 \times 10^{-3}$, or $\omega \geqq 4.8 \times 10^{7}$, or $\Lambda \leqq 3930$ cm. For this limiting value of α, which is quite arbitrary, the theory as developed is accurate for wavelengths not exceeding 40 meters. (b) The total self-inductance M of a bridge of length 10 centimeters made of No. 12 copper wire is readily computed.[10] M is found to be about 0.09μh. The resistance of this same bridge at $\omega = 4 \times 10^{8}$ is $4.3 \times 10^{-2}\Lambda$. This is clearly negligible compared with the inductive reactance $\omega M = 36\Omega$. For a shorter or longer bridge the ratio $R/\omega M$ remains the same.

(c) For $\alpha \leqq 8 \times 10^{-5}$, a maximum error of 5 per cent in neglecting $\alpha^2 S^2$ in comparison with unity requires that $S \leqq 2800$ cm. For $\alpha \leqq 0.8 \times 10^{-5}$, S should not exceed 28,000 cm. This condition is readily satisfied in most cases.

(d) For the approximate values of M and l computed above, the equivalent length of a bridge 10 centimeters long is $k = M/l = 5$ cm, or half the separation of the wires.[11] With this value of k and the above value of β, i.e. $\beta = 1.33 \times 10^{-2}$, $(\beta k)^2 = 4.45 \times 10^{-3}$, which is certainly negligible compared with unity. For an error of not over 5 per cent in neglecting $(\beta k)^2$ in comparison with unity, $\beta \leqq 0.045$ for $k = 5$. This corresponds to $\omega \leqq 1.35 \times 10^{9}$ or $\Lambda \geqq 140$ cm. For $k = 1$, corresponding about

[9] The value of g was computed from the approximate conductivity of the air, $\lambda = 10^{-4}$ electrostatic units.

[10] Bureau of Standards Circular No. 74, formula (130).

[11] This relation between k and the separation of the wires is approximately true only when the bridge is of the same size and material as the wires and is perfectly straight.

to a separation of 2 cm of the wires, $\beta \leqq 0.22$, $\omega \leqq 6.6 \times 10^9$, $\Lambda \geqq 27$ cm. For the usual range of wavelengths measured with parallel wires, condition (d) is seen to be readily satisfied.

Summarizing the above conclusions, the theory expressed in (18) applies to circuits for which $25 \leqq \Lambda \leqq 4000$ cm, or $1.6 \times 10^{-3} \lesseqqgtr \beta \lesseqqgtr 0.22$ cm^{-1}, for $\alpha \leqq 8 \times 10^{-5}$ cm^{-1}, if the separation of the wires or the inductance of the bridges is properly chosen to satisfy the condition on k. For a different limiting value of α the range of wavelength is, of course, not the same as that given above.

In computing the resonance curves for a particular circuit, values will be arbitrarily assigned to α, β, and k. The values selected will not be chosen to fit exactly any circuit actually used experimentally, but rather to provide a typical example which is, at the same time, arithmetically relatively simple to handle. Thus a choice of $\Lambda = 400$ cm or $\beta = 0.0157$ is mathematically convenient and at the same time reasonably near the wavelength used in several experimental determinations. In deriving the wavelength characteristics of this same type of circuit,[1] k was found to equal 0.044 for $\Lambda = 4$ (measured in units of primary length) for one experimental case. Hence a choice of $k = 4$ cm with a wavelength of $\Lambda = 400$ cm is reasonable and convenient. With β and k thus assigned a choice of $\alpha = 3.93 \times 10^{-5}$ corresponds to the very convenient value of $kq = 1$ or $q = 1/4$. It will be observed that this choice of constants falls well within the limits specified above.

With the three constants α, β, and k thus selected to agree with both the requirements of the theory and the values encountered in experiment, it only remains to consider the range over which the variables s_1, s_2, and y need be studied. To be sure, an upper limit to the extension of any or each one of these has already been set in restriction (c), and it may appear at first thought that no further discussion is needed. This is true in the case of s_2 and y, but not entirely so for s_1. By definition s_2 is simply the distance along the parallel conductors measured from the bridge B_1 to the bridge B_2. Similarly y is the distance measured from B_1 to the reference point of the source of electromotive force. With s_1 the situation is not quite so simple. It will be recalled that the length of the primary is the distance from an impedanceless ammeter at $x = 0$ to the bridge B_1 at $x = s_1$. Now, from the experimental point of view an impedanceless ammeter is a pure fiction, and it is certainly true that the screen-grid resonance indicator used in experimental determinations has an impedance which is not at all negligible. In order to bring the theory as developed into harmony with this experimental fact, it will now be demonstrated that the impedance of the indicating device is electrically equivalent to a hypothetical extension of the

primary beyond its obvious length. That is, it will be shown that a pair of parallel conductors of a specified length bridged by an ammeter of impedance Z_a at one end corresponds electrically to a primary of considerably greater length bridged at the end by an impedanceless ammeter. The difference in length between the fictitious or extended primary and the actual measured length will be called the equivalent length of the impedance Z_a.

Consider a pair of parallel conductors of length S bridged at the end $x=S$ by a device with an admittance Y_a. The input admittance of such a circuit arrangement has already been given in (6). In terms of Y_a it is:

$$Y_i = \frac{1}{N}\left\{\frac{Y_aN \cosh KS + \sinh KS}{Y_aN \sinh KS + \cosh KS}\right\}. \tag{34}$$

It is desired to represent this line of length S and terminal impedance Z_a by a fictitious line of length S' (greater than S) and terminal impedance zero. The input admittance of such a line is readily obtained from (34) by letting Y_a become infinite. It is:

$$Y_i' = \frac{1}{N} \coth KS'. \tag{35}$$

If these two input admittances are to be equal, the following relation must be satisfied:

$$\frac{Y_aN \cosh KS + \sinh KS}{Y_aN \sinh KS + \cosh KS} = \coth KS' \tag{36}$$

or,

$$Y_aN(\cosh KS \sinh KS' - \sinh KS \cosh KS') = \cosh KS \cosh KS' - \sinh KS \sinh KS'. \tag{36a}$$

Using familiar transformation formulas this expression reduces to:

$$Y_a = \frac{1}{N} \coth K(S' - S). \tag{37}$$

Upon comparing (35) and (37) it is clear that the terminal admittance Y_a may be represented by a pair of parallel conductors of length $S_e = S' - S$. This length is determined by (37); it is the equivalent length S_e of the impedance Z_a. If it can be determined by experimental means, the impedance Z_a of the current indicator may be obtained using (37).[12]

[12] It may be noted that a method is here outlined for actually measuring the input impedance of ultra-high-frequency receivers. A further analysis and development of the method is reserved for a later paper.

If the length of the primary s_1 be now redefined as the total fictitious length S' corresponding to the measured length plus the equivalent length of the impedance of the ammeter, the theory as developed may be applied to the experimental case at hand. This will be true provided the length of the primary so defined does not exceed the limits imposed by restriction (c). In order to verify that it does not, and at the same time in order to obtain a general notion of the range of length of the fictitious primary with which one has to deal using the screen-grid

TABLE II

Numerical values of θ and Δ from Table I.
The value of D for Special Case 2.
$\beta=\pi/200$; $k=4$; $q=\frac{1}{4}$, ($\alpha=3.93\times10^{-5}$) $s_1=2000$

$s_2$cm	Θ	Δ	D
1	28.6	172	11.6
6	22.2	40.6	10.95
16	19.0	10.5	10.5
46	16.9	2.0	10.2
96	15.9	1.0 min.	9.95
146	14.9	2.0	9.74
176	12.8	10.5	9.0
186	9.6	40.6	7.66
191	3.2	160	3.11
192.06	0.0	257	1.75 min.
193	− 4.7	426	4.4
194	−14.1	954	8.4
195.5	−47.7 min.	8100	11.25
195.94	0.0	16000	
196	15.9	16200 max.	11.68
196.5	79.5 max.	8100	11.8
197	66.7	3240	11.8
199	36.6	426	11.7
201	28.6	160	
206	22.2	40.6	10.95
216	19.0	10.5	10.5
246	16.9	2.0	10.2
296	15.9	1.0 min.	9.95
346	14.9	2.0	9.74
376	12.8	10.5	9.0
386	9.6	40.6	7.66
391	3.2	156	3.22
392	0.99	238	3.01 min.
392.27	0.0	271	3.20
393	− 3.18	405	4.69
394	− 9.54	810	7.49
395	−15.9 min.	2025	9.60
395.73	0.0	2340	
396	15.9	4050 max.	10.75
397	47.7 max.	2025	11.2
398	41.4	810	11.6
399	35.0	405	11.40
400	30.9	238	11.38
401	28.6	156	
406	22.2	40.6	10.95
416	19.0	10.5	10.5
446	16.9	2.0	10.2
496	15.9	1.0 min.	9.95

resonance indicator, recourse must be had to experimental data. It will be shown and discussed in detail in conjunction with *Special Case 3b* that the equivalent length of the screen-grid resonance indicator at a frequency corresponding to a wavelength of 434 cm is 1467.5 cm. The total fictitious length s_1 of the primary is therefore obtained by

adding the length of the parallel conductors measured from the indicator to the bridge B_1 to this equivalent length. Referring to restriction (c) it is clear that for $\alpha \doteq 4 \times 10^{-5}$ this measured length must not exceed about 5600–1467.5 cm using the screen-grid indicator at this particular frequency. The range of s_1 is thus determined.

In concluding this section, it may be noted that the values of the three circuit constants and the ranges of the three circuit variables have been fitted to both theory and experiment. In the following section the theoretical equations will be used to compute the amplitude characteristics of a typical circuit.

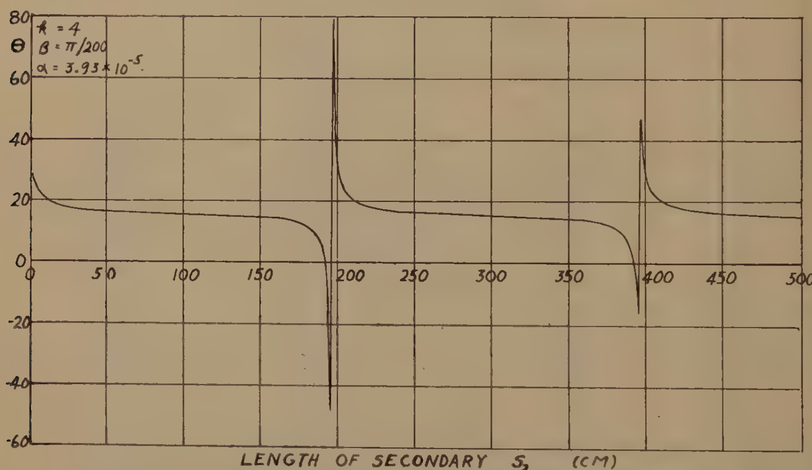

Fig. 2—The variation of θ with s_2 for the constants indicated.

V. The Resonance Curves of a Particular Circuit

In the preceding section numerical values were selected for the constants α, β, and k, and the ranges of the variables s_1, s_2, and y were discussed. In addition to appearing explicitly in the several equations, the three constants and the variable s_2 occur in the quantities θ and Δ. Hence, a first step in the application of the theory to a special circuit is the evaluation of these two quantities over the desired range of s_2. This has been done in Table II in which the values of θ and Δ are shown over a range of secondary length corresponding to a complete wavelength. Table II was evaluated from the relations given in Table I and the chosen values of the constants. Fig. 2 shows the values of θ from Table II plotted against s_2. The variation of Δ is readily visualized without plotting a curve.

Before turning to the evaluation of the special cases it will be convenient to tabulate the important quantities as follows:

Name of Quantity	Symbol	Numerical value or range
Damping constant	α	$3.93\ 10^{-5}\ \mathrm{cm}^{-1}$
Propagation constant	β	$\pi/200\ \mathrm{cm}^{-1}$
Equivalent length of bridge	k	4 cm
Wavelength of source	$\Lambda=2\pi/\beta$	400 cm
	$q=\alpha\Lambda/\beta k$	$\frac{1}{4}$
Secondary argument	$\varphi=\beta(s_2+k)$	$(\pi/200)(s_2+4)$
Amplitude	$D=\lvert I_0 lv/E_x\rvert$	
Secondary length	s_2	$s_2<5600$ cm
Primary length	s_1	$1470<s_1<5600$ cm
Position of E_x	x	$1470<x<s_1$ cm

Special Case 1: By choosing $n=1$ and $m=10$, the general conditions and the special requirements of this case, as discussed in the theoretical study, are satisfied. Then,

$$\varphi = \pi/2;\ s_2 = 96 \text{ cm};\ \theta = 15.9;\ \Delta = 1$$
$$s_1 = 2000 \text{ cm}.$$

Using array (19″) and neglecting $s_2/s_1=0.05$ in comparison with unity, the following simplification may be made:

$$\left\{\frac{1+\theta^2}{\alpha^2 F_s{}^2 \sin^2(\cot^{-1}\theta+\gamma_s)}\right\}^{1/2} \doteq \frac{1}{\alpha s_1} = 12.7.$$

Since θ^2 is large compared with unity, the following is true:

$$\frac{F_y}{F_s} \doteq \frac{y}{s_1} = 1 - \frac{x}{2000}\,.$$

Hence, (22) and (22b) yield the following:

$$D = 12.7\cos\beta x = 12.7\cos\pi x/200 \qquad (38)$$
$$1470 < x < 2000;\ x \neq 1500,\ 1700,\ 1900$$
$$D = (1 - x/2000) \text{ at } x = 1500,\quad 1700,\ 1900 \qquad (38a)$$

or,

x cm	D
1500	0.25
1700	0.15
1900	0.05

Fig. 3 shows the resonance curve plotted according to (38) and (38a).

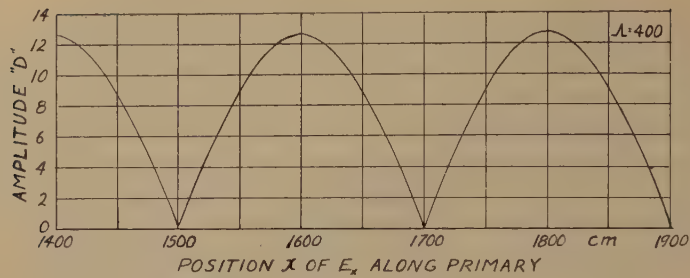

Fig. 3—Theoretical resonance curve for *Special Case 1.*

Special Case 2: By again choosing $m=10$ or $s_1=2000$ and setting $\beta x=8\pi$, the special conditions for this case are satisfied. Upon substituting in (24a), the following formula is obtained:

$$D = \left\{\frac{\theta^2}{1+6.18\times10^{-3}\theta^2}\right\}^{1/2} \quad \left.\begin{matrix}1\\201\\401\end{matrix}\right\} < s_2 < \left\{\begin{matrix}191\\391.\\591\end{matrix}\right. \tag{39a}$$

In the same way (24b) yields:

$$D = \left\{\frac{\theta^2+1.54\times10^{-9}s_2{}^2\Delta^2}{(3.08\times10^{-6}s_2\Delta+1)^2+6.18\times10^{-3}\theta^2}\right\}^{1/2}$$
$$\left.\begin{matrix}191\\391\end{matrix}\right\} < s_2 < \left\{\begin{matrix}201\\401\end{matrix}\right.. \tag{39b}$$

Using the values of θ and Δ obtained from Table II, the amplitude D is readily calculated as a function of the secondary length s_2. These values of D are also listed in Table II. Fig. 4 shows the resonance curve for *Special Case 2.*

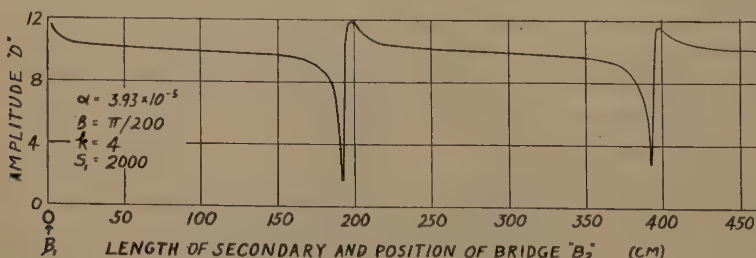

Fig. 4—Theoretical resonance curve for *Special Case 2.*

Special Case 3a: Let the bridge B_1 be moved from $s_1=1900$ to $s_1=2100$ with the total length s fixed near 2400. It is found that a very limited range of values of s yields resonance curves which completely picture

this special case. Beyond this range *Special Case 3a* merges into *Special Case 3b* in a readily visualized way. This range of s is from $s=2383$ to $s=2395$ cm. Five curves have been computed over this range of s by substituting the required values in (29a) and (30a). The computation

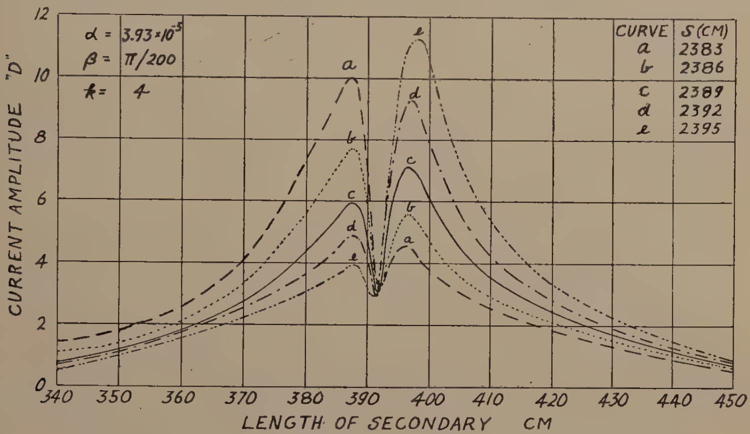

Fig. 5—Theoretical resonance curve for *Special Case 3a*.

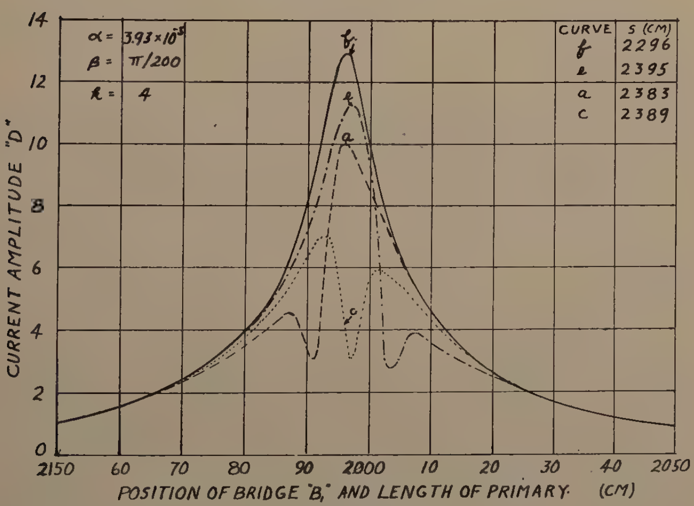

Fig. 6—Theoretical resonance curves: curves e, a, c for *Special Case 3a;* curve for *Special Case 3b*.

in this case is somewhat tedious since the formulas are not simple. The results are represented in Figs. 5 and 6. In Fig. 5 the variation in the amplitude D corresponding to the five values of s is plotted as a function of the secondary length s_2. In Fig. 6 the same amplitude of three of the five curves is plotted against the primary length s_1 as abscissa.

Special Case 3b: In this case the total length s is chosen to be $s=2296$ to satisfy the requirement that it be near $(2m'+1)\Lambda/4$. In view of the conclusions drawn in the theoretical discussion of this special case, only (32) needs to be evaluated. It is found that the range from $s_1=2050$ to $s_1=2150$ completely covers the region where the amplitude D is not small. Using formula (32) curve f of Fig. 6 was readily computed.

In this section typical resonance curves corresponding to four special cases have been computed for a particular circuit from the equations derived earlier in the paper. In the next section the method of obtaining corresponding experimental curves will be briefly described and the resonance curves will be displayed. A careful discussion and comparison of the two sets of curves is reserved for Section VII.

VI. A Review of Experimental Technique and a Display of Experimentally Obtained Resonance Curves

In a theoretical study such as this one, an appeal is made to experimental data primarily to demonstrate that approximations and restrictions made in the course of the mathematical analysis have not been so severe that the theory actually does not fit the facts it purposes to explain. If it can be shown that the theoretically derived general formulas, such as (18) in this case, lead to results in representative special cases which agree well with the corresponding experimental ones, then it is safe to assume the mathematical picture a good one. Hence, no attempt will be made at this point to explain in detail an experimental technique which has already been discussed in another paper.[2] A brief description of the apparatus and its manipulation must suffice.

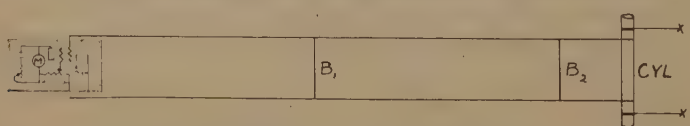

Fig. 7—Schematic diagram of the experimental arrangement. At the left is the screen-grid resonance indicator in its shielded case. B_1 and B_2 are the movable bridges. At the right is shown the brass cylinder which winds up the parallel conductors as it simultaneously unwinds the supporting cords.

The experimental set-up is shown schematically in Fig. 7. The diagram is self-explanatory. The current indicator represented is in this case the compact linear detector designed as a receiver of ultra-high frequencies. It consists of the screen-grid voltmeter[13] with all necessary batteries and control devices contained in or mounted on a shielded case. The device is described in considerable detail in another paper.[14]

[13] R. King, "A screen-grid voltmeter," Proc. I.R.E., vol. 18, p. 1388, (1930).
[14] G. H. Brown and R. King, "High Frequency Models in Antenna Investigations."

Due to the extensive shielding, which is connected to the cathode of the 224 tube, the detector is relatively insensitive as a resonance indicator if the two parallel wires are connected, respectively, to the control grid and the cathode of the tetrode. On the other hand, if only one of the wires is attached to the control grid, while the other is left free, the capacitive coupling between this latter and the shielding of the indicator case is sufficient to make the instrument highly sensitive.

The source of electromotive force is a small high-frequency oscillator coupled inductively to the two parallel conductors. Sufficiently loose coupling is maintained throughout to prevent close-coupling effects.

Special Case 1: The oscillator was mounted on a small truck in such a way that it could be moved parallel to the two wires which were stretched one above the other 10 cm apart. Precautions were taken to

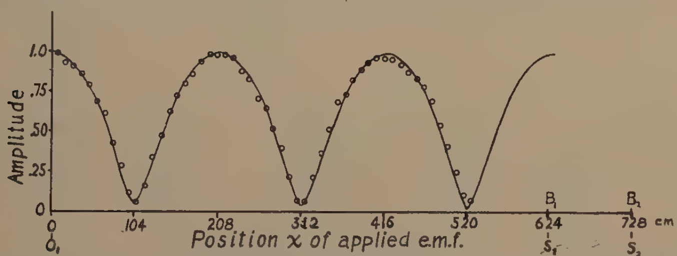

Fig. 8—Comparison of experimental and theoretical results for *Special Case 1.* The solid curve is computed; the small circles are experimental points. In each case the amplitude is reduced to unity for the first maximum on the left.

maintain a uniform coupling distance. With the oscillator coupled at any arbitrary point, a bridge B_1 was placed across the wires in a position, several half wavelengths from the indicator, such that a maximum deflection was observed. (In the theory, $(\beta s_1 + \delta_s) = m\pi$.) The remote end was then adjusted by means of the telescoping tubes or the brass cylinder so that the secondary length, i.e., the distance from the bridge B_1 to the bridged end B_2, was an odd multiple of a quarter wavelength; (in the theory, φ near $n\pi/2$). With this adjustment completed the oscillator was moved step by step along the parallel conductors, readings being taken of the indicator deflection at the successive positions along the wires of the arbitrary reference point on the oscillator. Taking the first maximum amplitude as unity, the deflections obtained are shown plotted as small circles in Fig. 8. Fig. 9 shows the same experimental data plotted according to (23). The solid curve of Fig. 8 is one computed from the theoretical formulas (22) and (22b) for the wavelength used in this experiment. The amplitude is also taken as unity.

Special Case 2: The bridge B_1 was fixed to give a maximum deflection in the same way as above, but for practical reasons at a point several half wavelengths nearer the indicator; (in the theory, $\beta s_1 = m\pi$). The oscillator was coupled to the wires at a point between B_1 and the indicator where it produced a maximum deflection; (in the theory, $\beta x = n\pi$). Since it was impossible to change the length of the secondary from zero to a whole wavelength by means of the end ad-

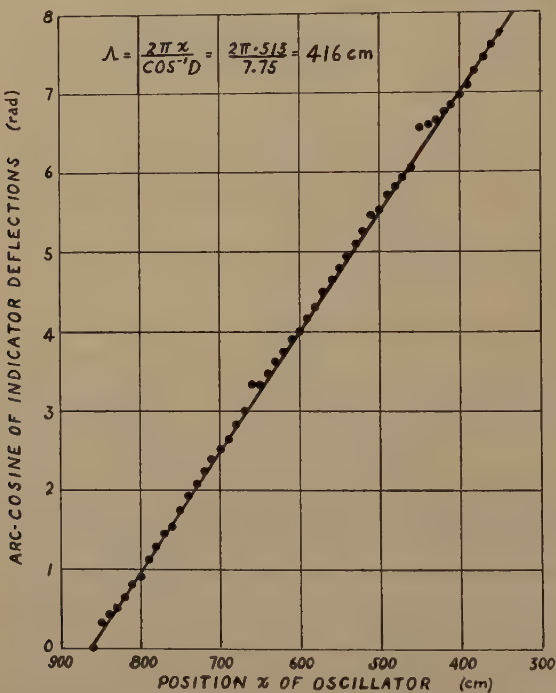

Fig. 9—The experimental points of Fig. 8 replotted according to the indicated equation. The straight-line locus is determined by these points. Its slope gives the wavelength of the source as shown.

justing device which allowed a range of only a half wavelength, the conclusions drawn in the theory in conjunction with the arrays (19′) and (19″) were invoked. Accordingly, by adjusting the length beyond the bridge B_1 in such a way that it was an odd multiple of a quarter wavelength, it had essentially no effect on the rest of the circuit. By now moving a second bridge B_2 from B_1 toward this end, the secondary (i.e. the length between the two bridges) was effectively varied as required, while the length beyond the bridge B_2, a tertiary circuit, could have essentially no effect upon the remainder of the circuit. The varia-

tion in the deflection of the current indicator with a progressive change in the length of the secondary circuit is shown in Fig. 10. Fig. 11 shows a similar characteristic observed on conductors made of flat copper braid.

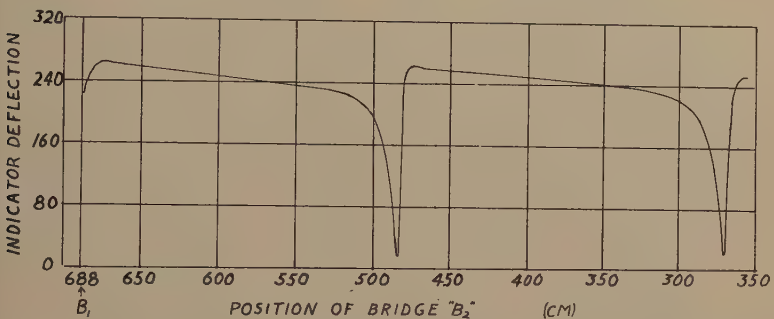

Fig. 10—Experimental resonance curve for *Special Case 2*. The conductors were No. 12 copper wire.

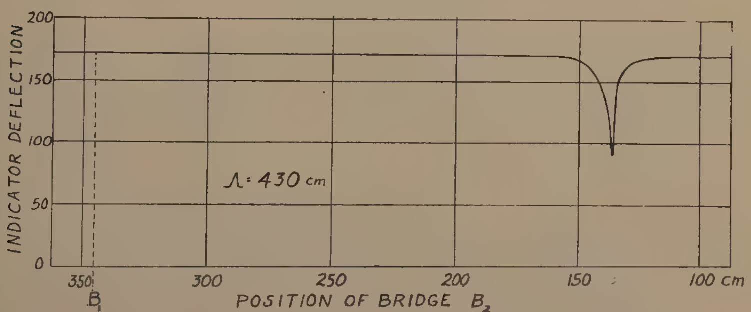

Fig. 11—Experimental resonance curve for *Special Case 2*. The conductors were flat copper braid.

Special Case 3a: With the oscillator coupled as above, and the total length of the wires adjusted to an odd multiple of a quarter wavelength beyond a point at which a single bridge on the wires produced a maximum deflection, bridge B_2 was placed successively at the points indicated in Fig. 11. For each position of B_2, B_1 was moved along the conductors and the indicator deflection was noted. The curves of Fig. 12 and of Fig. 13 are typical of the characteristics observed at intervals of a half wavelength along the wires. In Fig. 12 the abscissa is the secondary length (i.e., the length between the two bridges); in Fig. 13 the abscissa is the position of B_1 referred to the primary. Figs. 7 and 8 of reference 2 show additional characteristics of this type. Fig. 14 shows a family of curves corresponding to those shown in Fig. 12, but observed for a wire system of flat braid.

Special Case 3b: With B_2 set as indicated for curve f of Fig. 13, the bridge B_1 was moved along the wires and indicator deflections were recorded. At intervals of a half wavelength curves like f of Fig. 12 were

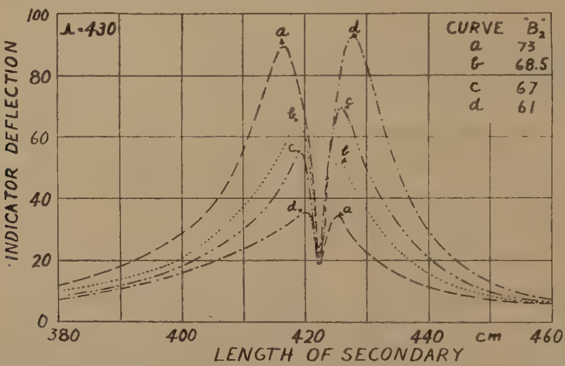

Fig. 12—Experimental resonance curve for *Special Case 3a.* The conductors were No. 12 copper wire.

observed. Figs. 6 and 8 of reference 2 show similarly obtained characteristics. Curve G of Fig. 13 is the corresponding curve observed on the flat braid parallel wire system.

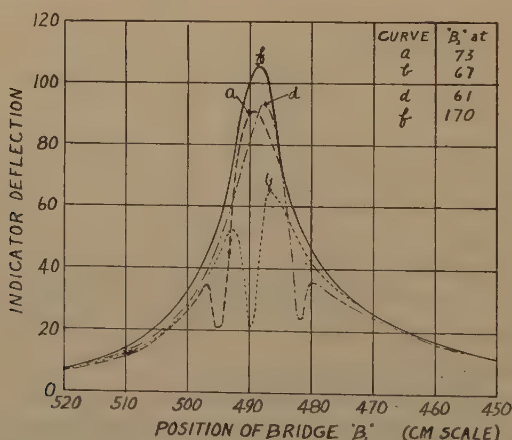

Fig. 13—Experimental resonance curves: curves a, b, d for *Special Case 3b;* curve f for *Special Case 3a.* The conductors were No. 12 copper wire.

In this section experimentally obtained resonance curves for the four special cases are displayed. They will be discussed and compared with the corresponding theoretical ones in the next section.

VII. Interpretation and Significance of the Theoretical and Experimental Results

A preliminary survey of the computed and experimentally derived curves displayed in the preceding sections cannot but leave a smile of satisfied conviction on the lips alike of the theorist and of the experimenter. The adequacy of the theory and the justification of the restrictions imposed in its derivation could hardly be better demonstrated than by comparing in the preceding sections the corresponding pairs of characteristics. In the sequel each of the special cases will be discussed; a few general comments are reserved as a conclusion to this section.

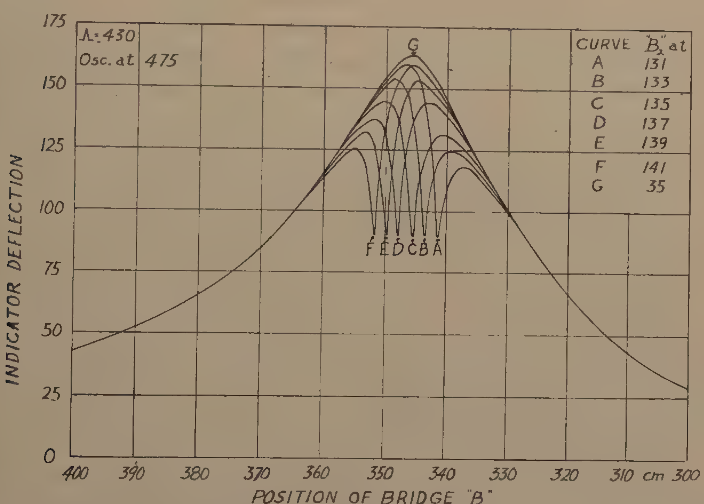

Fig. 14—Experimental resonance curves: curves *A* to *F* for *Special Case 3b;* curve *G* for *Special Case 3a.* The conductors were flat copper braid.

Special Case 1: The (solid) theoretical curve of Fig. 8 and the experimentally determined points (small circles) are in exact agreement if due allowance is made for fluctuations in the experimental values due to no very accurate control over the coupling distance between the oscillator and the parallel wire system. This distance may easily have varied by 5 per cent; (see reference 2 for details). It will be observed that this special case completely verifies the form of (22), but that it throws no light on the quantities contained in the amplitude factor, since both in the theory and the experiment this is purely relative.

The excellent correspondence between theory and experiment and the great simplicity of (22) suggests that a method might well be

devised for the measurement of ultra-radio waves using the arrangement of this special case. As Hoag[6] has recently pointed out, the usual Lecher wire method of determining the separation between resonance peaks (of the type to be discussed in Special Case 3b) is not precise when wavelengths of the order of a meter or less are to be measured. This is a consequence of the fact that it is not practicable to increase the accuracy with which the position of resonance peaks can be determined beyond a certain limit regardless of the wavelength. The relative error for short wavelengths is therefore larger than for long ones. In the following method, suggested by that of Hoag and by (23), this difficulty is avoided.

Consider a small parallel wire system so arranged that it can be moved relative to the source of the frequency which is to be measured. If it is more convenient the source may be moved instead of the wire system, but the former method involves no practical difficulties since the Lecher wires need not be over 150 or 200 centimeters long. They may be stretched one above the other over a suitable board equipped with a scale, and with the resonance indicator mounted on one end. With either arrangement the only precautions to be observed are that the coupling distance between the source and the wires must be maintained constant as the two are moved relative to each other, and that it be not so short that close coupling effects are observable. The preliminary adjustment of the wire system involves nothing further than the placing of a bridge at some point near the end remote from the indicator where a satisfactory deflection is obtained in this latter. The wire system is now moved relative to the source a centimeter or two at a time, and the deflection D of the indicator recorded. By plotting the position x along the wires, as measured from any convenient reference point, against the arc-cosine of the ratio D/D_{max}, the slope of the straight line drawn through the points is $\Lambda/2\pi$. Here Λ is the wavelength of the source. It will be observed that no critical adjustments, such as that of the input admittance of the wire system in the method of Hoag, are required in this case; (see footnote 7). In Fig. 9 the experimental data of Fig. 8 are replotted according to the method just outlined. It is an easy matter to draw a straight line through this large number of points and at once determine the wavelength from its slope. Several points seem to lie a relatively large distance from the line; actually the error in the deflection observed for these points is not over 3 per cent. By suitably constructed apparatus this method may be made both convenient and precise for measuring ultra-short waves.

Special Case 2: In *Special Case 1* the constants α and k entered only into the amplitude factor and not at all into the factor determining the

shape of the resonance curve. In this case all the constants are important in affecting both the amplitude and the shape of the characteristic. In order to reveal the part played by each of the constants, as well as

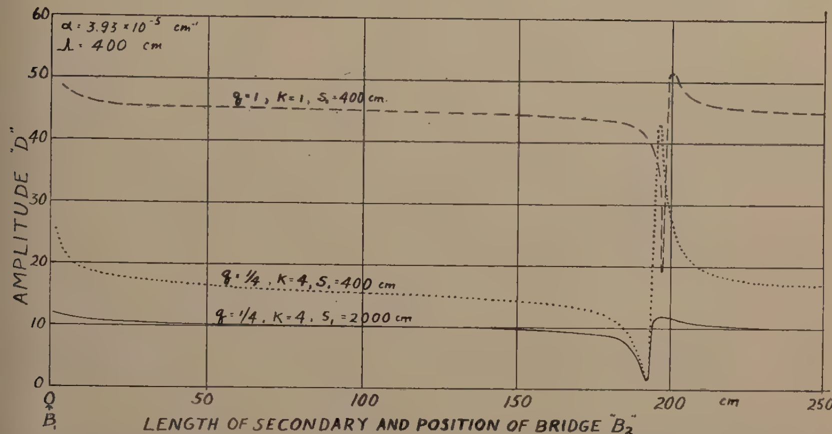

Fig. 15—Theoretical resonance curves for *Special Case 2* for different values of the constant k and the length s_1.

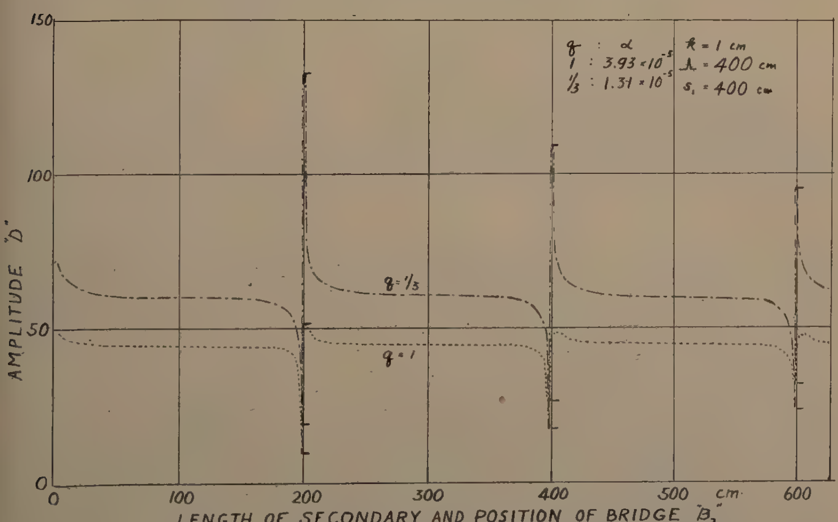

Fig. 16—Theoretical resonance curves for *Special Case 2* for two different values of the damping constant α.

by the total length s_1 of the primary, the curves of Figs. 15 and 16 were computed from (25a) and (25b) in the same way as Fig. 4. Completely new computations of θ and Δ were, of course, involved. It is seen that the position of the minima relative to the points $s_2 = n\Lambda/2$

are determined primarily by the value of k. They are all shifted toward the indicator by an amount roughly equal to the sum of the equivalent lengths of the two bridges B_1 and B_2. This is entirely reasonable. In this case the shift is approximately $2k$ since the bridges are alike. The amplitude, especially of the maximum points, is determined largely by α and the length s_1. A comparison of the theoretical curve of Fig. 4, with the experimental one of Fig. 10 shows good agreement. The theoretical damping constant is evidently somewhat larger than that of the system of No. 12 copper conductors used in obtaining Fig. 9. On the other hand the value of α in the experimental curve of Fig. 11, which was obtained using conductors of flat copper braid is clearly larger than the value used in the theory. A difference in k, of course, also plays a part.

As a method of wavelength measurement this method, previously referred to as the minimum deflection method, is entirely satisfactory.

TABLE III

Special Case 2, Minimum Deflection Method

Position of minimum	Half Wavelength
1391.5* cm	210.5** cm
1181.0	217.0
964.0	217.0
747.0	217.0
530.0	217.0
313.0	

* This is the position of the fixed bridge B_1.

** In agreement with the theory the distance from B_1 to the first minimum is less than a half wavelength. The amount of this shortening should be approximately $2k$ centimeters. In this case, then, k is about 3.25 centimeters. Since this data was taken on a wire system made of flat copper braid while the bridge was of No. 12 copper wire, $k = M/l$ would not be one half the wire separation.

The distance from the fixed bridge B_1 to the first minimum or "dip" is about $2k$ less than a half wavelength, but the separation of the succeeding "dips" is very nearly a half wavelength. Table III shows the experimental data obtained on a long parallel wire system. It agrees entirely with the statements just made.

Special Case 3a: This is the "double-hump" phenomenon discussed in various ways by Takagishi,[3] Mohammed and Kantabet,[15] and more recently by Hikosaburo.[16] A comparison of the curves of Figs. 5 and 11, or of Figs. 6 and 13, shows that the present theory completely describes the experimental observations. Fig. 14 shows curves analogous to those of Fig. 13 but for the circuit having higher damping. Figs. 5 and 10 show that here, just as in the preceding case, there is a shift of about $2k$ toward the indicator end. This is, of course, to be expected since both bridges again play a part. Clearly the double peaks occur when-

[15] Proc. I.R.E., vol. 19, p. 1983, (1931).
[16] Proc. I.R.E., vol. 21, p. 303, (1933).

ever the primary comes into resonance at or near the same position of the movable bridge B_1 as does the secondary. The way in which the double peaks grow and shrink with different adjustments of the total length is readily followed in the curves. The extent to which the constants of the circuit determine the depth of the "dips" may be analyzed using (29a).

The double peaks are not convenient for wavelength measurement. They have been considered here primarily to show that the "double-hump" is, in fact, no remarkable phenomenon at all. The appearance of two or more peaks in the amplitude characteristics of filter circuits having two or more similar sections is well known. The fact that in this case the circuits have distributed constants instead of lumped ones in no way alters the general theory underlying the problem. This is evident from the results here given.

Special Case 3b: The amplitude characteristics obtained in this case are the ordinary resonance peaks of the conventional way of measuring wavelength by the Lecher wire method. The theory shows and experiment agrees that the maxima occur at intervals of exactly a half wavelength. Their shape and amplitude depend upon α and s_1; their position relative to the points $s_1 = m\Lambda/2$ is determined by the value of k. In this case all the peaks are shifted exactly k centimeters toward the resonance indicator. The theoretical and experimental curves of Figs. 6, 13, and 14 show that the peaks obtained in this case are the envelopes of the double peaks described above. For wavelengths of over a meter the method of this special case is the most convenient and quite accurate.

In concluding Section IV it was stated that the equivalent length of the resonance indicator was experimentally determined to be 1467.5 centimeters. The method by which this value was obtained will now be described, since it depends upon *Special Case 3b*. It was shown by (32c) that the maximum amplitude of the peaks in this case is inversely proportional to their half wavelength number m. That is, if the first peak nearest the impedanceless ammeter has an amplitude 1, the second one will be one-half as high, the third one-third as high, or in general, the mth peak will be $1/m$ times the height of the first peak. In the fourth column of Table IV are tabulated the observed amplitudes of six resonance peaks as measured by the deflections of the current indicator located at the scale point recorded in the table. By dividing these amplitudes by the factor 925, the decimals given in the fifth column are obtained. A comparison of these with the values of $1/m$ given in the sixth column, shows that these six peaks are peak numbers

TABLE IV

Observed peak No.	Scale position in cm*	Half wavelength $\Lambda/2$	Observed amplitude	Observed amplitude divided by 925	Theoretical $1/m$	Theoretical peak No.
2	1391.5	217.0	117	0.126	1/8 = 0.125	8
3	1174.5	217.5	101	0.110	1/9 = 0.111	9
4	957.0	217.0	92	0.100	1/10 = 0.100	10
5	740.0	217.0	84	0.091	1/11 = 0.091	11
6	523.0	216.5	78	0.084	1/12 = 0.083	12
7	306.5		71	0.077	1/13 = 0.077	13

Current indicator at 1660.0; Oscillator coupled at 1590; *To nearest 0.5 cm.

Equivalent length of current indicator (8×217) − (1660 − 1391.5) = 1467.5 cm.

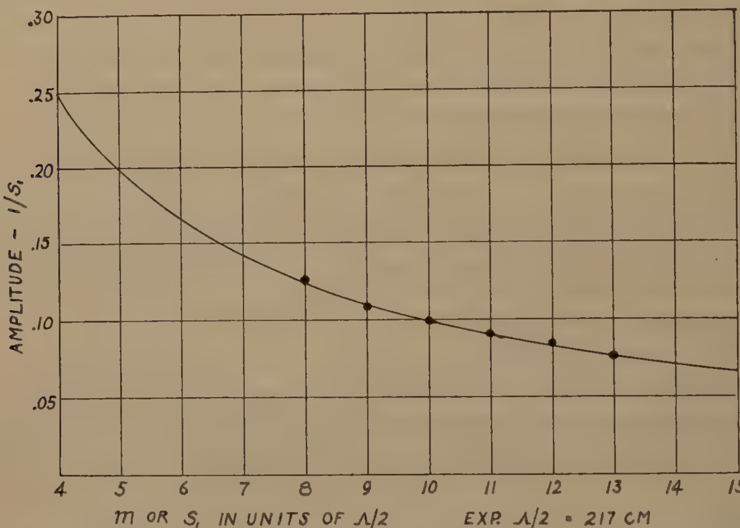

Fig. 17—Theoretical $1/s$ curve and six experimental amplitudes plotted as points.

8 to 13 on an equivalent parallel system bridged by an impedanceless ammeter. Actually they are peaks numbers 2 to 7 on the system bridged by an ammeter having an impedance Z_a. The last two columns of Table IV are shown plotted in Fig. 17. The solid curve is a $1/s$ curve, the plotted points are the experimentally observed amplitudes reduced to a suitable scale.

From the measured wavelength of 434 cm, the length of the fictitious system from observed peak number 2 (theoretical peak number 8) to the hypothetical impedanceless ammeter can be readily calculated to be 1736 cm. The actual distance from this peak to the current indicator was 1660 − 1391.5 = 268.5 cm. Hence the equivalent length of the indicator is 1736 − 268.5 = 1467.5 cm. From the constants of the parallel wire system and this length the actual impedance of the current in-

dicator may be readily computed using (37). The significance of this result should not be underestimated. Let it be emphasized that an experimental method has been devised by which impedances may be measured accurately at ultra-high frequencies. For if the impedance of the detector is known, small impedances connected in series with it may be measured.

In this section the beautiful and complete agreement of theory and experiment has been pointed out, and the significance of the several special cases has been discussed. In the application of the theory to a particular circuit, let it be recalled, no attempt was made to select constants such that the computed curves would exactly fit the experimental data available. The values selected were chosen, rather, as representative, hence the theoretical characteristics are not to be expected to coincide identically with the experimental ones. As a matter of fact they do correspond very closely.

A word is in order with regard to the comparative amplitudes of the characteristics of the several special cases. For the theoretical curves the amplitude "D" is plotted as ordinate in each case, so that an intercomparison of characteristics is possible. With the experimental data, however, the indicator deflection plotted as ordinate differs in almost every instance, since the respective curves were recorded at different times using two different forms of the indicator with conveniently adjusted sensitivity. Evidently, then, an intercomparison of amplitudes is not possible. For this reason data were taken successively for the three special cases to compare the maximum amplitudes. It was found that this was essentially the same in all three cases; that is, the amplitude of Fig. 8, the maximum point of Fig. 9, and the peak of Fig. 12 would all be very nearly the same, if the same indicator adjusted to the same sensitivity had been used for each. A comparison of the theoretical curves shows that here, too, the amplitudes are practically the same.

Throughout the analysis it has been tacitly assumed that the current indicating device is an impedanceless ammeter the deflections of which are proportional to, or at least a known function of the high-frequency current flowing through the instrument. It was theoretically and experimentally shown that it is possible to substitute for the resonance indicator with its impedance Z_a, an impedanceless fictitious ammeter and a definite length of parallel conductors. But whether it be the actual current indicator or the fictitious one that is considered, it is none the less true that the theoretical as well as the experimental curves have been plotted on the assumption that the amplitude "D" and the observed indicator deflection are linearly related to the resonance current passing through the device. The question evidently

arises: Is the deflection of the indicating milliammeter a linear function of the resonance current? Or, more in particular, does the screen-grid voltmeter connected across the ends of a pair of parallel wires actually function as an impedanceless ammeter at the end of a fictitious length of line? It was shown in a previous paper[14] that the screen-grid volt-meter when used as a detector of ultra-radio waves in space is indeed a linear rectifier. An even more conclusive proof than that referred to above is, however, the agreement between theory and experiment in each and all of the cases here analyzed. If the screen-grid detector did not have the linear characteristic as presupposed, then the points on Fig. 8a for example, could not possibly lie along a straight line. A further significant result of the theoretical analysis is, therefore, the development of an experimental means for studying the detection characteristics of short-wave receivers. In particular, the linear characteristic of the screen-grid voltmeter has been definitely verified.

VIII. Summary and Conclusions

The following are the significant achievements of this theoretical investigation supplemented by experimental studies:

(1). The basic mathematical theory of bridge-coupled circuits having distributed constants has been developed and applied to important special cases. (Sections I, II, and III.)

(2). A careful study has been made of the physical conditions under which the theory may be applied to actual circuits. (Section IV.)

(3). The theory and all its implications have been shown to be completely verified by a detailed comparison of computed and observed amplitude characteristics in four widely different and important special cases. (Sections V, VI, and VII.)

(4). A new precision method for measuring ultra-short waves has been described and demonstrated. (*Special Case 1*, Section VII.)

(5). The maximum deflection and the minimum deflection methods for the measurement of wavelengths are shown to be exact. (*Special Cases 3b* and *2*, Section VII.)

(6). The "double-hump" phenomenon is discussed and shown to be merely a special case of the coupled circuit theory here developed. (*Special Case 3a*, Section VII.)

(7). A method is described for experimentally determining the characteristics of short-wave detectors and for measuring their input impedance at ultra-high frequencies. The method is applied to show that the screen-grid voltmeter has a linear resonance current indicator deflection characteristic, and that its input impedance is the same as that of a definite length of parallel conductors.

Finally this investigation has once again demonstrated the fruitfulness of combined theoretical and experimental study. It is hoped that the results obtained may prove of value in the ultra-high-frequency field.

Appendix

The Evaluation of the Quantities θ and Δ

Before proceeding to derive the expressions for θ and Δ from (14) and (15) the following condition will be assumed satisfied by the constant k:

Restriction d: The equivalent length of each bridge B is sufficiently small to satisfy the inequality:

$$(\beta k)^2 \ll 1. \tag{d}$$

As a consequence of (d) it is also true that

$$\tan \beta k \doteq \beta k. \tag{d'}$$

Let the following notation be introduced:

$$\begin{aligned} \varphi &= (\beta s_2 + \tan^{-1} \beta k) \doteq \beta(s_2 + k) \\ a &= (\cos \beta s_2 - \beta k \sin \beta s_2) = \sqrt{1 + \beta^2 k^2} \cos \varphi \doteq \cos \varphi \\ b &= (\sin \beta s_2 + \beta k \cos \beta s_2) = \sqrt{1 + \beta^2 k^2} \sin \varphi \doteq \sin \varphi. \end{aligned} \tag{I–1}$$

With these symbols (14) and (15) give:

$$\begin{aligned} \alpha s_2 \Delta - j\theta &= -j/\beta k + \left\{ \frac{a + j\alpha s_2 b}{\alpha s_2 a + jb} \right\} \\ &= \frac{\alpha s_2 (a^2 + b^2)}{\alpha^2 s_2^2 a^2 + b^2} - j\left\{ 1/\beta k + \frac{ab(1 - \alpha^2 s_2^2)}{\alpha^2 s_2^2 a^2 + b^2} \right\}. \end{aligned} \tag{I–2}$$

Upon neglecting $\alpha^2 s_2^2$ as compared with unity according to (c), the complete expressions for θ and Δ are:

$$\theta = 1/\beta k + \frac{1}{\alpha^2 s_2^2 \cot \varphi + \tan \varphi} \tag{I–3}$$

$$\Delta = \frac{1}{\alpha^2 s_2^2 \cos^2 \varphi + \sin^2 \varphi}. \tag{I–4}$$

For the argument φ (as defined by (I–1)) not near $n\pi$, ($n = 1, 2, 3, \cdots$), these expressions reduce to the simple forms given below:

$$\theta = 1/\beta k + \cot \varphi \tag{I–5}$$

$$\Delta = \csc^2 \varphi \tag{I–6}$$

For the argument φ near $n\pi$ the following relations are true:

$$\tan\varphi \doteq \sin\varphi \doteq \varphi;\ \cos\varphi \doteq 1 \tag{I-7}$$

$$s_2 = n\Lambda/2 + \bar{s}_2$$

$$\alpha^2 s_2^2 = \alpha^2 n^2 \Lambda^2/4.$$

Here $\bar{s}_2$ is a small length measured in either the positive or negative direction of s_2 from the point $s_2 = n\Lambda/2$.

With these approximations θ and Δ have the following values in the neighborhood of the points $s_2 = n\Lambda/2$:

$$\theta_n = \frac{1}{\beta k} + \frac{\varphi}{\alpha^2 s_2^2 + \varphi^2} = \frac{1}{\beta k} + \frac{4\beta(\bar{s}_2 + k)}{\alpha^2 n^2 \Lambda^2 + 4\beta^2(\bar{s}_2 + k)^2} \tag{I-8}$$

$$\Delta_n = \frac{1}{\alpha^2 s_2^2 + \varphi^2} = \frac{4}{\alpha^2 n^2 \Lambda^2 + \beta^2(\bar{s}_2 + k)^2}. \tag{I-9}$$

It is now convenient to introduce a new constant to replace the damping constant α. Let the quantity q be defined as follows:

$$q = \frac{\alpha\Lambda}{\beta k}. \tag{I-10}$$

In terms of this new constant, (I–8) and (I–9) become:

$$\theta_n = \frac{1}{\beta k}\left[1 + \frac{4(1 + \bar{s}_2/k)}{q^2 n^2 + 4(1 + \bar{s}_2/k)^2}\right] \tag{I-8a}$$

$$\Delta_n = \frac{1}{\beta^2 k^2}\left[\frac{4}{q^2 n^2 + 4(1 + \bar{s}_2/k)^2}\right]. \tag{I-9a}$$

In the range of φ near $n\pi$, (or what is practically the same, s_2 near $n\Lambda/2$), there are several important and interesting points. These include the maxima, the minima, and the zeros of θ_n and the maxima of Δ_n. By equating θ_n in (I–8a) to zero, the vanishing points of θ_n are found to be at

$$\bar{s}_{2,n}''' = \frac{n\Lambda}{2} + \bar{s}_{2,n}''' = \frac{n\Lambda}{2} - \frac{k}{2}(3 \mp \sqrt{1 - q^2 n^2}). \tag{I-11}$$

By differentiating θ_n with respect to s_2 in (I–8a) and equating the derivative to zero, the extreme values of θ_n are easily shown to be at

$$s_{2,n}'' = \frac{n\Lambda}{2} + \bar{s}_{2,n}'' = \frac{n\Lambda}{2} - k\left(1 \mp \frac{nq}{2}\right). \tag{I-12}$$

Here the upper sign refers to the position of the maxima, the lower sign to the position of the minima.

By equating the derivative of Δ_n with respect to s_2 in equation (I–9a) to zero, Δ_n is found to have maxima at the following points:

$$s'_{2,n} = \frac{n\Lambda}{2} + \bar{s}'_{2,n} = \frac{n\Lambda}{2} - k. \tag{I–13}$$

With the aid of the values of s_2 obtained above, Table I, showing the values of θ and Δ, was easily evaluated. From it the general variations of θ and Δ with s_2 are readily visualized as follows. In general shape and period θ follows a cotangent curve having for its zero line the positive ordinate $1/\beta k$. The argument is $\beta(s_2+k)$. From this it is clear that there is an effective shortening of the secondary by an amount k. The name, equivalent length of the bridge, for k is thus seen to have a definite meaning. Instead of becoming infinite as the cotangent, θ reaches a definite maximum for values of s_2 slightly less than $n\Lambda/2-k$, and then drops to a minimum slightly beyond this value. This minimum will be positive, zero, or negative according as qn is greater than, equal to, or less than 1. If it is negative θ_n will have two zero points symmetrically placed with respect to the abscissas $s_2=n\Lambda/2-3k/2$. The variation of Δ with s_2 follows very closely the curve of the cosecant squared of the argument $\beta(s_2+k)$. Instead of becoming infinite, however, a definite maximum is reached at the points $s_2=n\Lambda/2-k$.

The convenience of using the constant q instead of α is apparent from Table I and the above discussion. Throughout it is the quantity nq which enters into the expressions for the significant quantities.

Proceedings of the Institute of Radio Engineers
Volume 21, Number 8 *August, 193*

FREQUENCY MODULATION AND THE EFFECTS OF A PERIODIC CAPACITY VARIATION IN A NONDISSIPATIVE OSCILLATORY CIRCUIT*

By
W. L. Barrow
(Massachusetts Institute of Technology, Round Hill Research Division, South Dartmouth, Mass.)

Summary—*Certain fundamental characteristics of the theory of frequency modulation for arbitrarily large degrees of modulation and unrestricted modulation frequencies are developed from the differential equation for a dissipationless circuit with fixed inductance and variable capacitance. The several modes of modulating the frequency are discussed and classified; it is shown that they give the same results only when the amount of modulation is very small. The case of "inverse capacity modulation" is then treated in detail. This treatment discloses the possibility of unstable oscillations occurring with certain values of the parameters; the nature and physical significance of these unstable oscillations are determined, and it is explained why they are not ordinarily observable in radio-frequency modulation or in the warble tone generator. The frequency spectrum of the stable oscillations is found, and a means of calculating the amplitude given. For certain adjustments of the circuit the oscillations may be represented by a true Fourier series, while in general this is not the case. Frequency modulation in radiotelephony, the warble tone, and the special case where the natural period of the unmodulated circuit and the frequency of modulation are of comparable magnitude, represent successively more complicated cases of the same general phenomena; the latter is of special interest. The nature of the phenomena accompanying other than a sinusoidal inverse capacity variation is mentioned.*

Introduction

Lord Rayleigh seems to have been the first to have given a theoretical explanation of the oscillations of a system in which the stiffness parameter is periodically varied, and in 1887 published[1] an excellent discussion of some of the types of oscillations of a string whose tension is periodically altered. His mention at that time of the corresponding situation in an electric circuit anticipated the interest to be given this kind of vibratory motion some thirty years later in the fields of radio communication and electro-acoustics. In 1922 J. R. Carson[2] discussed from the point of view of radiotelephony the actual electric circuit with inductance and a sinusoidally varying capacitance. During the last several years quite a few workers have given attention to various aspects of such modulation phenomena, especially in connection with its effects on the quality of wireless telephone transmis-

* Decimal classification: R148. Original manuscript received by the Institute, March 2, 1933.

[1] Numbers refer to Bibliography.

sion. The introduction of a "warble tone," often described as a tone whose frequency is periodically varied but whose amplitude, i.e. whose envelope, remains constant, into the technique of acoustical measurements for the purpose of mitigating undesired space and time interference has also supplied a growing interest in this kind of an oscillation, since it is usually by means of a vacuum tube oscillator in conjunction with a rotating condenser that the warble tone is produced.

Lord Rayleigh's treatment may be safely said to deal only with the case where the frequency of variation of the capacitance is twice the natural frequency of the circuit. The radio application discussed by Carson, on the other hand, is characterized by having both the frequency of variation of the capacitance and the magnitude of this variation (expressed as a variation of the frequency) so small compared to the natural frequency of the circuit that they may both be considered as second-order effects. Often the magnitude of the frequency variation in the warble tone is of the same order of magnitude as the natural frequency, and the frequency of variation is by no means a small quantity, so that in this case neither of the above theories is suitable. The nature of some of the types of oscillation occurring here have been discussed by the author from experimental evidence.

A theoretical treatment of the warble tone case is of considerable importance and displays some phenomena not at once apparent from the experimental work done heretofore. Besides this there are several points that may well receive attention in the radio case and which, it is believed, are not generally recognized. Finally, the physically very interesting situation existing when the natural period of the circuit and the period of the variation are of the same order of magnitude well deserves a detailed analysis.

The present paper attempts to give the theory of frequency modulation in its broadest sense without imposing limitations peculiar to any particular application. In doing this the individual characteristics of the several special applications will be developed and correlated.

The Differential Equation

The circuit under consideration consists of a pure inductance of constant value L connected in series with a pure capacitance $C(t)$, which is varied in some definite periodic way with the time t; there is no resistance in the circuit. One way to approximate physically the above conditions is to associate a three-electrode vacuum tube with an R, L, C circuit in one of the many oscillator connections, the effect of which may be considered as introducing just sufficient negative resistance to cancel the actual (positive) resistance R of the circuit, giving

as a result a circuit composed only of inductance and capacitance. The circuit thus formed differs from the idealized one treated in this paper as nonlinearity of the vacuum tube, etc., may prevent the oscillator from functioning so that the total resistance of the tuned circuit is exactly zero at every instance of time (the condition assumed in the following analysis), but for the purposes of this discussion the idealized representation of $R \equiv 0$ will suffice to bring out the salient characteristics of the actual oscillator.

Equating the potential difference across the inductance to that across the capacitance gives at once, where Q denotes the charge on the condenser and the dots denote differentiation with respect to time,

$$\ddot{Q} + \frac{1}{L \cdot C(t)} Q = 0 \tag{1}$$

which is the differential equation determining the performance of the circuit.

It is now necessary to select a specific function of t for the varying capacitance $C(t)$. The latter may, by suitably designing the plates of a rotating condenser, etc., be varied in almost any manner, but of all possible types of variation only three have any particular importance for us. Accordingly, the coefficient of Q in (1), viz., $1/L \cdot C(t)$, and the corresponding differential equation will be derived for these three cases.

First, it will be assumed that the capacitance is so varied that it has the form $C(t) = C_0 + \Delta C \cos \alpha t$. Assuming $\Delta C < C_0$, which is always true in a practical circuit, and denoting the natural frequency* of the circuit without variation $\sqrt{1/L \cdot C_0}$ by ω_0, a binomial expansion of $C(t)$ leads directly to the expression

$$\frac{1}{L \cdot C(t)} = \omega_0^2 - \omega_0^4 (L \cdot \Delta C) \cos \alpha t + \omega_0^6 (L \cdot \Delta C)^2 \cos^2 \alpha t - \cdots. \tag{2}$$

From (2) it is at once clear that the general equation (1) has the form

$$\ddot{Q} + (\theta_0 + \theta_1 \cos \alpha t + \theta_2 \cos 2\alpha t + \cdots) Q = 0 \tag{3}$$

where,

$$\theta_0, \theta_1, \theta_2, \cdots$$

are the constants obtained after completing the operations contained

* For brevity in text and formulas the word *frequency* will be used throughout this paper to mean *angular velocity* $= \omega_0 = 2\pi f$.

in (2) and rearranging according to ascending frequencies $\alpha, 2\alpha, \cdots$.† It seems quite reasonable to call this type of variation "direct capacity modulation," which term will be used throughout this paper. If the limitation be imposed that $\Delta C/C_0 \ll 1$ the square and higher power terms in (2) can be neglected; there is then no difficulty in showing that

$$\frac{1}{L \cdot C(t)} \cong \omega_0^2\left(1 - \frac{\Delta C}{C_0}\cos\alpha t\right) \cong \omega_0^2\left(1 + 2\frac{\Delta\omega}{\omega_0}\cos\alpha t\right), \tag{4}$$

where $\Delta\omega$ denotes the absolute frequency change, i.e. the difference between ω_0 and $\omega_0(1-\Delta C/C)^{1/2}$, so that the differential equation for this limited case becomes

$$\ddot{Q} + (\omega_0^2 + 2\omega_0 \cdot \Delta\omega \cos \alpha t) = 0, \qquad \Delta C \ll C_0. \tag{3a}$$

The conditions imposed on (3a) allow validity only when the absolute frequency change is very small compared to the natural frequency; this is thought to be true in frequency modulation occurring in radiotelephony, and indeed (3a) forms the basis of the analyses given for this case by Carson, van der Pol[3] and others.

A second type of variation of interest may be constituted as follows: We note that our fundamental equation (1) is of the form

$$\ddot{Q} + \Omega^2(t) \cdot Q = 0 \tag{5}$$

where $\Omega^2(t)$ is a periodic function of the time, and would correspond to the square of the frequency if $\Omega = \text{constant} \neq \Omega(t)$. Instead of formulating our problem for a sinusoidally varying capacity let us take such a variation that $\Omega(t) = \omega_0 + \Delta\omega \cos \alpha t$, whereupon (5) gives the differential equation

$$\ddot{Q} + \left(\omega_0^2 + \frac{\Delta\omega^2}{2} + 2\omega_0 \cdot \Delta\omega \cos \alpha t + \frac{\Delta\omega^2}{2} \cos 2\alpha t\right)Q = 0 \tag{6}$$

valid for all values of ω_0 and $\Delta\omega$.

This second type of variation leading to (6) will be called "pure frequency modulation." When $\Delta\omega$ is allowed to assume a relatively large magnitude compared to ω_0 the equation as above must be solved, but if small variations alone are of interest this reduces to

$$\ddot{Q} + (\omega_0^2 + 2\omega_0 \cdot \Delta\omega \cos \alpha t)Q = 0, \qquad \Delta\omega \ll \omega_0 \tag{6a}$$

† This equation is of the Hill type and presents formidable difficulties. Only when the highest θ present is θ_2 are the properties of the solutions known. (Reference: Ince, "Ordinary Differential Equations," p. 507.) Equation (6) is a particular case of the Hill equation, called the Whittaker equation;[4] of particular interest here is Ince's discussion of the existence, stability, etc., of the periodic solutions.[5]

which is identically the equation arising for small variations with direct capacity modulation, i.e. (3a).

A third type of variation is of great importance; first, because it corresponds to the important practical case of a condenser microphone connected in an oscillating circuit (such, for example, as the circuit used with the Siemens-Halske condenser microphone), and second, because it leads to the simplest differential equation. This type of variation is characterized by having the distance between the condenser plates oscillate in a simple harmonic manner about a mean distance d_0; if $h \cdot d_0 (h<1)$ is the amplitude of this oscillation and α the frequency, the capacitance as a function of time is given by $C(t) = \text{const.}/(d_0 + hd_0 \cos \alpha t)$, and (1) assumes the form

$$\ddot{Q} + (\omega_0^2 + h \cdot \omega_0^2 \cos \alpha t)Q = 0. \tag{7}$$

A comparison with (3) and (6) shows that the general equation here is far simpler than in the other two types of variation previously discussed. In view of the way in which (7) arises this third type of variation will be called "inverse capacity modulation." It is easy to show that when $h \ll 1$, (7) also reduces to the common form (3a) or (6a) assumed by all types of modulation for small variations.

The term *frequency modulation* is now generally applied only to the radio case where both the magnitude of the variation and the variation frequency are small compared to the natural frequency. In a discussion such as is undertaken in this paper, it seems advisable to use the term without reservation, but to state expressly the limitations imposed when special cases are being considered. The reasons for the distinction made above between "direct capacity," "pure frequency," and "inverse capacity" modulations are made, it is thought, sufficiently clear.

Tabulating the results of this section, it is seen that the three principal types of modulation lead to the following differential equations representing the phenomena in the circuit for all values of the parameters:

I. Direct capacity modulation:

$$\ddot{Q} + \left(\omega_0^2 + \omega_0^2 \frac{\Delta C}{C} \cos \alpha t + \omega_0^2 \left(\frac{\Delta C}{C}\right)^2 \cos 2\alpha t + \cdots \right)Q = 0.$$

II. Pure frequency modulation:

$$\ddot{Q} + \left(\omega_0^2 + \frac{\Delta\omega^2}{2} + 2\omega_0 \cdot \Delta\omega \cos \alpha t + \frac{\Delta\omega^2}{2} \cos 2\alpha t\right)Q = 0.$$

III. Inverse capacity modulation:

$$\ddot{Q} + (\omega_0^2 + \omega_0^2 \cdot h \cos \alpha t)Q = 0.$$

IV. For small variations all three equations become:

$$\ddot{Q} + (\omega_0^2 + 2\omega_0 \cdot \Delta\omega \cos \alpha t)Q = 0.$$

The equations I, II, and III represent three special types of frequency modulation as indicated. There are still other types of interest, for example, a square-wave type of variation to be mentioned later. Also, as will be pointed out, frequency modulation may be accomplished by varying the inductance periodically, under which circumstance the results of the present paper are generally applicable, and phenomena similar in character to those occurring with periodic capacity variation to be expected.

Solution of the Differential Equation

The equation III for inverse capacity modulation will be dealt with specifically, for reasons of mathematical simplicity as well as for the fact that it approaches closest to the actual cases of greatest practical interest. Our equation is therefore (III); making a convenient change of variable $\alpha t = \tau$ and denoting differentiation with respect to τ by primes this becomes

$$Q'' + (W + A \cos \tau)Q = 0$$

$$W = \left(\frac{\omega_0}{\alpha}\right)^2, \quad A = \left(\frac{\omega_0}{\alpha}\right)^2 \cdot h = Wh. \tag{8}$$

The solutions of (8) for the different values of the parameters W and A give the answer to our problem. This is the Mathieu equation and, fortunately, enough is known* about its solution to allow a complete discussion of the physical behaviour of the circuit. Floquet's theory† of linear differential equations with periodic coefficients shows that a particular solution of Mathieu's equation is $e^{i\mu\tau} \cdot \phi(\tau)$, where $\phi(\tau)$ is a periodic function with period 2π, μ is (in general) a complex number, the characteristic exponent, to be determined, and $i = \sqrt{-1}$. Since an imaginary charge or current has no physical significance only the *real part* of the solution is to be taken; this will be implied here in all cases.

* A standard reference for the theory of Mathieu's equation is Humbert,[6] while the most modern developments are presented in the recent work by Strutt.[7] Introduced originally by Mathieu[8] in connection with the oscillation of an elliptical membrane this equation is now one of the important ones of theoretical physics, appearing in numerous branches from the most classical to the newest quantum theory. Of particular interest here are papers by Goldstein,[9] van der Pol and Strutt,[10,11] and Morse.[12]

† Whittaker and Watson, "Modern Analysis," p. 412, 1927 edition.

Changing τ to $-\tau$ does not alter the equation, so that a fundamental set of solutions of (8) is

$$Q = C_1 e^{i\mu\tau}\cdot\phi(\tau) + C_2 e^{-i\mu\tau}\cdot\phi(-\tau) \tag{9}$$

where C_1 and C_2 are arbitrary constants.

Accordingly, let a particular solution be assumed

$$Q = e^{i\mu\tau}\cdot \sum_{n=-\infty}^{+\infty} b_n e^{in\tau}. \tag{10}$$

Substituting this into the differential equation and equating to zero coefficients of equal powers of the exponential gives the recurrence relationship for the coefficients b_n

$$[W - (\mu + n)^2]b_n + \tfrac{1}{2}A(b_{n-1} + b_{n+1}) = 0. \tag{11}$$

Equation (11) determines the ratio of all of the b's in terms of any one of them, say b_0, which may be regarded as an arbitrary constant. This relationship forms a set of homogeneous algebraic equations which must be mutually consistent for the existence of a solution; the condition for consistency is that the determinant obtained by eliminating all the b's must vanish. This determinant can be put in the following convergent form by dividing the recurrence formula by $[W-(\mu+n)^2]$, giving

$$\square(\mu) \equiv \begin{vmatrix} \cdot & \cdot & \cdot & \cdot & \cdot & \cdot & \cdot \\ \cdots & \dfrac{A}{2[W-(\mu+1)^2]} & 1 & \dfrac{A}{2[W-(\mu+1)^2]} & 0 & 0 & \cdots \\ \cdots & 0 & \dfrac{A}{2[W-\mu^2]} & 1 & \dfrac{A}{2[W-\mu^2]} & 0 & \cdots \\ \cdots & 0 & 0 & \dfrac{A}{2[W-(\mu-1)^2]} & 1 & \dfrac{A}{2[W-(\mu-1)^2]} & \cdots \\ \cdot & \cdot & \cdot & \cdot & \cdot & \cdot & \cdot \end{vmatrix} \tag{12}$$

The infinite determinant $\square(\mu)$ equated to zero gives an equation determining μ as a function of W and A. Following Hill (12) may be written as

$$\sin^2 \mu\pi = \square(0)\cdot\sin^2 W^{1/2}\pi. \tag{13}$$

From (12) and (13) it is at once clear that for very small values of A the characteristic exponent μ becomes approximately $\sqrt{W}$. For any given value of μ, (13) defines certain associated values of W and A; this relationship is best represented graphically by contours of constant μ-values drawn in the WA plane.

Now, from (10) it is easily seen that when μ is real or zero the solution remains finite as the time increases indefinitely; the solution is

then of a purely oscillatory character and is called "stable." On the other hand, when μ has an imaginary part not identically zero Q either becomes infinite with the time, or becomes vanishingly small; this type is referred to as "unstable." If we plot in the WA plane curves of constant μ some of these will represent stable and other unstable solutions. It is thus possible to divide the WA plane into areas where the oscillation is oscillatory and stable, and those where it is unstable. The two types of solutions are of prime importance in interpreting the electric oscillations of the resonant circuit. Therefore, the location, shape, etc., of the areas of stable and unstable oscillation becomes the subject of principal concern for the physical problem at hand.

Let us investigate the nature of μ in general. According to Hill another determinant $\nabla(0)$ may be defined as

$$\nabla(0) = 2\square(0) \sin^2 W^{1/2}\pi \tag{14}$$

so that the expression for μ may be written

$$\cos 2\mu\pi = 1 - \nabla(0).$$

Since $\cos 2\mu\pi$ is itself always real, let us suppose that $2\mu\pi$ is complex, i.e. $\mu = a + ib$, a and b real. Then,

$$\cos 2\mu\pi = \cos(2a\pi)\cos(2ib\pi) - \sin(2a\pi)\sin(2ib\pi)$$

and the reality of $\cos 2\mu\pi$ requires either that $b \equiv 0$ or $a = n/2$, n an integer. In the first case μ is real, while for the second case we have

$$\cos 2\mu\pi = \pm \cos 2ib\pi = 1 - \nabla(0)$$

which gives only one (real) value of b. If $1 - \nabla(0)$ is positive, then,

$$\mu = \pm ib + n,$$

but if negative $\cos 2\mu\pi = -\cos 2ib\pi$, whence,

$$\mu = \pm ib + n + 1/2.$$

Thus it has been demonstrated that when μ is complex the real part is independent of A, which is of great importance. It is therefore possible, when μ is complex, to associate its real part with the exponential inside of the summation sign in (10), so that the solution is, for example, of form $e^{b\tau}\sum b_n \cdot e^{i\tau(n+1)}$. In this sense one can state that the characteristic exponent for the Mathieu equation is either real or imaginary, but not complex. This allows the regions of the WA plane to be classified as either areas of real or areas of imaginary μ.

The boundaries between the two kinds of regions are the contours along which $\mu = 0$, 1/2, 1, 1-1/2, $\cdots$, i.e., the contours along which

periodic solutions exist with a true period of π or 2π. These are in fact those solutions of the Mathieu equation known as the Mathieu functions and have been studied in detail. That periodic solution reducing to $\cos m\tau$ when $A=0$ in which the coefficient of $\cos m\tau$ is unity is de-

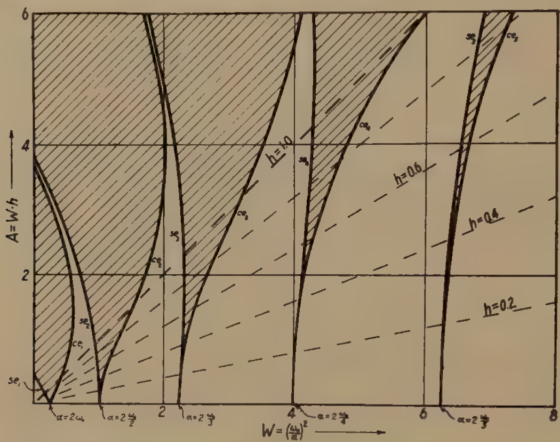

Fig. 1—WA plane graph, showing regions of stable (unshaded) and unstable (shaded) oscillations.

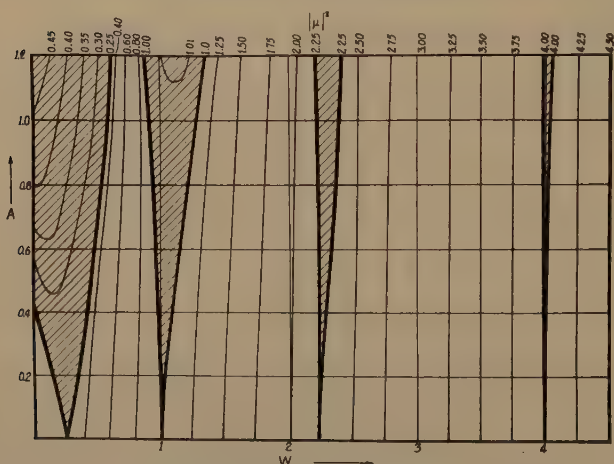

Fig. 2—Enlarged section of WA plane graph, showing contours of constant $|\mu|^2$ values.

noted by $ce_m(\tau)$; similarly, the solution which reduces to $\sin m\tau$ when $A=0$ is denoted by $se_m(\tau)$. Mathieu* gave in 1868 series approximations relating W and A for these particular solutions, the so-called

* Mathieu gave just enough terms to allow the computation for very small values of W and A; further terms could be obtained only with great labor.

"characteristic values," but the method of continued fractions of Ince and Hough[9] is vastly superior and has been used here. An example of the calculation is given in the Appendix.

The characteristic WA values are shown graphically in Fig. 1; shaded areas represent the sections within which the values of W and A give rise to unstable oscillation. Radial lines from the origin are the loci of constant h values. Fig. 2 shows a small part of the same diagram enlarged and with the contours giving associated values of W and A for particular values of $|\mu|^2$ equal a constant; this figure makes clear the way in which $|\mu|^2$ changes as one increases W or A. These curves are obtained by solving (18) after expanding the infinite determinant into an approximate series.† For all values of g in ce_g and se_g except g equal an integer or half integer the curves for ce and se are coincident; it is only when g has one of these values that the two curves separate and have an area of instability between them.

We must examine the actual cases of radio-frequency modulation and acoustical warble tone to determine the ranges of values for W and A in both instances before undertaking a discussion of the physical aspects of the problem; this will be treated in the next section.

Having determined the value of μ associated with any given set of values of W and A there remains only the evaluation of the coefficients b_n to complete the particular solution (10) and therefore the general solution (9). With b_0 arbitrary (say $=1$) equation (11) allows the calculation of these coefficients for any real value of μ, but it is more convenient first to transform this expression into the following continued fractions of Poole

$$\begin{aligned} \frac{b_n}{b_{n+1}} &= \frac{A}{S_n} \; \frac{A^2}{- S_{n-1}} \; \frac{A^2}{- S_{n-2}} \cdots - \\ \frac{b_n}{b_{n-1}} &= \frac{A}{S_n} \; \frac{A^2}{- S_{n+1}} \; \frac{A^2}{- S_{n+2}} \cdots - \end{aligned} \tag{14}$$

where $S_n = W-(\mu+n)^2$. With the evaluation of the b's the formal solution of the differential equation (8) is complete. We have yet to take the real part of the solution to secure the answer appropriate to the physical problem; one finds at once that the real part of

$$Q = C_1 \sum_{n=-\infty}^{+\infty} b_n e^{i\tau(\mu+n)} + C_2 \sum_{n=-\infty}^{+\infty} b_n' e^{-i\tau(\mu+n)}$$

† The writer is greatly indebted to Professor P. M. Morse of the Massachusetts Institute of Technology, Cambridge, Mass., for the use of some of the unpublished data from his paper "Quantum Mechanics of Electrons in Crystals," *Phys. Rev.*, vol. 35, p. 1310 (1930), used here and in Fig. 7.

is given by

$$Q = \sum_{n=-\infty}^{+\infty} (C_1 b_n + C_2 b_n') \cos \tau \, (\mu + n)$$

or, returning to the original variable t

$$Q = \sum_{n=-\infty}^{+\infty} (C_1 b_n + C_2 b_n') \cos (\mu + n)\alpha t \tag{15}$$

which is the final solution of our general equation and is valid for all values of the parameters ω_0, α and h for which stable oscillations exist. When, however, μ is imaginary the solution is no longer given by (15) but has the unstable form

$$\begin{aligned} Q &= C_1 e^{\beta t}\phi(t) + C_2 e^{-\beta t}\phi(-t), \ \beta \text{ real} \\ &\simeq C_1 e^{\beta t}\phi(t) \qquad\qquad\qquad, \ t \text{ large} \end{aligned} \tag{16}$$

and so becomes infinite with increasing time regardless of the ratio of C_1 to C_2, since the term with the positive exponential will rapidly swamp that with the negative exponential for any (finite) ratio of these constants.

Discussion of the Modes of Oscillation

Since h is never greater than unity it is clear that our interest lies only in the sector of the WA plane between the W axis and a 45-degree radial line from the origin. The region of this sector beginning at the origin and including the first several unstable areas is of considerable theoretical interest; this will be called Region I. A survey of the values of the parameters for the warble tone case, as used by a number of workers in experimental acoustics, gave the following representative values: $10^2 \leqq W \leqq 6\times10^6$, $0 < h \leqq 0.2$; this will be called Region II. In selecting specific values of the parameters for the case of frequency modulation in radiotelephony a difficulty is found, in that up to now such processes have been inadvertent auxiliary effects and almost no data are available. Probable values are, however; $10^5 \leqq W \leqq 3\times10^9$, $0 < h \leqq 0.05$; this will be called Region III. It is thus important to consider the oscillations occurring in the above three specific regions of the WA plane, which may be conveniently characterized by

Region I, of theoretical interest, $\begin{cases} \Delta\omega \simeq \omega_0 \\ \alpha \simeq \omega_0 \end{cases}$

Region II, acoustical warble tone, $\begin{cases} \Delta\omega < \omega_0 \\ \alpha \ll \omega_0 \end{cases}$

Region III, radio-frequency modulation, $\begin{cases} \Delta\omega \ll \omega_0 \\ \alpha \ll \omega_0 \end{cases}$

Fig. 3 shows the location of these regions in the WA plane. It is seen at once that only a very small part of the 45-degree sector is occupied by values occurring in practical applications.

Having determined the values of the parameters ω_0, α, and h for which stable and unstable solutions of the differential equation exist, as well as the precise form of these solutions and the values of the coefficients involved, let us now consider the nature of the electrical oscillations in general, and particularly those occurring in radio-frequency modulation, the acoustical warble tone generator, and when ω_0 and α are of comparable magnitude. The diagrams of Figs. 1, 2, and 3, together with equations (15) and (16), furnish at once the necessary information:

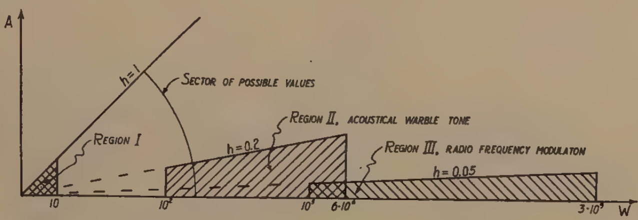

Fig. 3—Regions of the WA plane of particular interest.

To begin with, the significance of the shaded areas of Fig. 1 for the electrical and mechanical systems must be made clear. As already pointed out, the adjustment of ω_0, α, and h to such values that μ is imaginary (and so falls within a shaded area) gives rise to an oscillatory charge, or current, of continuously increasing amplitude (equation (16)). This represents a continual increase in the energy of the electric circuit which must be supplied by the energy expended in varying the capacity, for example, by the motor used for rotating the variable condenser of a warble tone generator or by the acoustic waves vibrating the moving element of a condenser microphone. Oscillations of this kind represent a special type of resonance phenomena between the electrical and mechanical parts of the system quite analogous to the forced oscillations of coupled electrical circuits. That the current cannot really become infinite in the physically realizable circuit is clear; a tendency in this direction must be very soon counterbalanced by a change in some of the parameters of the system, such that either ω_0, α, h are altered to give stable oscillations, or the premises upon which our original differential equation was based cease to be valid, and therefore the predications of the present theory inapplicable. For example, the amplitude of oscillation of the vacuum tube oscillator mentioned on page 1183 is inherently limited by the extent of the plate-current—grid-

voltage curve, the grid current, etc., which will prevent a current increase beyond a certain limit; before this limit is reached, however, it is certain that the assumption is no longer approximately true that the resistance of the oscillatory circuit is identically zero. As another example, if unstable oscillations begin to build up it might happen that the additional load demanded of the source responsible for the condenser variation (motor-driving the condenser, acoustic waves actuating condenser microphone, etc.) would cause a change in the speed of rotation or of the amount of variation just sufficient to make the oscillations again stable. An increase in the current through an iron-cored inductance used in the oscillatory circuit could change its properties so that ω_0 would be altered to give perfectly stable oscillation.

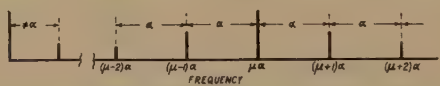

Fig. 4—Illustrating the frequency spectrum of oscillation type whose period is not that of the modulation.

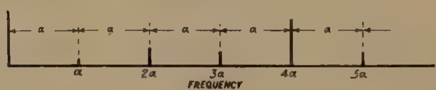

Fig. 5—Illustrating the frequency spectrum of oscillation type whose period is the same as that of the modulation.

Next, the unshaded areas of Fig. 1 where μ is real must be interpreted. When ω_0, α, h are given values such that μ falls into an unshaded area the charge is purely oscillatory of the form given by (15) and the amplitudes and frequencies of the components remain constant with time. It is important to notice, that corresponding to any real value of μ there are stable oscillations whose component frequencies are given by $(\mu+n)\alpha$, where $n= \cdots -3, -2, -1, 0, 1, 2, 3, \cdots$. This may be interpreted as a spectrum of the general form of Fig. 4. The electric oscillations are thus not in general of the same period as that of the capacitance variation, or any multiple of it (i.e. of period $2\pi/n\alpha$). It is only when $\mu=0, 1, 2, \cdots$, that the oscillation has the fundamental period $2\pi/\alpha$ of the capacitance variation. The contours bounding every alternate area of instability in the WA plane form the locus of associated values of ω_0, α, and h for this condition. This particular type of oscillation is characterized by the fact that the spectrum is representable by an ordinary Fourier series with fundamental frequency α and harmonics 2α, 3α, $\cdots$, as illustrated in Fig. 5. The boundaries of the remaining areas of unstable oscillation give values of

ω_0, α, h for which the oscillation has a Fourier series representation with fundamental frequency $\alpha/2$. Similarly, oscillations can take place having a Fourier series spectrum with a fundamental frequency of any integer fraction of α; these cases are of importance in some acoustical applications of the warble tone and have been observed and discussed by the author.[16]

With the above facts in mind a consideration of Fig. 1 makes the general character of the oscillations in the circuit quite clear. If we assume that the values of the inductance, capacity, etc., of the system are completely under our control and we vary these so as to go outward from the origin in the WA plane it is seen from Fig. 1 that the first instability occurs, with very small h, for $\alpha = 2\omega_0$; this is the case

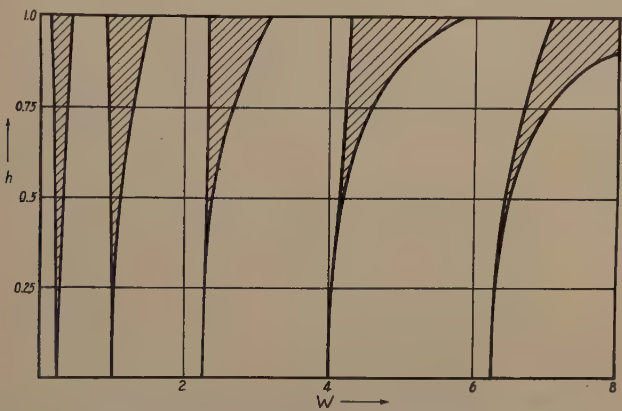

Fig. 6—Location of areas of stable and unstable oscillation for different values of h, ω_0, and α; $W = (\omega_0/\alpha)^2$.

discussed by Rayleigh[1] for a vibrating string and mentioned later by van der Pol[13] for an electric circuit. For larger h the unstable region broadens, until for $h = 1$ any value of α in the range from about 1.40 to 3.42 will cause unstable oscillation. This broadening with increasing h of the range of values of W causing an unstable condition in the circuit is typical of each successive area of unstable oscillation, although the amount of broadening is naturally slightly different.

Replotting Fig. 1 with the coördinates W and h, as in Fig. 6, gives a clear presentation of these areas of stable and unstable electric oscillations. It may be seen from this diagram that for small h almost any adjustment of ω_0 and α results in a stable oscillation, while as h increases the probability of having instability grows until for $h = 1$ this predominates, and indeed for large W and $h = 1$ there are only very narrow ranges of stable adjustment.

Proceeding outward along a line of constant but very small A in Fig. 1, the second instability occurs when $\alpha=\omega_0$, the third when $\alpha=2\omega_0/3$, the fourth when $\alpha=2\omega_0/4$, and in general when $\alpha=2\omega_0/n$, $n=1, 2, 3, 4, \cdots$. Each time that a new region of instability is traversed in progressing outward the range of these successive unstable values becomes smaller. Because the absolute value of the imaginary part of μ is smaller each successive instability has a lower magnitude than the preceding one, that is, the rapidity with which the current increases is less. This is made quite clear by a consideration of Fig. 7, where the real and imaginary values of μ (see p. 1189) are plotted for a

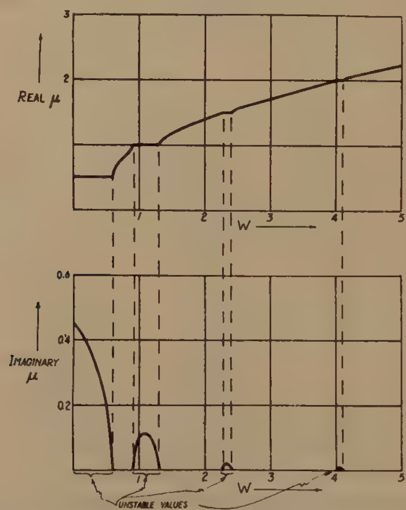

Fig. 7—Real and imaginary values of μ vs. $(\omega_0/\alpha)^2$ for $h=$constant.

particular value of $A=$constant. Since the value of the imaginary component alone determines the magnitude of the instability it may be seen at once that the successive unstable oscillations involve smaller and smaller ranges of W, and have successively smaller numerical values of imaginary μ, and are thus of a progressively lower magnitude of instability. Now, if we go out far enough the width of the unstable regions get exceedingly small, so that for small h they become, for practical purposes, simply a line. If it were then possible to give ω_0 and α the precise values required to make μ fall on one of these "lines" an unstable oscillation would occur, but because the absolute value of the imaginary μ is now so small the increase in amplitude of oscillation would take place very slowly. Nevertheless, the amplitude should finally increase beyond all bounds; but this is not likely to happen.

For, this would demand a very high degree of constancy of the magnitudes of both ω_0 and α and at the same time a continuously increasing load on the power sources of these two oscillatory motions; the maintenance of all of these conditions cannot be accomplished by any apparatus known to the writer. Since the particular range of ω_0/α for unstable oscillation is actually so very small, and because the apparatus would, if an attempt were made to adjust to this condition, undoubtedly stay at a stable condition represented by the *ce* or *se* lines to either side, this phenomena is not likely to be observable even with care in the radio or usual acoustic case. However, if h is not taken as a small quantity it is clear from the WA plane graph that the unstable oscillations would certainly make themselves noticeable, both directly in the oscillatory current and indirectly in the energy supplied for varying the condenser and for neutralizing the natural resistance of the circuit (i.e. the energy supplied to the vacuum tube oscillator).

It is only with the above provisions in mind that the solution of the frequency modulation problem as given by Carson,[2] van der Pol,[3] Salinger[14] and others is to be taken as strictly correct. Under the assumptions then made $\alpha \ll \omega_0$, $\Delta\omega \ll \omega_0$, in which case the solution sums up to

$$\left.\begin{aligned} Q &= C \cdot \sin\left(\omega_0 t - \frac{h\omega_0}{\alpha}\sin\alpha t\right) \\ &= C \cdot \sum_{n=-\infty}^{+\infty} J_n\left(\frac{\Delta\omega}{\alpha}\right) \sin 2\pi(\omega_0 + n\alpha)t \end{aligned}\right\} \tag{22}$$

where $J_n(\Delta\omega/\alpha)$ is the nth order Bessel function of argument $\Delta\omega/\alpha$ and C is an arbitrary constant.

Oscillations for Various Types of Modulation

A brief consideration of the general nature of the oscillations occurring in the circuit with a modulation other than the inverse capacity type is of interest. The foregoing detailed analysis is based on equation III, page 1187 for inverse capacity modulation. The general form of the equation for any periodic modulation is

$$Q'' + \psi(\tau) \cdot Q = 0$$

where $\psi(\tau)$ is a Fourier series determined by the way in which the capacity is varied. Equation III is thus a special case of the above obtained by putting $\psi(\tau) = \omega_0^2 + \omega^2 h \cos \tau$. Similarly, the equations I and II, for direct capacity modulation and pure frequency modulation, respectively, are special cases of the above general form obtained by assigning to $\psi(\tau)$ the particular expressions appearing in these equations

I and II. As a further example of an interesting special case there may be mentioned the type of frequency modulation occurring in radio-telegraph communication where the frequency is modulated abruptly in transmitting dots and dashes. In this instance $\psi(\tau)$ becomes the Fourier series representing a square-tooth wave.

A solution of the general equation written above is not at present possible (see footnote page 1185), but broad conclusions relative to the character of the solutions may be drawn with the assistance of the Floquet theory (reference, page 1187). From considerations of this nature it seems quite certain that all of the characteristics described for inverse capacity modulation will also accompany *any* periodic modulation. Thus, it is to be expected that the oscillatory charge will have the same type of spectrum, but with components of slightly different absolute values of frequency and amplitude, since μ will naturally be slightly different. Similarly, there will be certain, although somewhat different, values of ω_0, α, etc., for which unstable oscillations would tend to take place. For an arbitrary variation the mathematical difficulties of obtaining the *WA* plane representation are at present unsurmountable, but the case of telegraphic dots has been partly solved;[10] besides its application in radio communication this seems to be the only practical way of securing the adjustments $\alpha = 2\omega_0$, $\alpha = \omega_0$, $\cdots$, for large values of h and an ω_0 low enough to be satisfactorily oscillographed.

It is also to be expected from Floquet's theory that a periodic variation of the inductance would lead to essentially the same results as those predicted for the variable capacitance circuit. Such a circuit has been described by the author,[15] and the occurrence of periodic and non-periodic oscillations in the experimental circuit demonstrated.[16] The instability occurring when $\alpha = 2\omega_0$ in an R, L, C circuit containing a periodically varying, iron-cored inductance has been observed and explained by Winter-Günther.[17] There is, therefore, theoretical and experimental evidence that the findings for the circuit with a varying capacitance may also be applied to that with a varying inductance.

Conclusion

The most important aspects of the theory of frequency modulation for arbitrarily large degrees of modulation and unrestricted modulation frequencies have now been developed,* for, the frequency spectrum,

* The relative change in frequency measures the degree of modulation and the frequency at which this change takes place gives the modulation frequency. This nomenclature is directly analogous to that used in describing amplitude modulation, where the relative change in amplitude measures the degree of (amplitude) modulation, and the frequency at which this change takes place is the modulation frequency.

amplitudes, and stability of the oscillations may be obtained for given values of the circuit parameters and the nature of the oscillations have actually been studied throughout the range of these parameters. It is thought not amiss to conclude by summarizing the consequences of this analysis.

When the degree of modulation is small all types of frequency modulation result in exactly the same oscillation as given by equation IV, p. 1187. If, further, the modulating frequency is small the amplitudes and frequencies of the spectral components are given by Carson's[2] well-known solution. However, for large degrees of modulation and modulating frequencies it is essential to know the type of modulation used, as the amplitudes and frequencies of component oscillations will vary with the type. Besides, there is the important fact that unstable oscillations, that is, oscillations whose amplitude increases exponentially with time, tend to occur for certain values of the parameters of the circuit. The extent of the values producing instability, as well as the magnitude of the tendency toward increasing amplitude, becomes larger with increasing degree of modulation. That the current in an oscillatory circuit cannot increase indefinitely is clear. This tendency, however, may cause marked reactions on the circuit and associated apparatus.

In Region I, where $\alpha \cong \omega_0$ and $\Delta\omega \cong \omega_0$, stable or unstable oscillations are about equally divided, and the magnitude of the tendency toward instability, when this occurs, is relatively large. Instability occurs with small h when $\alpha = 2\omega_0/n$, $n = 1, 2, 3, \cdots$; for large h the range of α is extended. The magnitude of instability is largest when $\alpha \cong 2\omega$ and decreases with increasing ω_0/α and $1/h$. Stable oscillations may or may not be periodic in a Fourier series sense—in general they are not. The amplitude of the components depends in a complicated way on the circuit parameters, as does the real part of μ, which latter determines the frequencies of the components as $(\mu \pm n)\alpha$, $n = 0, 1, 2, \cdots$.

In the case of the warble tone, i.e., Region II where $\alpha \ll \omega_0$ and $\Delta\omega \lesssim \omega_0$, the oscillations are generally stable, with only a slight possibility of the unstable condition being set up. The oscillations are in general like the stable ones of Region I, except that for many of the values of ω_0, $\Delta\omega$, and α employed in acoustical practice, the approximate solution for Region III is valid. The oscillation is usually not periodic with period α, 2α, $\cdots$, but may be.

Frequency modulation in radiotelephony, Region III where $\alpha \ll \omega_0$ and $\Delta\omega \ll \omega_0$, represents the simplest possible situation. There is neither a question of instability nor one of nonperiodicity. The spectrum is composed of discrete frequencies $(\omega_0 \pm n\alpha)$ with amplitudes $J_n(\Delta\omega/\alpha)$,

$n=0, 1, 2, \cdots, J_n =$ Bessel function of nth order, as given by Carson's approximate solution.

Addendum

The preliminary results of an experimental investigation now in progress verify the above theoretical analysis quite well. Instability, manifested by comparatively large amplitudes of oscillations in the vacuum tube oscillator, amplitude, and the general character of the wave form, are all observable about as predicted. The results of these experiments will be published later.

Appendix

Calculation of μ for Mathieu Functions

This will be illustrated by means of the calculations for ce_3, as these are typical of all the others. Following the method of Goldstein,[9] we assume

$$ce_{2g+1} = b_1 \cos \tau + b_3 \cos 3\tau + \cdots + b_{2n+1} \cos (2n+1)\tau + \cdots.$$

Substituting this into the differential equation (8) gives the recurrence relation (11) in the special form

$$\frac{A}{2} b_{2n-1} + [W - (n+\tfrac{1}{2})^2] b_{2n+1} + \frac{A}{2} b_{2n+3} = 0, \quad n \geqq 1.$$

If b_{2n+3}/b_{2n+1} be denoted by v_n this can be written

$$\frac{A}{2(n+\frac{1}{2})^2} \cdot \frac{1}{v_{n-1}} - 1 + \frac{W}{(n+\frac{1}{2})^2} + \frac{A}{2(n+\frac{1}{2})^2} \cdot v_n = 0, \quad n \geqq 1$$

or,

$$v_{n-1} = -\frac{A}{2(n+\frac{1}{2})^2} \bigg/ \left(-1 + \frac{W}{(n+\frac{1}{2})^2} + \frac{A}{2(n+\frac{1}{2})^2} \cdot v_n \right) = 0, \; n \geqq 1.$$

Hence,

$$v_{n-1} = \frac{\dfrac{-A}{2(n+1)^2}}{-1 + \dfrac{W}{(n+\frac{1}{2})^2} -} \; \frac{\dfrac{A^2}{4(n+\frac{1}{2})^2(n+\frac{1}{2}+1)^2}}{-1 + \dfrac{W}{(n+\frac{1}{2}+1)^2} -} \; \frac{\dfrac{A^2}{4(n+\frac{1}{2}+1)^2(n+\frac{1}{2}+2)^2}}{-1 + \dfrac{W}{(n+\frac{1}{2}+2)^2} -} \cdots.$$

Also we have

$$-\frac{A}{2(n+\frac{1}{2})^2}\cdot v_n = -1+\frac{W}{(n+\frac{1}{2})^2}+\frac{4(n+\frac{1}{2})^2(n+\frac{1}{2}-1)^2}{\dfrac{A}{2(n+\frac{1}{2}-1)^2}\cdot v_{n-1}}$$

$$= -1+\frac{W}{(n+\frac{1}{2})^2}-\cfrac{\dfrac{A^2}{4(n+\frac{1}{2})^2(n+\frac{1}{2}-1)^2}}{-1+\dfrac{W}{(n+\frac{1}{2}-1)^2}-\cfrac{\dfrac{A^2}{4(n+\frac{1}{2}-1)^2(n+\frac{1}{2}-2)^2}}{-1+\dfrac{W}{(n+\frac{1}{2}-2)^2}-\cdots+\cfrac{\dfrac{A^2}{4(2+\frac{1}{2})^2(1+\frac{1}{2})^2}}{\dfrac{A}{2(1+\frac{1}{2})^2}\cdot v_1}}}.$$

But,

$$v_0 = -\left(\frac{A}{2}+\frac{1}{4}-W\right)\Big/\frac{A}{2},$$

so that:

$$-\frac{A}{2(1+\frac{1}{2})^2}\cdot v_1 = -1+\frac{W}{(1+\frac{1}{2})^2}-\frac{\dfrac{A^2}{4(1+\frac{1}{2})^2}}{\dfrac{A}{2}+\frac{1}{4}-W},$$

and therefore we secure the following equation determining the characteristic W and A values

$$L_n = -1+\frac{W}{(n+\frac{1}{2})^2}-H_n-K_n = 0$$

where,

$$H_n = \cfrac{\dfrac{A^2}{4(n+\frac{1}{2})^2(n+\frac{1}{2}-1)^2}}{-1+\dfrac{W}{(n+\frac{1}{2}-1)^2}-\cfrac{\dfrac{A^2}{4(n+\frac{1}{2}-1)^2(n+\frac{1}{2}-2)^2}}{-1+\dfrac{W}{(n+\frac{1}{2}-2)^2}-\cdots-\cfrac{\dfrac{A^2}{4(2+\frac{1}{2})^2(1+\frac{1}{2})^2}}{-1+\dfrac{W}{(1+\frac{1}{2})^2}-\cfrac{\dfrac{A^2}{4(1+\frac{1}{2})^2}}{\dfrac{A}{2}+\dfrac{1}{4}-W}}}}$$

$$K_n = \frac{-A}{2(n+\frac{1}{2})^2}\cdot v_n = \cfrac{\cfrac{A^2}{4(n+\frac{1}{2})^2(n+\frac{1}{2}+1)^2}}{-1+\cfrac{W}{(n+\frac{1}{2}+1)^2} - \cfrac{\cfrac{A^2}{4(n+\frac{1}{2}+1)^2(n+\frac{1}{2}+2)^2}}{-1+\cfrac{W}{(n+\frac{1}{2}+2)^2} - \cdots}}$$

For ce_3 n must be put equal to unity; for a particular value of A the characteristic value for W is found by solving the equation $L_1=0$ by successive approximations. For example, with $A=4$ we try $W=3.5$, which gives $L_1=+0.030$; a second try might be $W=3.52$, giving $L_1=-0.017$, which definitely fixes the correct value as intermediate between these two. Several further guesses, guided by the preceding work, give the value with four-figure accuracy as $W=3.512$. The rapid convergence of the continued fractions makes the calculations relatively easy, and if the first guess for W is fair, and it will be once computation has been started, the above accuracy is obtained quite rapidly. Goldstein[9] has given tables for ce_0, se_1, ce_1, se_2, ce_2; the other curves have been calculated as above, although Strutt[11] has published a graph of these. Quite complete tables of the Mathieu functions, characteristic values, etc., have just been published by Ince, *Proc. Royal Soc.* (Edinburgh), vol. 52, part 4, pp. 347–434, (1931–1932).

Bibliography

1. Lord Rayleigh, Scientific Papers, vol. 3, p. 1, (1887); vol. 2, p. 88, (1883).
2. J. R. Carson, Proc. I.R.E., vol. 10, p. 57, (1922).
3. Balth. van der Pol, Proc. I.R.E., vol. 18, p. 1194, (1930).
4. E. T. Whittaker, *Proc. Edinburgh Math. Soc.*, vol. 33, p. 22, (1914); vol. 32, p. 75, (1914).
   E. L. Ince, *Proc. Roy. Soc.* (Edinburgh), vol. 45, p. 106, (1925); *Proc. London Math. Soc.*, (2), vol. 25, p. 53, (1926).
5. E. L. Ince, *Proc. London Math. Soc.*, (2), vol. 23, p. 56, (1925).
6. Humbert, "Fonctions de Lamé et fonctions de Mathieu," *Memorial des Sc. Math.*, vol. 10, Paris, (1926).
7. M. J. O. Strutt, "Lamésche-, Mathieusche- und verwandte Funktionen in Physik und Technik," Ergebnisse der Math., Band I, Hirschwaldsche Buchhandlung, Berlin, (1932).
8. E. Mathieu, *Jour. de math. Purés et Appliquées*, vol. 13, p. 137, (1868).
9. S. Goldstein, *Trans. Cambridge Phil. Soc.*, vol. 23, p. 303, (1927).
10. Balth. van der Pol and M. J. O. Strutt, *Phil. Mag.*, vol. 5, p. 18, (1928).
11. M. J. O. Strutt, *Zeit. für Phys.*, vol. 69, p. 597, (1931).
12. P. M. Morse, *Phys. Rev.*, vol. 35, p. 1310, (1930).
13. Balth. van der Pol, *Exp. Wireless*, (1926).
14. H. Salinger, *E.N.T.*, vol. 6, p. 294, (1929).
15. W. L. Barrow, *Ann. der Phys.*, vol. 11, p. 147, (1931).
16. W. L. Barrow, Proc. I.R.E., vol. 20, p. 1626, (1932).
17. H. Winter-Günter, *Jahrbuch der draht. Tel. u. Tel.*, vol. 34, p. 1, (1929); and *Jahrbuch der draht. Tel. u. Tel.*, vol. 37, p. 172, (1931).

Proceedings of the Institute of Radio Engineers
Volume 21, Number 8 *August, 1933*

MODULATION PRODUCTS IN A POWER LAW MODULATOR*

By

A. G. Tynan

(Philadelphia, Pennsylvania)

Summary—*Expansion of the current as a function of the voltage in a multiple Fourier series is used to solve the problem of determining the amplitude of the various frequency components produced when a voltage is applied across a resistance, the current in which varies as a power of the voltage across it. Recurrence formulas are developed by which the higher order products can be computed from those of lower order. Certain of the integral coefficients in the Fourier series expansion are evaluated in the form of double summations. The method is applied to a specific case, and sample calculations carried through in detail. While the method is not as well adapted to obtaining qualitative results as are the usual forms of analysis, it does appear to have some advantages when numerical results are required, or when the effects of the contributions of higher order products are to be studied.*

The problem of determining the resultant current in a circuit containing a resistance varying as a function of the current through it has been attacked in a number of different ways. The usual method is to expand the current as a function of the applied voltage in a power or Taylor series. Another method, heretofore neglected, is available for this expansion. This method, expansion in a multiple Fourier series, appears to have been first applied by W. R. Bennett[1] who obtained by it a solution to the problem of a modulator operated through cut-off and obeying an integer power law over the conducting portion of the characteristic. We shall apply the method here to the case of a power law modulator not operated through discontinuities. This is the case considered in the usual treatment of the problem.

The current voltage characteristic is assumed to be of the form:

$$i = Ke^r \tag{1}$$

where,

i = instantaneous current
e = instantaneous voltage
K = a positive constant
r = a positive constant

* Decimal classification: R148. Original manuscript received by the Institute, January 3, 1933.

[1] This solution is given as an incidental part of a paper by W. R. Bennett entitled, "Note on relations between elliptic integrals and Schlömilch series," to be published soon in the *Bulletin of the American Mathematical Society*. Another paper by W. R. Bennett discussing the solution from a less mathematical standpoint has been prepared for publication.

For simplicity we shall limit ourselves to an input of the form:

$$e = E_0 + P \cos (pt + \theta_p) + Q \cos (qt + \theta_q). \tag{2}$$

Additional frequency terms would not alter the procedure but would increase the work involved. We can write more simply and without introducing any additional restrictions:

$$e = P(k_0 + k_1 \cos y + \cos x) \tag{3}$$

where,

$$k_0 = E_0/P \geqq 1 + k_1$$

$$k_1 = Q/P \leqq 1$$

$$x = pt + \theta_p$$

$$y = qt + \theta_q.$$

The first condition is the mathematical form of the limitation that the device shall not be operated through cut-off. In the plate circuit of a vacuum tube, or any power law device, when the sum of all the voltages, instantaneously present, becomes zero, current ceases to flow.

From (1) we have:

$$i = KP^r(k_0 + k_1 \cos y + \cos x)^r. \tag{4}$$

Expanding in a double Fourier series and using the plus and minus signs for the upper and lower side bands, respectively:

$$i = KP^r \sum_{n=0}^{n=\infty} \sum_{m=0}^{m=\infty} B_{mn} \cos (mx \pm ny) \tag{5}$$

$$B_{mn} = \frac{2}{\pi^2} \int_0^\pi \int_0^\pi (k_0 + k_1 \cos y + \cos x)^r \cos mx \cos ny \, dx \, dy. \tag{6}$$

If both m and n are zero the right-hand side is to be divided by two.

From (6) we can obtain recurrence formulas connecting the B_{mn}'s of different subscripts, thus reducing the number of integrals we shall be required to evaluate. The Fourier series expansion appears to be the only method that permits of a simple derivation of such formulas. To obtain them we note that:

$$\int_0^\pi \int_0^\pi \frac{d}{dx} [(k_0 + k_1 \cos y + \cos x)^{r+1} \sin (m + 1)x \cos ny] dy = 0 \tag{7}$$

and,

$$\int_0^\pi \int_0^\pi \frac{d}{dy} [(k_0 + k_1 \cos y + \cos x)^{r+1} \cos mx \sin (n + 1)y] dx = 0. \tag{8}$$

Differentiating under the integral sign, after collecting terms, and using the trigonometric sum and difference relations, we have from (7) and (8):

$$2k_0B_{(m+1)n} + k_1(B_{(m+1)(n+1)} + B_{(m+1)(n-1)}) + \left(1 - \frac{r+1}{m+1}\right)B_{mn} + \left(1 + \frac{r+1}{m+1}\right)B_{(m+2)n} = 0 \tag{9}$$

$$2k_0B_{m(n+1)} + B_{(m+1)(n+1)} + B_{(m-1)(n+1)} + k_1\left(1 - \frac{r+1}{n+1}\right)B_{mn} + k_1\left(1 + \frac{r+1}{n+1}\right)B_{m(n+2)} = 0. \tag{10}$$

If both of the subscripts in (9) or (10) are zero, we must divide that term by two. Another relation that may sometimes be of interest is obtained in the same way. Using a superscript to indicate the value of the exponent in (1), a relation between products of modulators having different exponents can be written:

$$2B^{r+1}_{(m+1)n} = \frac{r+1}{m+1}(B_{mn}{}^{r} - B^{r}{}_{(m+2)n}) \tag{11}$$

$$2B^{r+1}_{m(n+1)} = k_1\frac{r+1}{n+1}(B_{mn}{}^{r} - B_{m}{}^{r}{}_{(n+2)}). \tag{12}$$

Equations (9) and (10) give relations between terms having subscripts of order, $(m+n-1)$, $(m+n)$, $(m+n+1)$, $(m+n+2)$. Specifically we have the following relations between coefficients of zero to third order inclusive:

$$\begin{aligned}
&-rB_{00} + 4k_0B_{10} + 4k_1B_{11} + 2(2+r)B_{20} = 0 \\
&-rk_1B_{00} + 4k_0B_{01} + 4B_{11} + 2k_1(2+r)B_{02} = 0 \\
&(1-r)B_{10} + 4k_0B_{20} + (3+r)B_{30} + 4k_1B_{21} = 0 \\
&(1-r)k_1B_{01} + 4k_0B_{02} + k_1(3+r)B_{03} + 4B_{12} = 0 \\
&-2k_1rB_{10} + 4k_0B_{11} + 2k_1(2+r)B_{12} + 2B_{21} = 0 \\
&-2rB_{01} + 2k_1B_{10} + 4k_0B_{11} + 2k_1B_{12} + 2(2+r)B_{21} = 0.
\end{aligned} \tag{13}$$

It is evident that if B_{00}, B_{01}, B_{10}, and B_{11} are known, the remaining coefficients can be calculated from (13) or similar sets of equations. The problem is then reduced to the evaluation of four integrals. Unfortunately, there appears to be no way of obtaining a solution in a

finite number of terms, except, of course, when r is an integer, which is a trivial case. The solutions here found for the integrals are in the form of double summations. The first four coefficients might also be obtained by measurement or by use of the customary expansions, and (13) then used to obtain the remaining terms. The process of evaluating the integral B_{00} is given in detail in the appendix. The others can be readily found in the same manner. The final results are:

$$
\begin{aligned}
B_{00} = k_0^r \Bigg[1 &+ \sum_{s=1}^{s=\infty} \frac{r(r-1)\cdots(r-2s+1)}{(2s)!} \cdot \frac{1\cdot 3\cdot 5\cdots(2s-1)}{2\cdot 4\cdots 2s} \cdot \frac{k_1^{2s}}{k_0^{2s}} \\
&+ \sum_{v=1}^{v=\infty} \frac{r(r-1)\cdots(r-2v+1)}{(2v)!} \cdot \frac{1\cdot 3\cdot 5\cdots(2v-1)}{2\cdot 4\cdots 2v} \cdot \frac{1}{k_0^{2v}} \\
&+ \sum_{s=2}^{s=\infty} \sum_{v=1}^{v=s-1} \frac{r(r-1)\cdots(r-2s+1)}{(2s-2v)!(2v)!} \cdot \frac{1\cdot 3\cdot 5\cdots(2v-1)}{2\cdot 4\cdots 2v} \\
&\cdot \frac{1\cdot 3\cdot 5\cdots(2s-2v-1)}{2\cdot 4\cdots(2s-2v)} \cdot \frac{k_1^{2s-2v}}{k_0^{2s}} \Bigg]
\end{aligned}
\tag{14}
$$

$$
\begin{aligned}
B_{10} = 2k_0^{r+1} \Bigg[&\sum_{s=1}^{s=\infty} \frac{r(r-1)\cdots(r-2s+2)}{(2s-1)!} \cdot \frac{1\cdot 3\cdot 5\cdots(2s-1)}{2\cdot 4\cdots 2s} \cdot \frac{1}{k_0^{2s}} \\
&+ \sum_{s=2}^{s=\infty} \sum_{v=1}^{v=s-1} \frac{r(r-1)\cdots(r-2s+2)}{(2s-2v)!(2v-1)!} \cdot \frac{1\cdot 3\cdot 5\cdots(2v-1)}{2\cdot 4\cdots 2v} \\
&\cdot \frac{1\cdot 3\cdot 5\cdots(2s-2v-1)}{2\cdot 4\cdots(2s-2v)} \cdot \frac{k_1^{2s-2v}}{k_0^{2s}} \Bigg]
\end{aligned}
\tag{15}
$$

$$
\begin{aligned}
B_{01} = 2\frac{k_0^{r+1}}{k_1} \Bigg[&\sum_{s=1}^{s=\infty} \frac{r(r-1)\cdots(r-2s+2)}{(2s-1)!} \cdot \frac{1\cdot 3\cdot 5\cdots(2s-1)}{2\cdot 4\cdots 2s} \cdot \frac{k_1^{2s}}{k_0^{2s}} \\
&+ \sum_{s=2}^{s=\infty} \sum_{v=1}^{v=s-1} \frac{r(r-1)\cdots(r-2s+2)}{(2s-2v-1)!(2v)!} \cdot \frac{1\cdot 3\cdot 5\cdots(2v-1)}{2\cdot 4\cdots 2v} \\
&\cdot \frac{1\cdot 3\cdot 5\cdots(2s-2v-1)}{2\cdot 4\cdots(2s-2v)} \cdot \frac{k_1^{2s-2v}}{k_0^{2s}} \Bigg]
\end{aligned}
\tag{16}
$$

$$
\begin{aligned}
B_{11} = 2k_0^r \Bigg[&\sum_{s=2}^{s=\infty} \sum_{v=1}^{v=s-1} \frac{r(r-1)\cdots(r-2s+3)}{(2s-2v-1)!(2v-1)!} \cdot \frac{1\cdot 3\cdot 5\cdots(2v-1)}{2\cdot 4\cdots 2v} \\
&\cdot \frac{1\cdot 3\cdot 5\cdots(2s-2v-1)}{2\cdot 4\cdots(2s-2v)} \cdot \frac{k_1^{2s-2v-1}}{k_0^{2s-2}} \Bigg].
\end{aligned}
\tag{17}
$$

These equations can be written somewhat more compactly as follows:

$$B_{00} = k_0^r \left[1 + \sum_{s=1}^{s=\infty} \frac{r(r-1)\cdots(r-2s+1)}{[2\cdot 4 \cdots 2s]^2} \cdot \frac{k_1^{2s}}{k_0^{2s}} + \sum_{v=1}^{v=\infty} \frac{r(r-1)\cdots(r-2v+1)}{[(2\cdot 4 \cdots 2v)]^2} \cdot \frac{1}{k_0^{2v}} + \sum_{s=2}^{s=\infty} \sum_{v=1}^{v=s-1} \frac{r(r-1)\cdots(r-2s+1)}{[2\cdot 4\cdots 2v]^2[2\cdot 4 \cdots (2s-2v)]^2} \cdot \frac{k_1^{2s-2v}}{k_0^{2s}} \right] \quad (14\text{A})$$

$$B_{10} = 2k_0^{r+1} \left[\sum_{s=1}^{s=\infty} \frac{r(r-1)\cdots(r-2s+2)}{[(2\cdot 4\cdots 2s)]^2} \cdot \frac{2s}{k_0^{2s}} + \sum_{s=2}^{s=\infty} \sum_{v=1}^{v=s-1} \frac{r(r-1)\cdots(r-2s+2)2v}{[(2\cdot 4\cdots 2v)]^2[2\cdot 4\cdots(2s-2v)]^2} \cdot \frac{k_1^{2s-2v}}{k_0^{2s}} \right] \quad (15\text{A})$$

$$B_{01} = \frac{2k_0^{r+1}}{k_1} \left[\sum_{s=1}^{s=\infty} \frac{r(r-1)\cdots(r-2s+2)2s}{[(2\cdot 4\cdots 2s)]^2} \cdot \frac{k_1^{2s}}{k_0^{2s}} + \sum_{s=2}^{s=\infty} \sum_{v=1}^{v=s-1} \frac{r(r-1)\cdots(r-2s+2)(2s-2v)}{[(2\cdot 4\cdots 2v)]^2[2\cdot 4\cdots(2s-2v)]^2} \cdot \frac{k_1^{2s-2v}}{k_0^{2s}} \right] \quad (16\text{A})$$

$$B_{11} = \frac{2k_0^{r+2}}{k_1} \sum_{s=2}^{s=\infty} \sum_{v=1}^{v=s-1} \frac{r(r-1)\cdots(r-2s+3)(2s-2v)2v}{[2\cdot 4\cdots 2v]^2[2\cdot 4\cdots(2s-2v)]^2} \cdot \frac{k_1^{2s-2v}}{k_0^{2s}}. \quad (17\text{A})$$

These series are convergent for all values of r, k_0, and k_1. However, their rate of convergence does depend upon these constants. They will converge most rapidly for r near unity, k_1 small and k_0 large, or, in other words, they converge most rapidly for those values that correspond to the least curvature in the current-voltage characteristic over the operating range. However, for most curvature type modulators, they converge sufficiently rapidly for practical use.

The series are somewhat formidable in appearance but are comparatively easily handled. As an illustration of the use of the method, let us assume certain values for r and k_0 and carry out the work in detail. Assume $r=3/2$ and $k_0=2$. This corresponds approximately to the case of a vacuum tube amplifier working into a low plate load resistance. Since for these values of the constants the series converge quite rapidly, it will be sufficient to take terms up to $s=3$. Writing out the terms:

$$B_{00} = k_0^r \left[1 + \frac{3/2 \cdot 1/2 \cdot}{2^2} \cdot \frac{k_1^2}{k_0^2} + \frac{3/2 \cdot 1/2 \cdot 1/2 \cdot 3/2 \cdot}{(2 \cdot 4)^2} \cdot \frac{k_1^4}{k_0^4} \right.$$

$$+ \frac{3/2 \cdot 1/2 \cdot 1/2 \cdot 3/2 \cdot 5/2 \cdot 7/2 \cdot}{(2 \cdot 4 \cdot 6)^2} \cdot \frac{k_1^6}{k_0^6} + \frac{3/2 \cdot 1/2 \cdot}{2^2} \cdot \frac{1}{k_0^2}$$

$$+ \frac{3/2 \cdot 1/2 \cdot 1/2 \cdot 3/2 \cdot}{(2 \cdot 4)^2} \cdot \frac{1}{k_0^4} + \frac{3/2 \cdot 1/2 \cdot 1/2 \cdot 3/2 \cdot 5/2 \cdot 7/2 \cdot}{(2 \cdot 4 \cdot 6)^2} \cdot \frac{1}{k_0^6}$$

$$+ \frac{3/2 \cdot 1/2 \cdot 1/2 \cdot 3/2 \cdot}{2^2 \cdot 2^2 \cdot} \cdot \frac{k_1^2}{k_0^4} + \frac{3/2 \cdot 1/2 \cdot 1/2 \cdot 3/2 \cdot 5/2 \cdot 7/2 \cdot}{2^2 (2 \cdot 4)^2} \cdot \frac{k_1^4}{k_0^6}$$

$$\left. + \frac{3/2 \cdot 1/2 \cdot 1/2 \cdot 3/2 \cdot 5/2 \cdot 7/2 \cdot}{2^2 \cdot (2 \cdot 4)^2} \cdot \frac{k_1^2}{k_0^6} \right]$$

$$= k_0^{3/2} \left[\left(1 + \frac{0.1875}{k_0^2} + \frac{0.0088}{k_0^4} + \frac{0.00214}{k_0^6} \right) \right.$$

$$+ 0.1875 \frac{k_1^2}{k_0^2} \left(1 + \frac{0.1875}{k_0^2} + \frac{0.1025}{k_0^4} \right)$$

$$\left. + 0.00875 \frac{k_1^4}{k_0^4} \left(1 + \frac{2.187}{k_0^2} \right) + 0.00214 \frac{k_1^6}{k_0^6} \right].$$

Substituting k_0 equals 2:

$$B_{00} = 2.96 + 0.139 k_1^2 + 0.00239 k_1^4 + 0.000095 k_1^6.$$

Similarly we have:

$$B_{10} = 2.10 - 0.033 k_1^2 - 0.00198 k_1^4$$

$$B_{01} = k_1 (2.08 - 0.0205 k_1^2 - 0.000647 k_1^4)$$

$$B_{11} = k_1 (0.265 + 0.00062 k_1^2).$$

To obtain the current amplitude, these coefficients are multiplied by KP^r.

Appendix

Evaluating B_{00} we have:

$$B_{00} = \frac{1}{\pi^2} \int_0^\pi \int_0^\pi (k_0 + k_1 \cos y + \cos x)^r dx\, dy$$

$$= \frac{k_0^r}{\pi^2} \int_0^\pi \int_0^\pi \left(1 + \frac{k_1}{k_0} \cos y + \frac{1}{k_0} \cos x \right)^r dx\, dy \qquad (1)$$

applying the binomial theorem:

$$B_{00} = \frac{k_0^r}{\pi^2}\int_0^\pi\int_0^\pi\left(1+\sum_{s=1}^{s=\infty}\frac{r(r-1)\cdots(r-s+1)}{s!k_0^s}(k_1\cos y + \cos x)^s\right)dx\,dy \tag{2}$$

$$= \frac{k_0^r}{\pi^2}\int_0^\pi\int_0^\pi\left(I+\sum_{s=1}^{s=\infty}\frac{r(r-1)\cdots(r-s+1)}{k_0^s}\sum_{v=0}^{v=\infty}k_1^{s-v}(\cos y)^{s-v}\cos^v x\right)dx\,dy. \tag{3}$$

Integrating, we note that for odd values of L:

$$\int_0^\pi\int_0^\pi \cos^L x dx = 0 \tag{4}$$

and for even values:

$$\int_0^\pi\int_0^\pi \cos^L x\,dx = \frac{L-1}{L}\int_0^\pi\int_0^\pi \cos^{L-2} x\,dx. \tag{5}$$

Applying (4) and (5) to (3) we have after rearranging terms:

$$B_{00} = k_0^r\left[1+\sum_{s=1}^{s=\infty}\frac{r(r-1)\cdots(r-2s+1)}{(2s)!}\cdot\frac{1\cdot3\cdot5\cdots(2s-1)}{2\cdot4\cdots2s}\cdot\frac{k_1^{2s}}{k_0^{2s}}\right.$$
$$+\sum_{v=1}^{v=\infty}\frac{r(r-I)\cdots(r-2v+1)}{(2v)!}\cdot\frac{1\cdot3\cdot5\cdots(2v-1)}{2\cdot4\cdots2v}\cdot\frac{1}{k_0^{2v}}$$
$$+\sum_{s=2}^{s=\infty}\sum_{v=1}^{v=s-1}\frac{r(r-1)\cdots(r-2s+1)}{(2s-2v)!(2v)!}\cdot\frac{1\cdot3\cdot5\cdots(2v-1)}{2\cdot4\cdots2v}$$
$$\left.\cdot\frac{1\cdot3\cdot5\cdots(2s-2v-1)}{2\cdot4\cdots(2s-2v)}\cdot\frac{k_1^{2s-2v}}{k_0^{2s}}\right]. \tag{6}$$

For values of k_1 and k_0, respectively, less and greater than unity the series is convergent. The rapidity of convergence will depend upon the values of r, k_0, and k_1.

Proceedings of the Institute of Radio Engineers
Volume 21, Number 8 *August, 1933*

A METHOD FOR CALCULATING TRANSMISSION PROPERTIES OF ELECTRICAL NETWORKS CONSISTING OF A NUMBER OF SECTIONS*

By

Andrew Alford
(Los Angeles, California)

Summary—*The solution of certain electrical networks can be made to depend on the solution of a much-studied mathematical problem in difference equations. This fact, while recognized for some time, has not received as much attention as it deserves. On the following pages we have worked out several relatively simple electrical networks by the method of difference equations. Our aim was not to obtain the solutions of the particular cases considered, but rather to illustrate the procedure involved.*

LET us first consider a well-known network made up of a number of symmetrical T sections (see Fig. 1). Let,

z_m be the impedance of the series element of mth T section
Z_m be the impedance of the shunt element of mth section
i_m be the current in the series element of the mth T section
I_m be the current in the shunt element of the mth T section
V_m be the voltage across the input of the mth section.

Let Z_1' and Z_2' be the terminal impedances of the network.

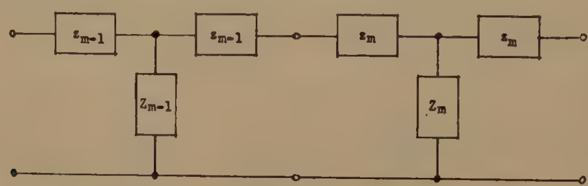

Fig. 1

The following set of equations can be readily derived by application of well-known laws:

$$I_m + i_{m+1} = i_m \tag{1}$$

$$I_{m+1} + i_{m+2} = i_{m+1} \tag{1'}$$

$$V_{m+1} + z_m i_{m+1} + z_m i_m = V_m \tag{2}$$

$$I_m Z_m + z_m i_m = V_m \tag{3}$$

$$I_{m+1} Z_{m+1} + z_{m+1} i_{m+1} = V_{m+1}. \tag{3'}$$

* Decimal classification: R140. Original manuscript received by the Institute, January 4, 1933.

If in (2) we replace V_{m+1} and V_m by their values in terms of I_m, i_m, I_{m+1}, and i_{m+1} as given by (3) and (3′), we get

$$Z_{m+1}I_{m+1} - I_mZ_m + (z_m + z_{m+1})i_{m+1} = 0. \tag{4}$$

Since by (1) and (1′), I_m and I_{m+1} may be expressed in terms of i_m, i_{m+1}, and i_{m+2}, we may write in place of (4)

$$(Z_{m+1} + Z_m + z_{m+1} + z_m)i_{m+1} - Z_mi_m - Z_{m+1}i_{m+2} = 0. \tag{5}$$

If i_1 and i_2 were given we could by repeated use of (5) written successively for $m=1, 2, 3, \cdots$, etc., calculate $i_3, i_4 \cdots i_m$ for any value of m. It seldom occurs, however, that i_1 and i_2 are given or can be easily calculated. Usually the conditions at the two ends of the network are given instead, and the best that one can do is to set up two independent equations involving four unknowns i_1, i_2, i_N, i_{N+1}. Theoretically speaking, this is equivalent to knowing i_1 and i_2, but in practice it is difficult to express i_N and i_{N+1} in terms of i_1 and i_2 by repeated use of (5). Indeed if N is a large number successive use of (5) becomes a laborious operation. This difficulty could be overcome if it were possible to express i_m in terms of two arbitrary constants C_1 and C_2 and one or more known functions of m.[1]

Suppose, for example, that it were possible to find $\phi_1(m)$ and $\phi_2(m)$ such that

$$i_m = C_1\phi_1(m) + C_2\phi_2(m), \tag{6}$$

where C_1 and C_2 are arbitrary constants not necessarily i_1 and i_2 but merely constants. Then the problem would be solved, for i_1, i_2, i_N, and i_{N+1} could be expressed in terms of C_1 and C_2, and the terminal conditions would reduce to two equations with two unknowns, C_1 and C_2.

Let us show how $\phi_1(m)$ and $\phi_2(m)$ can be obtained in several simple cases.

I.

Suppose that $z_{m+1}=z_m$; $Z_{m+1}=Z_m$ that is, that all T sections are identical. If we write, for simplicity $z_m=z$ and $Z_m=Z$; $\lambda=z/Z$, equation (5) becomes

$$2(1 + \lambda)i_{m+1} - (i_m + i_{m+1}) = 0. \tag{7}$$

Assume that $i_m=\phi(m)=Cq^m$ where C and q are independent of m. Then we have

$$i_{m+1} = Cq^{m+1}$$

$$i_{m+2} = Cq^{m+2}.$$

[1] See G. W. Pierce, "Electric Oscillations and Waves," Chap. XVI.

If (7) is to be satisfied, we must have

$$2(1+\lambda)q - q^2 - 1 = 0 \tag{8}$$

so that q may be equal to either

$$\left.\begin{aligned} q_1 &= 1+\lambda+\sqrt{(1+\lambda)^2-1} \\ \text{or,} \qquad & \\ q_2 &= (1+\lambda)-\sqrt{(1+\lambda)^2-1} = \frac{1}{q_1}. \end{aligned}\right\} \tag{9}$$

On the other hand C may have any value. We see that $C_1 q_1{}^m = i_m$ and $C_2 q_2{}^m = C_2 \; 1/q_1{}^m \; = i_m$ both satisfy (7). The sum $C_1 q_1{}^m + C_2 q_2{}^m$ too, satisfies (7).

Thus, if we prefer, we may write[2]

$$i_m = C_1 q_1{}^m + C_2 \frac{1}{q_1{}^m}. \tag{10}$$

Equation (10) contains the same information as does (7), but in more usable form. C_1 and C_2 are left arbitrary because (7) alone is not sufficient to fix the value of i_m. Terminal conditions must be given before C_1 and C_2 can be evaluated. Suppose, for example, that there is a generator in series with terminal impedance Z_1'. If the generator voltage is E, we have

$$V_1 = E - i_1 Z_1'.$$

On the other hand,

$$V_1 = I_1 Z + z i_1$$

$$i_1 = i_2 + I_1,$$

therefore,

$$(Z + z + Z_1')i_1 - i_2 Z = E. \tag{11}$$

If there is no source of voltage at the other end of the network

$$V_{N+1} = Z_2' i_{N+1}$$

but since,

$$V_{N+1} + z i_{N+1} + z i_N = V_N = z i_N + Z I_N$$

and,

$$i_N = i_{N+1} + I_N$$

[2] Equation (10) is the complete solution of (7). In general C_1 and C_2 are not constants but periodic functions of m with periods equal to unity. Since we are concerned with only integral values of m we may consider these periodic functions as constants. An excellent treatment of the theory of linear difference equations is found in Paul M. Batchelder's "Introduction to Linear Difference Equations," The Harvard University Press, 1927.

we may write,

$$(Z + z + Z_2')i_{N+1} - Zi_N = 0. \tag{12}$$

From (10),

$$i_1 = C_1 q_1 + C_2 \frac{1}{q_1}$$

$$i_2 = C_1 q_1^2 + C_2 \frac{1}{q_1^2}$$

$$i_N = C_1 q_1^N + C_2 \frac{1}{q_1^N}$$

$$i_{N+1} = C_1 q_1^{N+1} + C_2 \frac{1}{q_1^{N+1}} \cdot$$

If these values are introduced into (11) and (12), we get

$$C_1[Z + z + Z_1' - q_1 Z]q_1 + C_2\left[Z + z + Z_1' - \frac{1}{q_1} Z\right]\frac{1}{q_1} = E \tag{13}$$

$$C_1\left[Z + z + Z_2' - \frac{1}{q_1} Z\right]q^N + C_2[Z + z + Z_2' - q_1^2]\frac{1}{q^N} = 0 \tag{14}$$

but since,

$$Z + z = Z(1 + \lambda)$$

$$1 + \lambda - \frac{1}{q_1} = \sqrt{(1 + \lambda)^2 - 1}$$

$$1 + \lambda - q_1 = -\sqrt{(1 + \lambda)^2 - 1}$$

it follows that,

$$C_1[Z_1' - ZQ]q_1 + C_2[Z_1' + ZQ]\frac{1}{q_1} = E \tag{15}$$

$$C_1[Z_2' + ZQ]q_1^N + C_2[Z_2' - ZQ]\frac{1}{q_1^N} = 0 \tag{16}$$

where,

$$Q = \sqrt{(1 + \lambda)^2 - 1}.$$

Hence,

$$C_1 = \frac{E(Z_2' - ZQ)q_1^{-N}}{(Z_1' - ZQ)(Z_2' - ZQ)q_1^{-N+1} - (Z_2' + ZQ)(Z_1' + ZQ)q_1^{N-1}} \tag{17}$$

$$C_2 = \frac{E(Z_2' + ZQ)q_1^N}{(Z_2' + ZQ)(Z_1' + ZQ)q_1^{N-1} - (Z_1' - ZQ)(Z_2' - ZQ)q_1^{-N+1}} \cdot \tag{18}$$

Therefore,

$$i_m = C_1 q_1^m + C_2 \frac{1}{q_1^m} \text{ is known for every value of } m.$$

Other quantities, V_m, I_m can be readily calculated from (1), (2), and (3). In a special case, when

$$Z_1' = Z_2' = ZQ; \quad C_1 = 0; \quad C_2 = \frac{E}{2Z_1'}q = \frac{E}{2ZQ}q$$

$$i_m = \frac{E}{2Z_1'}q^{-m+1}.$$

It follows, incidentally, that

$$i_1 = \frac{E}{2Z_1'}.$$

This means that the impedance looking into the network is equal to

$$Z_1' = ZQ = Z\sqrt{\left(1 + \frac{z}{Z}\right)^2 - 1}.$$

This impedance is often called the *iterative impedance* of the network. From (17) and (18) it is also quite evident that when N is very large and $|q_1| > 1$, $C_1 = 0$ and

$$C_2 = \frac{Eq}{Z_1' + ZQ}; \qquad i_1 = \frac{E}{Z_1' + ZQ}$$

so that the network behaves as though it were equivalent to impedance ZQ even if $Z_1' \neq Z_2'$.

II.

Let us next assume that

$$z_m = \alpha^m z_0$$

$$Z_m = \alpha^m Z_0$$

Equation (5) then becomes

$$(Z_0 + z_0)(1 + \alpha)i_{m+1} - Z_0 i_m - \alpha Z_0 i_{m+2} = 0. \tag{19}$$

The solution of this equation again has the same general form as in I.

$$i_m = C_1 q_1^m + C_2 q_2^m$$

except that, this time

$$q_2 = \frac{1}{\alpha}\,\frac{1}{q_1}$$

and q_1 and q_2 are to be determined from the following equation

$$(Z_0 + z_0)(1 + \alpha)q - Z_0 - \alpha Z_0 q^2 = 0. \qquad (20)$$

III.

Consider now the so-called tapered line

$$z_m = z_0 + m \cdot z_1$$

$$Z_m = Z_{m+1} = Z.$$

Equation (5) reduces to

$$(2Z + 2z_0 + 2mz_1 + z_1)i_{m+1} - Z(i_m + i_{m+2}) = 0 \qquad (21)$$

or,

$$\frac{2(m + m_0)}{\dfrac{Z}{z_1}} i_{m+1} - i_m - i_{m+2} = 0 \qquad (22)$$

where,

$$m_0 = \frac{2Z + 2z_0 + z_1}{2z_1}.$$

If m_0 is not a real integral number (22) is satisfied by

$$i_{m+1} = C_1 J_{m+m_0}\left(\frac{Z}{z_1}\right)$$

and,

$$i_{m+1} = C_2 J_{-(m+m_0)}\left(-\frac{Z}{z_1}\right)$$

where $J_{m+m_0}(Z/z_1)$ and $J_{-(m+m_0)}(-Z/z_1)$ are Bessel's functions of the first kind. Indeed these functions satisfy the following well-known equations:

$$\frac{2n}{x} J_n(x) = J_{n+1}(x) + J_{n-1}(x)$$

$$-\frac{2n}{x} J_{-n}(x) = J_{-(n+1)}(x) + J_{-(n-1)}(x).$$

If we let $n=m+m_0$, $x=Z/z_0$, $J_n(x)$ and $J_{-n}(-x)$ obviously satisfy (23). When n is not an integer J_{-n} is independent of J_n and we may write as a complete solution

$$i_{m+1} = C_1 J_{m+m_0}\left(\frac{Z}{z_1}\right) + C_2 J_{-(m+m_0)}\left(-\frac{Z}{z_1}\right).$$

If m_0 is an integral number we must use $K_n(x)$ in place of $J_{-n}(-x)$. $K_n(x)$ is a Bessel function of the second kind. This solution is not as convenient as those previously discussed, yet, in some cases, it may prove of value since various types of expansions are available for Bessel's functions.

IV.

So far we have discussed networks made up of one row of T sections. The method is equally applicable to networks made up of more complicated elements. Let us now consider the network shown in Fig. 2.

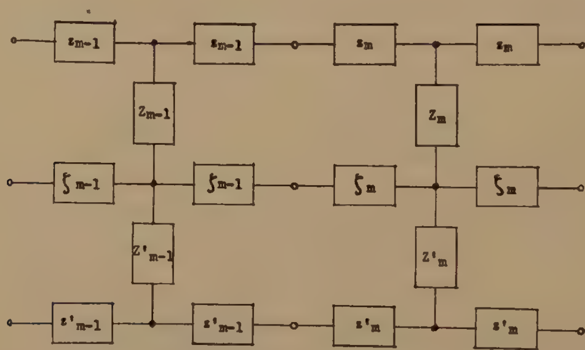

Fig. 2

$z=z_{m-1}=z_m$; $Z=Z_{m-1}=Z_m$
$z'=z'_{m-1}=z'_m$; $Z'=Z'_{m-1}=Z'_m$
$\zeta=\zeta_{m-1}=\zeta_m$

i_m current through z_m and z_{m-1}
I_m current in Z_m
θ_m current through ζ_m and ζ_{m-1}
i'_m current through z'_m and z'_{m-1}
I'_m current in Z'_m

The following equations may be easily obtained:

$$2zi_{m+1} + Z(I_{m+1} - I_m) + 2\zeta\theta_{m+1} = 0 \tag{1}$$

$$i_m = i_{m+1} + I_m \tag{2}$$

$$i_{m+1} = i_{m+2} + I_{m+1} \tag{3}$$

$$2z'i'_{m+1} + Z'(I'_{m+1} - I_m') + 2\zeta\theta_{m+1} = 0 \tag{4}$$

$$i'_m = i'_{m+1} + I'_m \tag{5}$$

$$i'_{m+1} = i'_{m+2} + I'_{m+1} \tag{6}$$

$$I_m + I_m' + \theta_{n+1} - \theta_m = 0. \tag{7}$$

Eliminating θ_m and θ_{m+1} from (7) by means of (4) and (1) written for $(m-1)$, and replacing $I_{m-1}, I_m, I_{m+1}, I_m', I'_{m+1}$ by their values in terms of $i_{(n-1}, i_m, i_{m+1}, i_{m+2}, i_m', i'_{m+1}, i'_{m+2}$ we get,

$$\begin{aligned}&- Zi_{m-1} + 2(z + Z + \zeta)i_m - (Z + 2\zeta)i_{m+1}\\&+ (Z' + 2\zeta)i'_m - 2(z' + Z' + \zeta)i'_{m+1} + Z'i'_{m+2} = 0.\end{aligned} \qquad (8)$$

On the other hand by subtracting (4) from (1) we obtain

$$\begin{aligned}&- Zi_m + 2(z + Z)i_{m+1} - Zi_{m+2}\\&+ Z'i'_m - 2(z' + Z')i'_{m+1} + Z'i'_{m+2} = 0.\end{aligned} \qquad (9)$$

Let,

$$\frac{z}{Z} = \lambda; \quad \frac{\zeta}{Z} = \mu; \quad \frac{Z'}{Z} = \nu; \quad \frac{z'}{Z} = \lambda', \quad \frac{z'}{Z'} = x$$

Then,

$$\begin{aligned}&- i_{m-1} + 2(\lambda + 1 + \mu)i_m - (1 + 2\mu)i_{m+1}\\&+ (\nu + 2\mu)i'_m - 2(\lambda' + \nu + \mu)i'_{m+1} + \nu i'_{m+2} = 0\end{aligned} \qquad (10)$$

$$\begin{aligned}&- i_m + 2(1 + \lambda)i_{m+1} - i_{m+2}\\&+ \nu i'_m - 2(\nu + \lambda')i'_{m+1} + \nu i'_{m+2} = 0.\end{aligned} \qquad (11)$$

Eliminating between (10) and (11) first i'_{m+2} and then i_m' we derive

$$\begin{aligned}- i_{m-1} + (2\lambda + 3 + 2\mu)i_m - (2\lambda + 3 + 2\mu)i_{m+1} + i_{m-2}&\\+ 2\mu(i'_m - i'_{m-1}) = 0&\end{aligned} \qquad (12)$$

$$\begin{aligned}&- \nu i_{m-1} + (3\nu + 2\lambda\nu + 2\mu\nu + 2\mu)i_m - (3\nu + 6\mu\nu + 2\lambda\nu + 4\mu)i_{m+1}\\&+ (2\mu + \nu)i_{m+2} + 2(2\mu\lambda' + \mu\nu)i'_{m+1} - 2\mu\nu i'_{m+2} = 0.\end{aligned} \qquad (13)$$

Writing (12) for $m+1$ and eliminating i'_{m+2} by means of (13) we get

$$\begin{aligned}&\nu i_{m-1} - (4\nu + 2\lambda\nu + 2\mu\nu + 2\mu)i_m + (6\nu + 4\lambda\nu + 8\mu\nu + 4\mu)i_{m+1}\\&\quad - (4\nu + 2\lambda\nu + 2\mu\nu + 2\mu)i_{m+2} + \nu i_{m+3} - 4\mu\lambda'i'_{m+1} = 0.\end{aligned} \qquad (14)$$

Writing (14) for $m+1$, subtracting the equation so obtained from (14) and combining the result with (12) we arrive at the following equation which contains only i's:

$$i_{m-1} - Qi_m + Ri_{m+1} - Ri_{m+2} + Qi_{m+3} - i_{m+4} = 0 \qquad (15)$$

where,

$$\begin{aligned}\nu \cdot Q &= 5\nu + 2\lambda\nu + 2\mu\nu + 2\mu + 2\lambda'\\\nu \cdot R &= 10\nu + 6\mu\nu + 6\lambda\nu + 6\mu + 4\lambda\mu + 4\lambda\lambda' + 6\lambda' + 4\lambda'\mu.\end{aligned}$$

We may now let $i_m' = Cq^m$. If (15) is to be satisfied q must be a root of the following equations

$$1 - Qq + Rq^2 - Rq^3 + Qq^4 - q^5 = 0 \tag{16}$$

or,

$$(1-q)[1 + q(1-Q) + q^2(1-Q+R) + q^3(1-Q) + q^4] = 0$$

$$(1-q)\left[\frac{1}{q^2} + q^2 + (1-Q)\left(\frac{1}{q} + q\right) + 1 - Q + R\right] = 0.$$

It is evident that one root $q_1 = 1$.
To get the remaining four roots let

$$x = q + (1/q).$$

Then,

$$q^2 + \frac{1}{q^2} = x^2 - 2$$

and we have,

$$x^2 + (1-Q)x + R - Q - 1 = 0$$

$$\left.\begin{aligned} x_1 &= -\frac{1-Q}{2} + \sqrt{\left(\frac{1-Q}{2}\right)^2 + Q + 1 - R} \\ x_2 &= -\frac{1-Q}{2} - \sqrt{\left(\frac{1-Q}{2}\right)^2 + Q + 1 - R} \end{aligned}\right\} \tag{17}$$

$$q + \frac{1}{q} = x_1 \qquad q + \frac{1}{q} = x_2. \tag{18}$$

It follows that $q_4 = 1/q_2$; $q_5 = 1/q_3$. q_4 and q_2 are roots of $(1/q) + q = x_1$ and q_5 and q_3 are the roots of $(1/q) + q = x_2$.

The complete expression for i_m therefore is

$$i_m = C_1 + C_2 q_2^m + C_3 q_3^m + C_4 \frac{1}{q_2^m} + C_5 \frac{1}{q_3^m}. \tag{19}$$

i'_m can now be obtained from (11) in the following manner. Consider the equation

$$-i_{m+1} + 2(1+\lambda)i_{m+1} - i_{m+2} = Aq^{m+a}. \tag{20}$$

Let,

$$i_m = \alpha q^m$$

Then,

$$\alpha[-1+2(1+\lambda)q-q^2]=Aq^a$$

$$\therefore \qquad i_m=\frac{A}{2(1+\lambda)q-1-q^2}\cdot q^{m+a} \tag{21}$$

f q is such that

$$2(1+\lambda)q-1-q^2=0. \tag{22}$$

This solution breaks down and we must have a special solution for his case.

Let,

$$i=mq^{m+a}\cdot\beta.$$

Then,

$$\beta[-m+2(1+\lambda)(m+1)q-(m+2)q^2]=Aq^a$$

$$\beta[-m+2(1+\lambda)qm-q^2m+2(1+\lambda)q-2q^2]=Aq^a.$$

But since q is assumed to satisfy (22) we have

$$\beta=\frac{A}{2(1+\lambda)q-2q^2}q^a$$

and,

$$i_m=\frac{A\cdot m}{2(1+\lambda)q-2q^2}q^{m+a}. \tag{23}$$

Therefore, the complete solution of (20) is

$$i_m=C_1'p_1^m+C_2'p_2^m+\frac{A}{2(1+\lambda)q-1-q^2}q^{m+a} \tag{24}$$

f q does not satisfy (22) and

$$i_m=C_1'p_1^m+C_2'p_2^m+\frac{A\cdot m}{2(1+\lambda)q-2q^2}q^{m+a} \tag{25}$$

f q satisfies (22). In either case p_1 and p_2 are roots of

$$2(1+\lambda)p-1-p^2=0.$$

t is now easy to show that if in place of (20) we had

$$-i_m+2(1+\lambda)i_{m+1}-i_{m+2}=Aq_1^{m+a_1}+Bq_2^{m+a_2}.$$

The complete solution would be

$$i_m=C_1'p_1^m+C_2'p_2^m+AL_1q_1^{m+a_1}+BL_2q_2^{m+a_2}$$

where,

$$L_n = \frac{1}{2(1+\lambda)q_n - 1 - q_n^2} \text{ if } q_n \text{ does not satisfy (22)}$$

and,

$$L_n = \frac{m}{2(1+\lambda)q_n - 2q_n^2} \text{ if } q_n \text{ does satisfy (22)}.$$

Applying similar procedure to (11), in which i_m', i'_{m+1}, i'_{m+2} have been replaced by their values obtained from (19), we get

$$\begin{aligned} i_m = C_1'p_1^m + C_2'p_2^m - C_1\frac{\lambda}{\lambda'} &+ C_2L_2[q_2^m - 2(1+\lambda)q_2^{m+1} + q_2^{m+2}] \\ &+ C_3L_3[q_3^m - 2(1+\lambda)q_3^{m+1} + q_3^{m+2}] \\ &+ C_4L_4[q_2^{-m} - 2(1+\lambda)q_2^{-m-1} + q_2^{-m-2}] \\ &+ C_5L_5[q_3^{-m} - 2(1+\lambda)q_3^{-m-1} + q_3^{-m-2}] \end{aligned}$$

$$\nu L_n = \frac{1}{2(1+\chi)q_n - 1 - q_n^2} \text{ if } q_n \textit{ is not} \text{ a root of } 2(1+\chi)q - 1 - q^2 = 0$$

and,

$$\nu L_n = \frac{m}{2(1+\chi)q_n - 2q_n^2} \text{ if } q_n \textit{ is} \text{ a root of } 2(1+\chi)q - 1 - q^2 = 0.$$

The arbitrary constants C_1, C_2, C_3, C_4, C_5, C_1', C_2' must be determined from the initial conditions.

Since $q = e^\alpha$ and $q^m = e^{\alpha m}$ if $\alpha = \log_e q$ we could express the solutions in terms of hyperbolic functions $\sinh \alpha m$ and $\cosh \alpha m$. We felt, however, that $e = 2.71 \cdots$ is entirely foreign to the problem itself and we preferred to avoid it.

BOOK REVIEWS

Theory of Thermionic Vacuum Tubes, by E. L. Chaffee. Published by McGraw-Hill Book Co., New York City. Price $6.00.

This splendid book by Dr. Chaffee is the most comprehensive work on the subject of low power vacuum tube theory which has so far appeared. The author states in his preface that the book was written primarily as a textbook but expresses the modest hope that it will serve also as a reference. That this hope will be fully realized is almost a foregone conclusion. The concise and yet complete discussions of fundamental vacuum tube theory are in keeping with the requirements of the classroom but are equally valuable to the engineer who desires a complete and authoritative reference book.

The writer of a book on any phase of radio engineering is faced with a difficult problem in separating important fundamentals from those short-lived engineering practices which soon become obsolete. Dr. Chaffee has wisely avoided extensive reference to current designs of tubes, choosing only a few typical cases which serve to illustrate the basic theory. Incidentally he shows some very fine X-ray photographs of these typical tubes. A similar course has been adopted with regard to the multitude of vacuum tube circuits, only those which are fundamental being discussed. The result is a work which has an excellent chance of remaining a standard reference for many years to come.

Much of the subject matter is new and obviously the original work of the author. There is also a collection and coordination of a large amount of material which has heretofore appeared only in fragmentary form in many scattered publications.

The opening chapters of the book include a brief historical introduction followed by a treatment of the basic physical phenomena which are important in the study of vacuum tube theory, such as atomic structure, conduction of electricity, electron emission, and space charge. This is followed by an excellent discussion of practical sources of electron emission and characteristics of the various emitters. Next the triode is very completely covered in a number of chapters, beginning with the basic structural relations in the tube itself then taking up the fundamental considerations of the triode and its attached circuits. Particular mention should be made of the excellent discussion of equivalent circuit theorems and the combined operating characteristics of tube and circuit. This material is much more complete than has appeared elsewhere. This is followed by a discussion of regeneration and three chapters on the various types of triode amplifiers. The operational characteristics of the diode and triode as detectors are discussed very completely, including operation with large electrical variations, a subject which has often been slighted in the literature. Tetrodes and pentodes are discussed in the closing chapter of the book.

The system of letter symbols used throughout the book recalls Dr. Chaffee's former publication on the subject and also his coöperation in the Vacuum Tube Committee of the Institute in its lengthy discussions of this difficult subject. Dr. Chaffee's system has the virtue of completeness and for a text book it appears to serve its purpose very well. However, this reviewer is still partial to the

simpler system finally adopted by the Institute, and believes that for a large majority of engineering uses it fully serves its purpose with a minimum of complication.

Two other minor criticisms might be mentioned. The classification of amplifiers (A, B, and C) is not in agreement with the system standardized by the Institute and in practically universal use by engineering organizations as well as by the Federal Radio Commission. There is also an omission in the discussion of the thoriated filament. The description of the activation and deactivation of the filament is very good but applies only to the untreated type of filament. The impression is left that this sort of filament is commonly used in medium-power transmitting tubes. As a matter of fact, the thoriated filament used in such tubes is invariably given a hydrocarbon treatment which entirely changes its rates of activation and deactivation. In fairness it should be added that nearly every other writer on thoriated filaments has made this same omission.

These criticisms are relatively unimportant however, and do not detract from the great value of the book as a whole. Unquestionably the book should become a permanent part of every radio engineer's technical library, and the promised second volume on high power tubes will be awaited with great interest.

*J. C. Warner

Radio International, by Ernst A. Pariser. Published by Union Deutsche Verlagsgesellschaft, Zweigniederlassung, Berlin SW 19, Germany. 81 pp. 5×7 in. Price, 3.50 Reichmarks.

A five-language dictionary of the more important and commonly used words on radio. The German words are arranged alphabetically, with the English, French, Spanish, and Italian equivalents in parallel columns. In addition, the words in the four latter languages are arranged in separate lists, with numbers referring to the German arrangement. Thus the dictionary is convenient and easy to use when translating from any one to any other of the five languages.

Nine hundred words in a radio dictionary may seem to be inadequate in view of the much larger lists that have already been published. But when it is considered that words common to all languages have been omitted, and that repetitions in compound words have been avoided as far as possible, this dictionary seems to fill its purpose of enabling the user to find the meaning of the common technical words that appear in foreign correspondence and periodicals.

There are a few errors in translation and spelling, but they are almost inevitable in the first edition of a polylingual dictionary and doubtless will be corrected in future editions.

†J. A. Sohon

(1) **An Appraisal of Radio Broadcasting in the Land-Grant Colleges and State Universities,** by Tracy Ferris Tyler. 150 pages, with tables and charts,
(2) **Some Interpretations and Conclusions of the Land-Grant Radio Survey,** by Tracy Ferris Tyler, 25 pages. Published by the National Committee on Education by Radio, Washington, 1933. A limited number of copies of these books are available from the publisher without charge.

Upon the initiative of the Radio Committee of the Association of Land-Grant Colleges and Universities, a survey has recently been made with the co-

* RCA Radiotron Company, Inc., Harrison, N. J.
† Engineering Societies Library, New York City.

operation of the National Committee on Education by Radio, the National Association of State Universities, the Association of Land-Grant Colleges, the Federal Office of Education, the National Advisory Council on Radio in Education and the United States Department of Agriculture. The desired data were collected from Land-Grant Colleges and State Universities in all of the forty-eight states. Publication (1) is the complete report of the survey, giving in detail the financial and administrative aspects of broadcasting, facilities, programs, opinions of college administrators, summary, and conclusions. In publication (2) a brief summary of the report is provided, with comments and conclusions. These two pamphlets are an important contribution to the literature on the use of radio in education, and they should be carefully studied by all who are related to this activity.

Of the seventy-one institutions surveyed, twenty-four owned and operated their broadcast stations. The discussion of the relative advantages and disadvantages of station ownership as contrasted with the use of commercial facilities is particularly timely and interesting, as is also the comparison of the investments and operating costs for different stations of the same power.

*W. G. CADY

* Wesleyan University, Middletown, Conn.

BOOKLETS, CATALOGS, AND PAMPHLETS RECEIVED

Copies of the publications listed on this page may be obtained gratis by addressing the manufacturer or publisher.

Switchboard and panel instruments of various sizes and types are covered in catalog No. 48 issued by the Roller-Smith Company, 233 Broadway, New York City.

In Bulletin 11 the Ward Leonard Electric Company of Mt. Vernon, N. Y. cover their vitrohm resistors. Bulletin 19 lists their vitrohm ribflex type resistors; Bulletin 25, resistor enclosures and mounts; Bulletin 106, midget magnetic relays; Bulletin 371, agastat, a pneumatic time delay relay; Bulletin 1105, vitrohm ring type rheostats; and Bulletin 75000, vitrohm stamped steel dimmer plates.

Leeds and Northrup Company of 4901 Stenton Avenue, Philadelphia, Pa. announce a portable Wheatstone testing set which is described in their Bulletin 1543. It is designed for locating faults in telephone and telegraph cables and other communication circuits and is sufficiently accurate and reliable for laboratory purposes.

Volume 1, No. 1 of the Shure Technical Bulletin is devoted to the advancement of microphone technique and is published by Shure Bros. Company of 337 W. Madison St., Chicago.

Data on general characteristics, installation and application of the following tubes are available from RCA Radiotron Company or E. T. Cunningham at 415 S. Fifth Street, Harrison, N. J.: 2A3, power amplifier triode, 2A5, power amplifier pentode, 2A6, duplex-diode high-mu triode, 6A4, power amplifier pentode, 2B7, duplex-diode pentode, 5Z3, full-wave rectifier, 1, half-wave vapor rectifier, 42, power amplifier pentode, 43, power amplifier pentode, 44, super control radio-frequency amplifier pentode, 49, dual-grid power amplifier, 53, class B twin amplifier, 75, duplex-diode triode, 77, triple-grid detector amplifier, 78, triple-grid supercontrol amplifier and 84, full-wave rectifier. Additional application notes have been released and are as follows: No. 5, the type 79 tube; No. 6, higher voltage ratings for the 36, 37, 38, 39–44, and 89; No. 7, higher voltage rating on the 79 tube, No. 8, the 2A6 as a resistance coupled audio-frequency amplifier; No. 9, recent advances in output design; No. 10, hum elimination in universal receivers, No. 11, use and operation of the 25Z5; No. 12, half-wave operation of the 25Z5; No. 13, recommended operating conditions for the 38, 41, 42, 43, and 89 tubes; No. 14, operating conditions for the 53; and No. 15, operation of the 48 as a triode.

RADIO ABSTRACTS AND REFERENCES

THIS is prepared monthly by the Bureau of Standards,* and is intended to cover the more important papers of interest to the professional radio engineer which have recently appeared in periodicals, books, etc. The number at the left of each reference classifies the reference by subject, in accordance with the "Classification of Radio Subjects: An Extension of the Dewey Decimal System," Bureau of Standards Circular No. 385, obtainable from the Superintendent of Documents, Government Printing Office, Washington, D.C., for 10 cents a copy. The classification also appeared in full on pp. 1433–1456 of the August, 1930, issue of the PROCEEDINGS of the Institute of Radio Engineers.

The articles listed are not obtainable from the Government or the Institute of Radio Engineers, except when publications thereof. The various periodicals can be secured from their publishers and can be consulted at large public libraries.

R000. RADIO (GENERAL)

R051 ×R200 A. Hund. High-Frequency Measurements (book). Published by McGraw-Hill Book Co., New York, N. Y. 1933. Price $5.00.

The book gives a thorough treatment of high-frequency measurements covering both theory and applications. The book is largely an amplification and modernization of "Hochfrequenzmesstechnik."

R100. RADIO PRINCIPLES

R111 F. D. McArthur. Electronics and electron tubes—Part I—Electron and atomic theories. *Gen. Elec. Rev.*, vol. 36, pp. 136–138; March, (1933).

A simple treatment of the theories of the electron and molecule is given. The Bohr atom is described.

R113 E. O. Hulburt. Ionization in the upper atmosphere at about 200 km above sea level. *Physics*, vol. 4, pp. 196–201; June, (1933).

From the skip distances of radio waves measured in temperate latitudes during 1927 and 1928 the average day ionization is calculated to be, at about 200 km above sea level with a maximum electron density, 7.5×10^5 and 5.6×10^5 for a summer and winter day, respectively, which agree with the observed virtual heights from radio echo experiments and the longest wave which at normal incidence pierces through the ionized layer.

R113 C. B. Feldman. The optical behavior of the ground for short radio waves. PROC. I. R. E., vol. 21, pp. 764–801; June, (1933).

The paper describes experiments undertaken to determine the limits of applicability of optical reflection equations and discusses the results. Particular emphasis is placed on the identification of direct and reflected waves. The existence of a surface wave, foreign to simple reflection theory, is recognized with vertical antennas, when the incident wave is not sufficiently plane. At angles of incidence between grazing and pseudo-Brewster value the requirements of planeness are severe. The relation of optics to Sommerfeld's theory is discussed. The experiments include tests made with the aid of an airplane.

R113.3 ×R521 H. Diamond. The cause and elimination of night effects in radio range beacon reception. *Bureau of Standards Journal of Research*, vol. 10, pp. 7–34; January, (1933). RP513; PROC. R.I.E. Vol. 21, pp. 808–832; June, (1933).

* This list compiled by Mr. A. H. Hodge and Miss E. M. Zandonini.

A new antenna system is described for use at radio range beacon stations which eliminates the troublesome night effects hitherto experienced in the use of the range beacon system. Data are given which show the severity of night effects. Because of the magnitude of these effects the range beacon is often useless over large distances. With the new antenna system developed, referred to as the transmission-line antenna system, the beacon course is satisfactory throughout its entire distance range, the night effects becoming negligible. An analysis is included which explains the occurrence of night effects with the range beacon system when using loop transmitting antennas. The significant element of the system consists of the use of transmission line for confining the radiation to the four vertical antennas.

R113.3 xR521 H. A. Chinn. A radio range-beacon free from night effects. Proc. I. R. E., vol. 21, pp. 802–807; June, (1933).

A radio range beacon, suitable for the guidance of aircraft along established airways, which is entirely free from atmospheric variations or "night effects," is described. Advantage is taken of the phenomenon that waves of frequencies higher than 30 megacycles per second, or thereabouts, are not usually refracted back to the earth by the Kennelly Heaviside layer. Multiple path transmission, variation in signal intensity and in polarization are thus avoided. A four-course aural beacon operating on 34.6 megacycles per second was employed for the experimental work. Results and applications are discussed.

R113.61 G. W. Kenrick. Records of the effective height of the Kennelly-Heaviside layer. *Physics*, vol. 4, pp. 194–195; May, (1933).

"The purpose of this note is to show characteristic changes in the effective height of the Kennelly-Heaviside layer recorded photographically with recently developed equipment." Some photographs are shown.

R140 C. H. Smith. Amplification of transients. *Wireless Eng. & Exp. Wireless* (London), vol. 10, pp. 296–298; June, (1933).

"A mathematical analysis which indicates discrepancies between the response of a receiver to steady tones and to transient waves, and suggests possible lines for fruitful experimental investigation."

R140 H. Kaiser. Beitrag zur Theorie der Eigenfrequenzen und der Selbsterregung in elektrischen Schwingungskreisen. (A contribution to the theory of the "eigen" frequency and self-generation in oscillating electric circuits.) *Elek. Nach. Tech.* vol. 10, pp. 123–143; March, (1933).

This article is a theoretical treatment of oscillating circuits.

R144 Stig. Ekelöf. Über den Wechselstromwiderstand von geraden Drühten mit kreisformigem Querschnitt, die aus mehreren konzentrischen Schichten bestehen. (On the alternating-current resistance of straight concentric conductors which consist of several layers.) *Elek. Nach. Tech.*, vol. 10, pp. 115–122; March, (1933).

Formulas are given by which one may calculate the high-frequency resistance of straight concentric conductors. The formulas are usuable for any frequency. As examples tin-plated and copper-oxide coated wire are treated.

R148 Series modulation. *Marconi Review*, no. 41, pp. 1–8; March-April, 1933.

A general review of the modulation systems commonly employed is given. Advantages of "series modulation" over other systems are discussed.

R.200. Radio Measurements and Standarization

R243.1 A valve voltmeter for audio frequencies calibrated by direct current. *Wireless Eng. & Exp. Wireless* (London), vol. 10, pp. 310–312; June, (1933).

The characteristics of this voltmeter are: (a) constant calibration for all frequencies in the audible range; (b) calibration independent of the valve characteristic to within one or two per cent, and independent of filament voltage over a wide range of variation of the latter; (c) fairly high input resistance; (d) range easily variable by a change of resistance, the lowest accurate range being about 20 to 30 volts for full scale deflection, making it suitable for measurement of loud speaker voltages; (e) linear scale; (f) calibration carried out by simple direct-current measurements.

R281 I. Saxl. How scientists are finding applications of the relation between electricity and crystals. *Radio News*, vol. 15, pp. 16–18; July, (1933).

Uses of quartz crystal (piezo-electricity) for loud speakers, microphones, and phonograph pick-ups.

R300. Apparatus and Equipment

R330 E. D. McArthur. Electronics and electron tubes—Part II—Elements of electron tubes. *Gen. Elec. Rev.*, vol. 36, pp. 177–181; April, (1933).

The electron emission of different types of filament is duscussed.

R330 E. D. McArthur. Electronics and electron tubes—Part III— Space charge and two-electrode high-vacuum tubes. *Gen. Elec. Rev.*, vol. 36, pp. 250–253; May, (1933).

A simple discussion of space charge and the conduction of electrons in a vacuum tube is given. Construction and application of two-electrode high-vacuum tubes are discussed.

R330 E. D. McArthur. Electronics and electron tubes—Control of electron space currents. *Gen. Elec. Rev.*, vol. 36,.pp. 282–289; June, (1933).

Methods of controlling space currents are discussed. Many tube characteristic curves are given.

R330 W. N. Tuttle. Dynamic measurement of electron tube coefficients. Proc. I.R.E., vol. 21, pp. 844–857; June, (1933).

Circuits are described for the dynamic measurement of amplification factor, electrode resistance, and transconductance; and are shown to be suitable for the measurement of both positive and negative values of all three coefficients over wide ranges. The analyses are for the grid-to-plate coefficients of a triode but are directly applicable to the measurement of grid-circuit coefficients or of coefficients relative to any pair of electrodes of a multielement tube. A description is given of a measuring instrument in which the three circuits are incorporated.

R330 The Catkin valve. *Wireless World*, vol. 32, pp. 340–341; May 12, (1933).

The new all-metal tubes of Marconi and Osram Companies are described.

R330 Trends in radio design and manufacturing. *Electronics*, vol. 6, p. 152; June, (1933).

The new all-metal tube is announced. It is a product of Osram-Marconi. The chief advantages are listed as: better support and mounting of electrodes, self-shielding, greater cooling, elimination of losses in the seal, nonmicrophonic, and retention of high vacuum.

R330 New receiver valves. *Electrician* (London), vol. 110, pp. 611–612; May 12, (1933).

A group of new tubes which use metal containers instead of glass bulbs are described.

R330 C. N. Symth and J. Stewart. The double-diode triode. *Wireless World*, vol. 32, pp. 355–356; May 19, (1933).

Practical data on the double-diode triode tube.

R330 L. Martin. New tube data. *RadioCraft*, vol. 5, pp. 14–17; July, (1933).

The following type vacuum tubes are described: 2A6, 2A7, 6A7, 2B7, 6B7, and 6F7.

R355 C. G. Dietsch. Suppression of transmitter harmonics. *Electronics*, vol. 6, pp. 167–169; June, (1933).

The problem of suppressing transmitter harmonics is discussed. Several circuits are given. Push-pull amplifiers in connection with low pass filters and antiresonant circuits in transmission line are recommended.

R355.9 J. S. McPetrie. Production of electronic oscillations with a two-electrode valve. *Nature* (London), vol. 131, pp. 691; May 13, (1933).

A two-electrode valve is described which may be used to generate high frequencies.

R356.3 D. D. Knowles. The Ignitron—A new controlled rectifier. *Electronics*, vol. 6, pp. 164–166; June, (1933).

A rectifier tube is described which uses a spark for forming a cathode spot. It requires no time delay, has a high overload capacity and longer life.

R357
×R361.2 C. L. Lyons. The Pentragrid converter—An American development in frequency changers. *Wireless World*, vol. 32, pp. 347–348; May 12, (1933).

Description of a single tube frequency changer which should simplify the construction of the superheterodyne. It combines in one envelope the electrodes necessary for a triode oscillator and a variable-mu first detector with the added advantage that aerial radiation and interaction between tuning circuits is avoided.

R361 J. M. Stinchfield and O. H. Schade. Reflex circuit considerations. *Electronics*, vol. 6, pp. 153–155; June, (1933).

This paper deals with the fundamental principles of reflex, the difficulties in using it, its advantages and some general comments on the design of reflexed circuits.

R361 R. W. H. Bloxam. Increasing bass response. *Wireless World*, vol. 32, pp. 334–336; May 12, (1933).

A method of arranging the parallel-fed low-frequency transformer in the circuit so as to increase the bass response is given. A diagram is given which shows at a glance the value of coupling condenser required for different transformers to effect the bass resonance at any required frequency.

R363 P. O. McDonald and T. W. Tweed. Operating constants for direct-current thermionic amplifiers. *Physics*, vol. 4, pp. 178–183; May, (1933).

The most sensitive operating value for a UX222 is found to be 1.5 volts giving a voltage sensitivity of 8×10^{-4} volt/mm in the simple circuit with no plate current compensation. By use of the screen grid, a grid filament resistance of 10^{14} ohms may be obtained, giving a current sensitivity of 8×10^{-15} amp/mm with an input resistor of 10^{11} ohms.

R363 J. R. Nelson. Class B amplifiers considered from the conventional class A standpoint. Proc. I.R.E., vol. 21, pp. 858–874; June, (1933).

The wave form of the output current of an ideal tube is analyzed when plate current cut-off occurs between zero and 180 degrees of the cycle. The theory thus developed is applied to practical tubes, and it is shown that one of the tubes operated in series may be represented as a hypothetical class A amplifier provided that twice the plate load resistance cuts off the plate current for the input voltage used. It is also shown that a diagram may be constructed from the characteristics of a tube for any operating condition from class A to class B with half the wave cut off. The load resistance used may then be transferred back to the characteristic.

R400. Radio Communication Systems

R423.21 N. Wells. Common wavelength relay broadcasting. *Marconi Review*, no. 41, pp. 20–27; March-April, (1933).

Some indication is given of the nature and possibilities of this form of broadcast transmission.

R500. Applications of Radio

R526.12 H. Diamond. Radio system for landing aircraft during fog. *Electronics*, vol. 6, pp. 158–161; June, (1933).

A description is given of the installation of radio equipment for blind landing at the Newark, N. J., airport.

R583 E. L. Q. Walker. Synchronization in television. *Marconi Review*, no. 41, pp. 9–19; March-April, (1933).

In this article the conditions which have to be met, and the difficulties which have to be overcome, are enumerated, and some details are given of systems of synchronization which have been applied in practice.

R583 G. D. Robinson. Theoretical notes on certain features of television receiving circuits. Proc. I.R.E., vol. 21, pp. 833–843; June, (1933).

Four main items are treated in these notes. The first is the determination of the product of capacity and resistance required in a television amplifier in order that the distortion of low-frequency flat-topped waves shall not exceed a specified percentage, the wave being passed through a single stage of resistance-coupled amplification. The second item deals with the addition of small amounts of inductance to the circuit of a resistance-coupled amplifier. A set of generalized graphs are presented for the purpose of greatly expediting computation of the best amount of inductance to use for given conditions. The third item shows the use of these curves by applying them to specific cases. The fourth item refers to the use of a type of push-pull detector circuit useful for minimizing the bypassing of desired high-frequency currents in the output of a detector.

R800. Nonradio Subjects

621.313.7 B. R. Hill. Applications and characteristics of copper-oxide rectifiers. *RadioCraft*, vol. 5, pp. 18–19; July, (1933).

Uses and limitations of copper-oxide rectifiers are discussed

CONTRIBUTORS TO THIS ISSUE

Alford, Andrew: Born August 5, 1904, at Samara, Russia. Graduated, University of California, December, 1924; university Fellow and graduate student, University of California, 1925–1927; teaching Fellow in physics, California Institute of Technology, 1927-December, 1928. Research engineer, West Coast division, Fox Film Corporation, 1929–1931; geophysical prospecting and consulting engineer, 1931 to date. Nonmember, Institute of Radio Engineers.

Baker, William George: Born May 27, 1902, at Clarendon, South Australia. Received B.S. degree, Sydney University, 1921; B.E. degree, 1923. Held Walter and Eliza Hall engineering traveling Fellowship, 1924–1927. Honorary lecturer in electrical engineering, University of Sydney, 1927; radio research worker under Council for Scientific and Industrial Research, Australia, 1929–1931; Amalgamated Wireless, Australasia, Ltd., 1931 to date. Received D.S. in engineering, Sydney University, 1932. Nonmember, Institute of Radio Engineers.

Barrow, W. L.: Born October 25, 1903, at Baton Rouge, Louisiana. Received B.S. degree in E.E., Louisiana State University, 1926; law student, Louisiana State University, 1926–1927; M.S. degree in E.E., Massachusetts Institute of Technology, 1929; D.C. degree in Physics, Technische Hochschule, Munich, Germany, 1931. Assistant, Electrical Engineering Department, Louisiana State University, 1925–1926; instructor, Communications Division, Electrical Engineering Department, Massachusetts Institute of Technology, 1928–1929; Redfield Proctor Fellow in physics, Technische Hochschule, Munich, 1929–1931; Round Hill, research and instructor, Communications Division, Massachusetts Institute of Technology, 1931 to date. Associate member, Institute of Radio Engineers, 1928.

Green, Alfred Leonard: Born February 3, 1905, at London, England, Educated at King's College, London University; B.S., 1925; M.S., 1929. Investigator to Radio Research Boards, Councils for Scientific and Industrial Research, Great Britain and Australia, 1927–1929, and 1929 to date. Associate member, Institute of Radio Engineers, 1928.

Hoag, J. Barton: Born September 22, 1898, at Colorado Springs, Colorado. Amateur radio experimenter since 1916. Instructor Army Radio School, Colorado College, 1918; received A.B. degree, Colorado College, 1920. Instructor in Physics, Colorado College, 1920–1921; assistant, 1922–1927. Instructor, University of Chicago, 1927–1930; Assistant Professor, 1930 to date. Received Ph.D. degree, University of Chicago, 1927. Member, American Physical Society. Member, Institute of Radio Engineers, 1928.

King, Ronold: Born September 19, 1905, at Williamstown, Massachusetts. Received A.B. degree, University of Rochester, 1927; M.S. degree, 1929; Ph.D. degree, University of Wisconsin, 1932. American-German Exchange Student, Munich, 1928–1929; White Fellow in physics, Cornell University, 1929–1930; University Fellow in electrical engineering, University of Wisconsin, 1930–1932. Associate member, Institute of Radio Engineers, 1930.

Kozanowski, Henry N.: Born August 15, 1907, at Buffalo, New York. Received B.S. degree, University of Buffalo, 1927; M.A. degree, 1929; Ph.D. degree in physics, 1930, University of Michigan. Graduate teaching assistantship, University of Buffalo, 1927–1928. Research assistant, University of Michigan, 1929–1930. Research assistant, power tube section, Westinghouse Electric and Manufacturing Company, 1930. Member, American Physical Society. Nonmember, Institute of Radio Engineers.

Lord, Harold W.: Born August 20, 1905, at Eureka, California. Received B.S. degree in E.E., California Institute of Technology, 1926. General Electric Test Course, 1926–1927; vacuum tube engineering department, General Electric Company, 1927 to date. Nonmember, Institute of Radio Engineers.

Mouromtseff, Ilia Emmanuel: Born December, 1881, at St. Petersburg, Russia. Received M.A. degree, Engineering Academy, St. Petersburg, 1906; received Diploma-Ingenieur degree, Institute of Technology, Darmstadt, Germany, 1910. Radio laboratory, Russian Signal Corps, 1911. Technical member, Westinghouse Electric and Manufacturing Company, 1923 to date. Nonmember, Institute of Radio Engineers.

Spitzer, Edwin E.: Born February 22, 1905, at Fitchburg, Massachusetts. Received B.S. and M.S. degrees in E.E., Massachusetts Institute of Technology, 1927. Research laboratory and vacuum tube engineering department, General Electric Company, 1927–1933; research and development laboratory, RCA Radiotron Company, 1933 to date. Associate member, Institute of Radio Engineers, 1928.

Thomas, H. P.: Born May 23, 1904, at Boston, Massachusetts. Received A.B. degree, Harvard College, 1925; M.S. degree in electrical communication engineering, Harvard Engineering School, 1927. Test and radio engineering department, General Electric Company, 1927 to date. Nonmember, Institute of Radio Engineers.

Tynan, A. G.: Graduated from Moore School of Electrical Engineering, University of Pennsylvania, 1930. Member, transmission research group, Bell Telephone Laboratories; designed and built apparatus for telephoto and television transmission, 1930–1932; Pilot Radio and Tube Corporation, 1933. Nonmember, Institute of Radio Engineers.